

Exponential number of equilibria and depinning threshold for a directed polymer in a random potential

Yan V. Fyodorov

King's College London, Department of Mathematics, London WC2R 2LS, United Kingdom

Pierre Le Doussal

CNRS-Laboratoire de Physique Théorique de l'École Normale Supérieure, 24 rue Lhomond, 75231 Paris, France

Alberto Rosso, Christophe Texier

LPTMS, CNRS, Univ. Paris-Sud, Université Paris-Saclay, 91405 Orsay, France

Abstract

By extending the Kac-Rice approach to manifolds of finite internal dimension, we show that the mean number $\langle \mathcal{N}_{\text{tot}} \rangle$ of all possible equilibria (i.e. force-free configurations, a.k.a. equilibrium points) of an elastic line (directed polymer), confined in a harmonic well and submitted to a quenched random Gaussian potential in dimension $d = 1 + 1$, grows exponentially $\langle \mathcal{N}_{\text{tot}} \rangle \sim \exp(rL)$ with its length L . The growth rate r is found to be directly related to the generalized Lyapunov exponent (GLE) which is a moment-generating function characterizing the large-deviation type fluctuations of the solution to the initial value problem associated with the random Schrödinger operator of the 1D Anderson localization problem. For strong confinement, the rate r is small and given by a non-perturbative (instanton, Lifshitz tail-like) contribution to GLE. For weak confinement, the rate r is found to be proportional to the inverse Larkin length of the pinning theory. As an application, identifying the depinning with a landscape “topology trivialization” phenomenon, we obtain an upper bound for the depinning threshold f_c , in the presence of an applied force, for elastic lines and d -dimensional manifolds, expressed through the mean modulus of the spectral determinant of the Laplace operators with a random potential. We also discuss the question of counting of stable equilibria. Finally, we extend the method to calculate the asymptotic number of equilibria at fixed energy (elastic, potential and total), and obtain the (annealed) distribution of the energy density over these equilibria (i.e. force-free configurations). Some connections with the Larkin model are also established.

Keywords:

PACS: 05.40.-a, 75.10.Nr

Email addresses: yan.fyodorov@kcl.ac.uk (Yan V. Fyodorov), ledou@lpt.ens.fr (Pierre Le

Preprint submitted to Elsevier

August 28, 2018

Contents

1	Introduction	3
2	Model and main results	4
2.1	The continuous model	4
2.2	The discrete model	5
2.3	Main results	5
2.4	Outline	8
2.5	Guideline	9
3	Counting of equilibria	9
4	Counting of equilibria in the presence of a force – Depinning	11
4.1	Growth of the total number of equilibria and of the number of stable equilibria .	11
4.2	The rate $r_{\text{tot}}(f)$ in the presence of an external force field	12
4.3	Rate for the number of stable equilibria : $r_{\text{st}}(f)$	17
5	Numerical calculation of the depinning threshold	18
6	Equilibria configurations: spatial correlations in the annealed measure	19
7	Relation with one-dimensional Anderson localization	20
7.1	From the number of equilibria to the generalized Lyapunov exponent	20
7.2	Stochastic Riccati equation	22
8	Generalized Lyapunov exponent and spectral analysis	26
8.1	Continuous time random walk with drift	27
8.2	Analysis of the differential equation $\mathcal{O}_q \Phi_0^R = \Lambda(q) \Phi_0^R$	28
8.3	Higher eigenvalues	30
9	WKB analysis of $\mathcal{E}_1(q)$	31
9.1	The double well effective potential	32
9.2	Weakly asymmetric double well ($ q + 1 \ll 1$)	33
9.3	Strongly asymmetric double well ($ q + 1 \gtrsim 1$)	34
10	The generalized Lyapunov exponent for even integer argument	38
10.1	Warming up : exact calculation of $\Lambda(2) = \widehat{\Lambda}(2)$	39
10.2	Analysis of $\widehat{\Lambda}(q)$ with $q \in \mathbb{N}^*$	40
10.3	Large deviations for the wave function amplitude	43
11	Mean number of equilibria at fixed value of the energy and annealed distribution of the energy of the line over the set of equilibria	44
11.1	Definitions and determinant formulae for Laplace transforms	44
11.2	Large deviations and rate functions in the large L limit	47
11.3	Mean number of equilibria at fixed value of the elastic energy for any L	57
12	Conclusion	60

Doussal), alberto.rosso@u-psud.fr (Alberto Rosso), christophe.texier@u-psud.fr (Christophe Texier)

Appendix A	Boundary conditions and determinants	61
Appendix A.1	Boundary conditions	61
Appendix A.2	Determinants	62
Appendix B	Pinning of the line for fixed boundary conditions	65
Appendix C	The Larkin model	66
Appendix D	Spectrum of the Fokker-Planck generator \mathcal{G}^\dagger in the presence of a non equilibrium stationary state – Spectrum of \mathcal{O}_q	67
Appendix D.1	Generator of the FPE	67
Appendix D.2	The spectrum of \mathcal{O}_q	69
Appendix E	WKB calculation for the ground state of the Fokker-Planck operator (written by David Saykin)	70
Appendix F	Action S_q of the WKB treatment in the $s \rightarrow 0$ limit	73
Appendix G	An inverse Laplace transform	74
Bibliography		75

1. Introduction

Various aspects of the behaviour of a directed polymer, i.e. an elastic line, in a quenched random potential keep attracting permanent research efforts of both physicists and mathematicians for more than three decades. Among other applications, it was at the center of attention as a model for vortex lines in superconductors, leading to important developments in the physics of pinning (see Refs. [1, 2] for reviews). Its connection to the Kardar-Parisi-Zhang growth (see Ref. [3] for review of earlier works) led to a recent outburst of interest, and it was shown that the probability density of the free energy for a long polymer converges to the famous Tracy-Widom distribution [4, 5, 6, 7, 8], extending the result for the ground state energy [9].

In this article we address a somewhat different aspect and consider the problem of counting the total number of *equilibria* for a directed polymer (DP), in general harmonically confined, immersed in a random potential. Those are defined as the stationary points (minima, maxima, or saddles) of an energy functional (see below). From a broader perspective, describing the statistical structure of the stationary points of random landscapes and fields of various types is a rich problem of intrinsic current interest in various areas of pure and applied mathematics [10, 11, 12, 13, 14, 15, 16, 17]. It also keeps attracting steady interest in the theoretical physics community, and this over more than fifty years [18, 19, 20, 21, 22, 23, 24, 25], with recent applications to statistical physics [26, 27, 28, 24, 25], neural networks and complex dynamics [29, 17, 30], string theory [31, 32] and cosmology [33].

Note, however, that all the previous works considered only the case of zero internal dimension, equivalent to dealing with a single-particle embedded in a random potential of arbitrary dimension. In such a setting the counting of equilibria (a.k.a, stationary points or force-free configurations) can be placed in a framework of the standard Random Matrix Theory, see Refs. [11, 34]. In contrast we aim here to address the counting problem

of manifolds of finite internal dimension. As was already anticipated in Ref. [34], in the latter case the problem turns out to be intimately related to properties of random Schrödinger operators appearing in the problems of Anderson localization. To the best of our knowledge, this aspect of the counting problem was never investigated before. Its treatment calls for a quite different technique and requires understanding of less studied properties of random Schrödinger operators, such as the modulus of its determinant and generalized Lyapunov exponents. We develop the corresponding approaches, mainly for the 1D case, in the present article.

2. Model and main results

2.1. The continuous model

We consider the following energy functional

$$\mathcal{H}[u(\tau)] = \int_0^L d\tau \left[\frac{\kappa}{2} \left(\frac{\partial u(\tau)}{\partial \tau} \right)^2 + \frac{m^2}{2} u^2(\tau) + V(u(\tau), \tau) \right] \quad (1)$$

where $u(\tau)$, $\tau \in [0, L]$ describes the polymer configuration trajectory and $\kappa \geq 0$ is the elastic energy coefficient (cf. Fig. 1). Unless stated otherwise, in the main text of the paper we assume the fixed ends configuration $u(0) = u(L) = 0$ for simplicity, other types of boundary conditions are briefly discussed in the Appendix A. The random potential $V(u(\tau), \tau)$ is chosen to be Gaussian with zero mean and with a translationally-invariant covariance

$$\langle V(u, \tau) V(u', \tau') \rangle = \delta(\tau - \tau') R(u - u'), \quad (2)$$

where we assume the symmetric function $R(u)$ to be at least four times differentiable at $u = 0$. To have a better defined problem, the polymer is considered to be confined inside a harmonic well of curvature $m^2 \geq 0$, called the mass parameter, which flattens the line beyond an infrared length, defined as

$$L_m := \sqrt{\kappa}/m \quad (3)$$

The limit $m \rightarrow 0^+$ is of special interest, as the system becomes critical, with a non trivial roughness exponent in the $L/L_m \gg 1$ limit [1, 2].

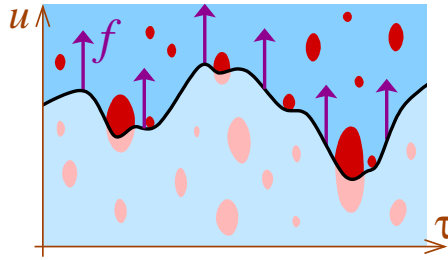


Figure 1: *Elastic line in a disordered medium submitted to a uniform force field.*

As is well known [1, 2, 35, 36] the zero temperature problem is characterized by the Larkin length L_c , which gives the order of magnitude of the scale above which

metastability (i.e. multiple extrema) sets in. Below that scale, there is typically a unique minimum and the system responds elastically (i.e. linearly) to perturbations, such as an external force $f(\tau)$, i.e. adding $-\int_0^L d\tau f(\tau) u(\tau)$ in (1). In the absence of a mass, standard estimates at weak disorder [1, 2] yield

$$L_c := (\kappa^2/R''''(0))^{1/3}, \quad (4)$$

taken here as a definition. It is also often expressed as $L_c = (\kappa^2 v_p^2/|R''(0)|)^{1/3}$, where $v_p = (|R''(0)|/R''''(0))^{1/2}$ is a characteristic scale of variation of the random potential. $L_c(m)$ in the presence of a mass, was also estimated: in the simplest (Gaussian replica variational) approximation, it corresponds to the scale beyond which replica symmetry breaking (RSB) occurs [37, 35] while in the more elaborate Functional Renormalization Group (FRG) treatment [38, 39, 2], it is associated with a cusp (non-analyticity) $R_{\text{ren}}'''(0^+) > 0$ which develops in the renormalized force correlator, signalling the appearance of shocks and avalanches [40, 35]. It also provides the so-called Larkin-Ovchinnikov (LO) estimate for the depinning threshold f_c under the action of a uniform force $f(\tau) = f$, as $f_c \sim \kappa v_p/L_c^2 = v_p R''''(0)^{2/3} \kappa^{-1/3}$ [1, 2], such that for $f > f_c$ there are no more barriers to motion [41, 1, 2, 42, 43, 44, 45, 46, 47, 48, 49]. These estimates are either dimensional (balancing elastic and pinning energy), or valid in large embedding dimension (RSB) or within an (internal) dimensional expansion (FRG), and at present there are no exact result for the number of minima, or even of equilibria, for a model of a directed polymer in one dimension.

2.2. The discrete model

Although most calculations will be performed within the continuous model, technically it will be often more easy to start from a discrete version of the model, passing to the continuous limit in the end of calculations. In this way we replace the continuous variable τ by a discrete lattice index $i = 1, \dots, K$ with $K = L/a$ (for simplicity we choose units such that the lattice spacing is $a = 1$). The energy of the polymer and the correlations of the random potential in such setting are given by

$$\mathcal{H}(\mathbf{u}) = \frac{\kappa}{2} \sum_{i=0}^K (u_i - u_{i+1})^2 + \sum_{i=1}^K \left[\frac{m^2}{2} u_i^2 + V_i(u_i) \right] \quad (5)$$

$$\langle V_i(u) V_j(u') \rangle = \delta_{ij} R(u - u'). \quad (6)$$

Configurations of the polymer are described by vectors of transverse coordinates $\mathbf{u} = (u_1, \dots, u_K)$, with $u_i \in \mathbb{R}$ for $i = 1, 2, \dots, K$. The fixed ends condition now reads $u_0 = u_{K+1} = 0$ (see Appendix A for a discussion of other boundary conditions). We will also consider the effect of an external force field, which requires to add a term $-\mathbf{f}^T \mathbf{u} = \sum_{i=1}^K f_i u_i$ to the energy (5) (the superscript T denotes transposition).

2.3. Main results

In the present article, we provide some exact results for this problem. Namely, for model (1) we show that the mean total number of equilibria grows exponentially at large L , and that the rate r is given in terms of the two length scales L_m and L_c defined above as

$$\langle \mathcal{N}_{\text{tot}} \rangle \sim e^{rL} \quad \text{with} \quad r = \frac{1}{L_m} g\left(\frac{L_m}{L_c}\right), \quad (7)$$

where $g(x)$ is a function calculated below. Although this result is derived for the continuous model (1) and Gaussian disorder, we argue that the function $g(x)$ is universal for a broader class of models, in the limit of weak disorder $L_c \gg a$ and small mass $L_m \gg a$ (where a is a UV cutoff, such as the lattice spacing). We obtain the asymptotic behaviours

$$g(x) \simeq \begin{cases} c_0 x^3 \exp\{-8/(3x^3)\} & \text{for } x \ll 1 \\ C x & \text{for } x \gg 1 \end{cases} \quad (8)$$

where the constant $c_0 = 1/(8\pi)$ has been calculated analytically (see Appendix E written by David Saykin), and we also obtained numerically both $c_0 \simeq 0.04$ and

$$C \simeq 0.46. \quad (9)$$

Correspondingly, we get

$$r = C/L_c \quad (10)$$

for the rate in the zero mass limit $m = 0$ (i.e. $L_m = \infty$): the rate of growth of the number of equilibria increases with the disorder strength as $r \sim R''''(0)^{1/3}$. In the other limit of large confinement, the rate is exponentially suppressed $r \sim \exp[-8m^3\sqrt{\kappa}/(3R''''(0))]$, which shows that as long as the elastic line is shorter than the exponentially large scale, $L \lesssim (L_c^3/L_m^2) \exp[8m^3\sqrt{\kappa}/(3R''''(0))]$, it is typically in a unique equilibrium configuration. This reflects exponentially rare metastable states of a strongly confined polymer induced by the rare events in the Gaussian tail of the disorder.

We can ask the question about the universality of our result Eq. (7). First it is immediate that (7) can be applied to the discrete model (5) in the limit $L_m, L_c \gg a$ with parameters κ and the same $R(u)$ function (in units such that $a = 1$). Our result (7) is based on the asymptotic analysis of the mean number of equilibria, expressed in terms of a ratio of determinants, see Eqs. (21) and (27) below. Below, the analysis is performed in the continuum limit, which leads to evaluating some functional determinants with the Gelfand-Yaglom method. In fact, although we will not pursue it here, one can extend the Gelfand-Yaglom method to calculate the ratio of discrete determinants (21), see Appendix A. It is a particular model since it has uncorrelated, Gaussian disorder, and quadratic elastic energy. First it is clear from our derivation that the precise shape of the correlator function $R(u)$ (within the Gaussian class) does not matter for fixed values of the second and fourth derivative at zero. We expect furthermore that the scaling form (7), up to two non-universal scales, L_c and L_m (which, in some cases, can be independently measured), extends to a broader class of elastic line models (e.g. with short-range correlations in the τ direction, and with non Gaussian disorder). A remaining question for future work is to which extent the function $g(x)$ is universal.

Furthermore, the method of calculation developed here is interesting in itself as it reveals connections to other stochastic problems such as, multifractality-like scaling of moments for the solution of the initial value problem associated with the 1D Schrödinger operator with a white noise random potential, reflecting anomalous fluctuations of finite-size Lyapunov exponents, thermally activated dynamics of a particle near depinning, and probably more.¹

1. For example the problem of calculating large deviation function addressed here is closely related to recent work in chaos theory [50], to be explored.

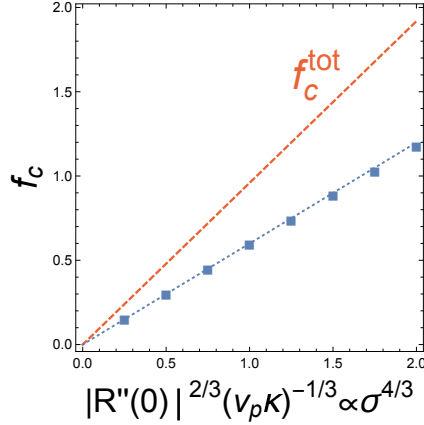


Figure 2: Depinning threshold as a function of the disorder strength $|R''(0)| = \sigma^2$ for the case of a random periodic disorder ; we compare numerics (squares) and the upper bound (11) in the continuum limit (dashed line) ; numerical calculations are performed with averaging over 100 realizations with chains of $K = 512$ monomers. For details, cf. Section 5.

As an application of our result we consider the depinning transition in the presence of a uniform applied force f . Predicting the value of f_c is a difficult problem in the theory of pinning. The value f_c of the depinning threshold is identified [42, 43] as the force f beyond which no metastable state survive. Depinning can thus be put in the broader framework of the so-called *topology trivialization* phenomenon, which has been studied recently in the context of spin glasses and other complex dynamical systems [28, 29, 17, 30]. Here we calculate $\langle \mathcal{N}_{\text{tot}} \rangle$ and obtain the value, f_c^{tot} at which it drops below unity. As we argue below, this provides an upper bound

$$f_c \leq f_c^{\text{tot}} = \frac{\sqrt{2C|R''(0)|R''''(0)^{1/3}}}{\kappa^{1/3}} = \sqrt{2C} \frac{|R''(0)|^{2/3}}{(v_p \kappa)^{1/3}}, \quad (11)$$

with the constant C given above. The formula for f_c^{tot} is compatible with the LO estimate, and we confirm from numerical simulations that (11) is a strict inequality, as shown in Fig. 2. For the random periodic disorder introduced in the numerical simulations, although the bound seems far from the numerical data, one should keep in mind that f_c^{tot} provides an upper bound depending only on $R''(0)$ and $R''''(0)$ but not the complete shape of the function $R(u)$, in particular irrespectively of its range.

We discuss the question of counting of stable equilibria in Section 4.3.

In Section 11, we also show how to extend the method to calculate the asymptotic number of equilibria $\langle \mathcal{N}_{\text{tot}}(H) \rangle \sim \exp\{r(m^2; H/L) L\}$ for which the line has a given energy H . This allows us to deduce the large deviation rate function $\Psi(h) = r(m^2) - r(m^2; h)$ controlling the (annealed) distribution of the energy density over the set of equilibria

$$\frac{\langle \mathcal{N}_{\text{tot}}(H) \rangle}{\langle \mathcal{N}_{\text{tot}} \rangle} \sim \exp\{-L \Psi(H/L)\} \quad \text{for } L \rightarrow \infty. \quad (12)$$

We obtain the precise limiting behaviours of the large deviation function :

$$\Psi(h) \simeq \begin{cases} \frac{h^2}{2R(0)} & \text{for } h \rightarrow -\infty \\ \frac{1}{2\sigma_h^2} (h - h^*)^2 & \text{for } h \sim h^* \\ \frac{m^2}{|R''(0)|} h & \text{for } h \rightarrow +\infty \end{cases} \quad (13)$$

where h^* is a typical value of the energy density described for various regimes below. We also study the annealed distribution, over the set of equilibria, of the elastic and disorder energy densities, respectively. Moreover, for the elastic energy, we can go beyond the large deviation analysis and study the distribution for arbitrary length. For weak confinement ($L_m \gg L_c$), the elastic energy dominates in typical configurations of equilibria and the typical energy density is $h^* \simeq |R''(0)|/(4m\sqrt{\kappa}) > 0$. We also show that the typical disorder energy is negative in general and, for weak confinement, takes the form $h_d^* = -a_1 |R''(0)|/(R''''(0)\kappa)^{1/3}$, with $a_1 \simeq 0.47$. The variance of the annealed distribution is also dominated by fluctuations of the elastic energy $\text{Var}_a(h) = \sigma_h^2/L \simeq [R''(0)^2/(8m^2\kappa)](L_m/L) \propto m^{-3}$. For strong confinement ($L_m \ll L_c$), the typical energy density is dominated by the disorder energy, which is negative and twice the elastic energy density in absolute value, thus $h^* \simeq -|R''(0)|/(4m\sqrt{\kappa}) < 0$. The variance is dominated by the disorder energy $\text{Var}_a(h) = \sigma_h^2/L \simeq R(0)/L$. Some connections with the simplified Larkin model (see definition in Appendix C) are made explicit: we show that (i) the (annealed) roughness of the elastic line, averaged over the set of all equilibria (ii) the annealed distribution of the elastic energy, both coincide exactly with the predictions of the Larkin model.

Finally, we further extend the upper bound for the depinning threshold f_c , to elastic manifolds of internal dimensionality d , relating it in Eq. (55) to the problem of evaluating the mean modulus of the spectral determinant of the Laplace operators with a random potential, as arises in Anderson localization problems.

2.4. Outline

In Section 3, starting from the Kac-Rice formula, we provide a representation of the mean number of equilibria as the disorder-averaged ratio of determinants (determinants of matrices for the discrete model and functional determinants of differential operators for the continuous model). In Section 4, we show that the rate r controlling the number of equilibria can be related to the depinning threshold. Section 5 briefly exposes the numerical simulations of the pinning of the elastic line. In Section 6 we determine the roughness of the elastic line over the annealed set of equilibria. In Section 7, we establish the relation between the counting of equilibria of the elastic line and the Anderson localization problem for a 1D Schrödinger equation with a random white-noise potential. Precisely, the rate r is given in terms of the generalized Lyapunov exponent (GLE), which is a moment-generating function characterizing the large-deviation type fluctuations of the solution $y(L)$ to the initial value problem associated with the random Schrödinger operator, $\langle |y(L)|^q \rangle \sim e^{L\Lambda(q)}$. Namely, the rate r is directly related to GLE function $\Lambda(q)$ at a special value of the argument equal to unity, $q = 1$. This allows us to perform a first-principle analysis of the GLE and to identify that r depends non-perturbatively on

the disorder strength for small disorder. Starting from the interpretation of the GLE as the eigenvalue of a spectral problem, we perform in Section 8 accurate numerical determination of the GLE. In Section 9, by using an improved WKB method, we obtain the value for the GLE, i.e. for the rate r . Section 10 shows that a simple determination of the GLE for even integer argument is possible, however it does not lead to the non-perturbative contribution which fully controls the rate r . This indicates that the attempts to calculate the mean number of equilibria by a naive replica-type analytic continuation may be problematic, reflecting that non-analyticity of the modulus of the determinant plays an important role in this problem. Section 11 presents the calculation of the large deviation rate functions for the elastic, disorder and total energy densities.

2.5. Guideline

This brief description of the content of the article leads us to propose two possible ways to read the article :

- Elastic line in disordered medium : Sections 3, 4, 6 and 11.
- 1D Schrödinger equation with a random potential and generalized Lyapunov exponent : Sections 7, 8, 9 and 10.

3. Counting of equilibria

As we shall see, the problem of counting equilibria for the energy function describing the lattice version of our model can be treated in a well-established mathematical framework². An equilibrium configuration is found as a solution of the system of K stationarity conditions which can be conveniently written as

$$\partial_i \mathcal{H}(\mathbf{u}) = [(m^2 \mathbf{1}_K - \kappa \Delta) \mathbf{u}]_i + V'_i(u_i) = 0, \quad i = 1, \dots, K \quad (14)$$

where $\partial_i \equiv \partial/\partial u_i$ is the partial derivative, $\mathbf{1}_K$ is the identity matrix of size K and Δ is the *discrete Laplacian matrix* for the underlying one-dimensional lattice, with the only non-zero entries for our choice of boundary conditions being $\Delta_{i,i} = -2, i = 1, \dots, K$ and $\Delta_{i,i-1} = \Delta_{i-1,i} = +1$ (see Appendix A). Note that in the continuum limit such a matrix approximates the standard one-dimensional Laplacian operator $d^2/d\tau^2$ with Dirichlet boundary conditions.

The total number, \mathcal{N}_{tot} , of solutions of such equations is then known to be given by the famous *Kac-Rice* formula, see Ref. [10] for a rigorous exposition, and Ref. [11] for a review. It can be written as follows

$$\mathcal{N}_{\text{tot}} = \int_{\mathbb{R}^K} d\mathbf{u} \rho(\mathbf{u}) \quad (15)$$

$$\rho(\mathbf{u}) = |\det(\partial_i \partial_j \mathcal{H})| \prod_{i=1}^K \delta(\partial_i \mathcal{H}), \quad (16)$$

where the Hessian is a $K \times K$ matrix given explicitly by

$$\partial_i \partial_j \mathcal{H} = [m^2 + V''_i(u_i)] \delta_{i,j} - \kappa \Delta_{i,j}. \quad (17)$$

2. Developing the corresponding formalism directly for the continuum model may represent an interesting mathematical problem.

The notation (15) allows to express more general quantities such as the total number of solutions $\mathcal{N}_A = \int_A d\mathbf{u} \rho(\mathbf{u})$ where \mathbf{u} belongs to a subset A of \mathbb{R}^K .

Eqs. (15,16) are valid in every disorder realization such that all equilibria are distinct (which happens almost surely). However for technical reasons we restrict our attention to the simplest, yet informative characteristics, the disorder average $\langle \mathcal{N}_{\text{tot}} \rangle$. To perform the disorder average we will use that (a) the potentials $V_i(u)$ and $V_j(u)$ are statistically independent for $i \neq j$ and (b) the variables $V'_i(u)$ are independent of $V''_i(u)$ for any i : indeed, from (6), one has

$$\langle V'_i(u) V''_i(u) \rangle = R'''(0) = 0 \quad (18)$$

since we have assumed differentiability ($R(u)$ being obviously an even function). More generally, the property (b) is an important consequence of translational invariance and the Gaussian character of the random function $V_i(u)$ [10]. Moreover, after taking the average the mod-Hessian factor is obviously independent of \mathbf{u} , and the average of each of the K δ -factors can be done independently over the distribution of the Gaussian variable $V'_i(u)$ with the variance $\langle [V'_i(u)]^2 \rangle = -R''(0)$, which gives

$$\langle \mathcal{N}_{\text{tot}} \rangle = \langle |\det(\partial_i \partial_j \mathcal{H})| \rangle J(m^2) \quad (19)$$

where

$$J(m^2) = \int \frac{d\mathbf{u}}{(2\pi|R''(0)|)^{K/2}} \exp \left\{ -\frac{[(m^2 \mathbf{1}_K - \kappa \Delta)\mathbf{u}]^2}{2|R''(0)|} \right\}. \quad (20)$$

The Gaussian integral yields the constant Jacobian factor $J(m^2) = |\det(m^2 \mathbf{1}_K - \kappa \Delta)|^{-1}$ finally implying that

$$\langle \mathcal{N}_{\text{tot}} \rangle = \frac{\langle |\det((m^2/\kappa) \delta_{ij} - \Delta_{ij} + U_i \delta_{ij})| \rangle}{|\det((m^2/\kappa) \delta_{ij} - \Delta_{ij})|}, \quad (21)$$

where the averaging goes over the set of independent and identically distributed (i.i.d.) mean-zero Gaussian random variables

$$U_j \equiv V'_j(u_j)/\kappa \quad (22)$$

with the covariance structure $\langle U_i U_j \rangle = 2D \delta_{ij}$, where the parameter

$$D = \frac{R''''(0)}{2\kappa^2} = \frac{1}{2L_c^3}, \quad (23)$$

measures the strength of the disorder in the problem, and is directly related to the Larkin length at $m = 0$ as defined in Eq. (4).

It is easy to see that Formula (21) obeys the exact bound $\langle \mathcal{N}_{\text{tot}} \rangle \geq 1$. Indeed, inside the average in the numerator one can use $|\det| \geq \det$, together with the following property

$$\langle \det((m^2/\kappa) \delta_{ij} - \Delta_{ij} + U_i \delta_{ij}) \rangle = \det((m^2/\kappa) \delta_{ij} - \Delta_{ij}) \quad (24)$$

which holds from the fact that the U_i are centered i.i.d random variables, and the determinant is a polynomial in the U_i of degree at most one in each variable. The disorder realizations with a single minimum $\mathcal{N}_{\text{tot}} = 1$ satisfy $|\det| = \det$. Note that replacing

$|\det| \rightarrow \det$ in our calculations would amount to neglect possibility of multiple minima and lead to the (simpler) Larkin model, described in Appendix C, which leads to a roughness exponent $\zeta = \zeta_L(d) = (4-d)/2 = \zeta_{\text{th}}(d-2)$ where $\zeta_{\text{th}}(d) = (2-d)/2$ is the thermal roughness of the disorder-free model. This is an example of the dimensional reduction property which holds for a broader class of models see [51, 52, 53, 54, 55, 56] and short review in [57], by which zero temperature observables in a disordered model – upon the replacement $|\det| = \det$ – formally identify with those of a pure model at finite temperature in two dimension less.

The continuous version of the problem is related to the pair of Schrödinger operators

$$H = -\frac{d^2}{d\tau^2} + U(\tau) \quad \text{and} \quad H_{\text{free}} = -\frac{d^2}{d\tau^2}, \quad (25)$$

where $U(\tau)$ is the Gaussian white-noise potential with mean zero and covariance

$$\langle U(\tau)U(\tau') \rangle = 2D \delta(\tau - \tau'). \quad (26)$$

Taking the appropriate continuous limit makes it rather apparent that the mean number of equilibria should be given in this case by a similar mean modulus of the ratio of two functional determinants for the operators (25) acting on functions vanishing at the two boundaries (Dirichlet boundary conditions) so that (21) takes the form

$$\langle \mathcal{N}_{\text{tot}} \rangle = \frac{\langle |\det(m^2/\kappa - \partial_\tau^2 + U(\tau))| \rangle}{|\det(m^2/\kappa - \partial_\tau^2)|}. \quad (27)$$

The calculation of these determinants will be performed in Section 7. In addition we will generalize the method to count equilibria at a given value of the energy in Section 11.

4. Counting of equilibria in the presence of a force – Depinning

Before evaluating the main objects of our interest, namely the ratios (21) or (27), which we postpone to Section 7, we discuss the effect of a uniform force field and show that the calculation of the rate r is modified in a simple way. This will allow us to establish the connection to depinning threshold.

4.1. Growth of the total number of equilibria and of the number of stable equilibria

Let us define, in a given disorder realization and with a uniform force f applied to the polymer, the total number equilibria $\mathcal{N}_{\text{tot}}(f)$ and the number of stable equilibria $\mathcal{N}_{\text{st}}(f)$. A stable equilibrium is characterized by a strictly positive Hessian matrix; to connect to the notations used earlier we note that $\mathcal{N}_{\text{tot}}(f=0) \equiv \mathcal{N}_{\text{tot}}$. We expect that before the depinning threshold is reached both $\mathcal{N}_{\text{st}}(f)$ and $\mathcal{N}_{\text{tot}}(f)$ grow exponentially with L , and define the rate functions as the following limits³ $\rho_{\text{st}}(f) := \lim_{L \rightarrow \infty} (1/L) \langle \ln \mathcal{N}_{\text{st}}(f) \rangle$, and similarly $\rho_{\text{tot}}(f) := \lim_{L \rightarrow \infty} (1/L) \langle \ln \mathcal{N}_{\text{tot}}(f) \rangle$. These two rates are expected to vanish at the *same* value of the applied force f , which defines the depinning threshold f_c . This is because

3. The limits presumably also exist in a given sample, i.e. these quantities are likely to be self-averaging.

- (i) the no-crossing rule (or Middleton theorems) [58, 59, 60], known to hold for interface depinning, implies that in any given sample the last equilibrium which disappears upon increasing f is a stable equilibrium,
- (ii) the sample-dependent threshold force at which this happens has fluctuations decaying to zero at large L (see e.g. Ref. [43]).

In this article, instead, we consider the "annealed" rates

$$r_{\text{tot}}(f) := \lim_{L \rightarrow \infty} \frac{1}{L} \ln \langle \mathcal{N}_{\text{tot}}(f) \rangle \quad \text{and} \quad r_{\text{st}}(f) := \lim_{L \rightarrow \infty} \frac{1}{L} \ln \langle \mathcal{N}_{\text{st}}(f) \rangle \quad (28)$$

and have defined the corresponding thresholds f_c^{tot} and f_c^{st} as the forces for which these rates vanish (i.e. when $\langle \mathcal{N}_{\text{tot, st}}(f) \rangle \sim 1$ for $f = f_c^{\text{tot, st}}$). From $\mathcal{N}_{\text{st}} \leq \mathcal{N}_{\text{tot}}$ and the convexity of the logarithm we obtain

$$f_c \leq f_c^{\text{st}} \leq f_c^{\text{tot}}. \quad (29)$$

In the next subsections, we determine the exact f -dependence of $r_{\text{tot}}(f)$ and $r_{\text{st}}(f)$. Together with the determination of the rate $r_{\text{tot}} \equiv r_{\text{tot}}(0)$ in Section 7, this will provide the value for f_c^{tot} displayed in (11). Obtaining the rates $\rho_{\text{tot, st}}(f)$ and the threshold f_c (and even f_c^{st} as we argue below) looks to us quite a challenging problem and goes beyond the scope of the present paper.

4.2. The rate $r_{\text{tot}}(f)$ in the presence of an external force field

4.2.1. Toy model ($d = 0$)

For simplicity let us start with a toy model of a single particle, of energy $\mathcal{H}(u) = m^2 u^2/2 + V(u) - fu$ (i.e. our discrete model (5) with $K = 1$ and $\kappa = 0$), in the presence of an external force f . Let us calculate the number of equilibria, denoted here $\mathcal{N}_{\text{tot}}^w(f)$, weighted by a function $\phi(u)$ of width w :

$$\mathcal{N}_{\text{tot}}^w(f) := \int du \rho(u) \phi(u) \quad (30)$$

$$\rho(u) = |m^2 + V''(u)| \delta(m^2 u - f + V'(u)) \quad (31)$$

where $\rho(u)$ is the mean density of equilibria at point u . For convenience, we will choose below the function $\phi(u)$ to be a Gaussian of width w . We will see that its introduction is necessary in order to connect the calculation of the number of equilibria to the threshold f_c^{tot} . From the text, its mean value is given by

$$\langle \mathcal{N}_{\text{tot}}^w(f) \rangle = G(m^2) J_w(m^2) \quad (32)$$

where

$$G(m^2) := \langle |m^2 + V''(u)| \rangle = \sqrt{\frac{2R''''(0)}{\pi}} e^{-m^4/(2R''''(0))} + m^2 \operatorname{erf} \left(\frac{m^2}{\sqrt{2R''''(0)}} \right) \quad (33)$$

where $\operatorname{erf}(x)$ is the error function [61]. We have $G(0) = \sqrt{2R''''(0)}/\pi$ and

$$J_w(m^2) := \langle \delta(m^2 u - f + V'(u)) \rangle = \int \frac{du \phi(u)}{\sqrt{2\pi|R''(0)|}} \exp \left\{ -\frac{1}{2|R''(0)|} (m^2 u - f)^2 \right\} \quad (34)$$

Now note that if we choose $\phi(u) = 1$, i.e. $w \rightarrow \infty$, then $J_\phi(m^2) = 1/m^2$ independently of f , and we obtain the mean total number of equilibria as $\langle \mathcal{N}_{\text{tot}}^\infty(f) \rangle = G(m^2)/m^2$. For $m^2 > 0$ it makes sense that it is independent of f , since the position of the center of the harmonic confining well is just shifted by f/m^2 . In the case most relevant for depinning, $m^2 \rightarrow 0^+$, this number diverges (as the particle can explore the whole real axis) and we cannot extract any information about the depinning threshold.

To have a better defined problem in the limit $m^2 \rightarrow 0^+$ we will now count the mean number of equilibria in a finite region of space u , of width w . In practice this is how a depinning force is defined, e.g. by restricting the particle to move on a cylinder of perimeter w . Here we could restrict $u \in [-w/2, w/2]$, but for calculational simplicity let us choose instead $\phi(u) = e^{-u^2/(2w^2)}$. This gives

$$J_w(m^2) = \int \frac{du}{\sqrt{2\pi|R''(0)|}} e^{-u^2/(2w^2) - \frac{1}{2|R''(0)|}(m^2u-f)^2} = \frac{e^{-f^2/[2(m^4w^2+|R''(0)|)]}}{\sqrt{m^4 + |R''(0)|/w^2}} \quad (35)$$

In the limit $m^2 \rightarrow 0^+$ we find

$$\langle \mathcal{N}_{\text{tot}}^w(f) \rangle = w \sqrt{\frac{2R'''(0)}{\pi|R''(0)|}} e^{-f^2/(2|R''(0)|)} \quad (36)$$

Hence we find that the mean number drops below unity when $f > f_c^{\text{tot}}$ with

$$f_c^{\text{tot}} = \sqrt{2|R''(0)| \left(\ln w + \frac{1}{2} \ln \frac{2R'''(0)}{\pi|R''(0)|} \right)} \quad (37)$$

This is the force such that the mean total number of equilibria drops below unity in the interval of width $\sim w$, in the u -space. Note that the effect of the mass m can be neglected as long as $w \ll \sqrt{|R''(0)|}/m^2$, and that in $d = 0$ the number of equilibria is at most of order twice the number of metastable states. The square-root logarithmic dependence in the width w is thus not surprising for the model of a particle as it originates from rare large barriers in the tail of the Gaussian-distributed potential, and is compatible with calculations of the depinning threshold in Ref. [46] on related models. Due to this effect there is no true finite depinning threshold force for the particle for $w \rightarrow +\infty$ (except for a bounded disorder). We now turn to the elastic line, which does admit a well-defined depinning threshold force in the thermodynamic limit, even for the Gaussian disorder.

4.2.2. Elastic line ($d = 1$) – discrete model

Let us now generalise the previous calculation to the DP model. Introducing the restriction

$$\phi(\mathbf{u}) = e^{-\mathbf{u}^2/(2w^2)} \quad (38)$$

in the integrals in Eqs. (15) and (20), we need to calculate

$$J_w(m^2) = \int \frac{d\mathbf{u}}{(2\pi|R''(0)|)^{K/2}} \exp \left\{ -\frac{\mathbf{u}^2}{2w^2} - \frac{[(m^2\mathbf{1}_K - \kappa\Delta)\mathbf{u} - \mathbf{f}]^2}{2|R''(0)|} \right\} \quad (39)$$

where we have added a term $-\sum_{i=1}^K f_i u_i = -\mathbf{f}^T \mathbf{u}$ to the energy (5). This equation obviously generalizes (35). Performing the integrals, this leads to a modification of (21)

$$\begin{aligned} \langle \mathcal{N}_{\text{tot}}^w(f) \rangle &= \frac{\langle |\det(m^2 \mathbf{1}_K - \kappa \Delta + \kappa U)| \rangle}{\sqrt{\det\left((m^2 \mathbf{1}_K - \kappa \Delta)^2 + \frac{|R''(0)|}{w^2} \mathbf{1}_K\right)}} \\ &\quad \times \exp \left\{ -\frac{1}{2w^2} \mathbf{f}^T \left[(m^2 \mathbf{1}_K - \kappa \Delta)^2 + \frac{|R''(0)|}{w^2} \mathbf{1}_K \right]^{-1} \mathbf{f} \right\} \end{aligned} \quad (40)$$

where U denotes the diagonal matrix with elements $U_i \delta_{ij}$. Using $\det[(a \mathbf{1}_K - \Delta)^2 + b^2 \mathbf{1}_K] = \det[a \mathbf{1}_K - \Delta + i b \mathbf{1}_K] \det[a \mathbf{1}_K - \Delta - i b \mathbf{1}_K]$, the expression can be further simplified as

$$\begin{aligned} \langle \mathcal{N}_{\text{tot}}^w(f) \rangle &= \frac{\langle |\det(L_m^{-2} \mathbf{1}_K - \Delta + U)| \rangle}{|\det((L_m^{-2} + i L_w^{-2}) \mathbf{1}_K - \Delta)|} \\ &\quad \times \exp \left\{ -\frac{1}{2(w\kappa)^2} \mathbf{f}^T [(L_m^{-2} \mathbf{1}_K - \Delta)^2 + L_w^{-4} \mathbf{1}_K]^{-1} \mathbf{f} \right\} \end{aligned} \quad (41)$$

We have introduced the two length scales (3) and

$$L_w := \frac{\sqrt{w\kappa}}{|R''(0)|^{1/4}} = L_c \sqrt{\frac{w}{v_p L_c^{1/2}}}. \quad (42)$$

The formula (41) is valid for an arbitrary number of monomers K and general boundary conditions, i.e. for all three types studied in Appendix A. Note that for $w = +\infty$ the result (40) is independent of \mathbf{f} : this is because one can shift the Gaussian integration measure on \mathbf{u} in (39) by \mathbf{u}_0 , using that there exist (for $m > 0$) a unique solution \mathbf{u}_0 to the equation $(m^2 \mathbf{1}_K - \kappa \Delta) \mathbf{u}_0 = \mathbf{f}$, which represents the new equilibrium position in the absence of disorder, displaced by the force.

The criterion $\langle \mathcal{N}_{\text{tot}}^w(f) \rangle \sim 1$ then allows to obtain a bound on the depinning threshold in the discrete setting (see below for an application).

4.2.3. Elastic line ($d = 1$) – continuous model

Taking the continuum limit is now straightforward. The presence of an external force is accounted for by adding the term $-\int_0^L d\tau f(\tau) u(\tau)$ to the energy functional (1). To restrict to a finite region in u -space we similarly introduce a functional

$$\phi[u] = \exp \left\{ -\frac{1}{2w^2} \int_0^L d\tau u(\tau)^2 \right\}. \quad (43)$$

Note that the dimension of w^2 is now $[u]^2[L]$. The extension of (41) is

$$\begin{aligned} \langle \mathcal{N}_{\text{tot}}^w(f) \rangle &= \frac{\langle |\det(L_m^{-2} - \partial_\tau^2 + U(\tau))| \rangle}{|\det(L_m^{-2} + i L_w^{-2} - \partial_\tau^2)|} \\ &\quad \times \exp \left\{ -\frac{1}{2(w\kappa)^2} \int_0^L d\tau d\tau' f(\tau) \langle \tau | \frac{1}{(L_m^{-2} - \partial_\tau^2)^2 + L_w^{-4}} | \tau' \rangle f(\tau') \right\} \end{aligned} \quad (44)$$

where we have used a quantum mechanical notation for the propagator. For $f = 0$ we recover (27). Expanding the force over the eigenmodes $\psi_n(\tau)$ of the Laplace operator (given in Appendix A for several boundary conditions) with components $\tilde{f}_n = \int_0^L d\tau \psi_n^*(\tau) f(\tau)$ we rewrite more explicitly

$$\langle \mathcal{N}_{\text{tot}}^w(f) \rangle = \frac{\langle |\det(L_m^{-2} - \partial_\tau^2 + U(\tau))| \rangle}{|\det(L_m^{-2} + i L_w^{-2} - \partial_\tau^2)|} \exp \left\{ -\frac{1}{2(w\kappa)^2} \sum_n \frac{|\tilde{f}_n|^2}{(L_m^{-2} + q_n^2)^2 + L_w^{-4}} \right\} \quad (45)$$

where $-\partial_\tau^2 \psi_n(\tau) = q_n^2 \psi_n(\tau)$. The determinant in the denominator is easily obtained for various boundary conditions, Dirichlet, Neumann or periodic (cf. Appendix A) [62] :

$$\det(\gamma - \partial_\tau^2) = \begin{cases} \frac{2}{\sqrt{\gamma}} \sinh \sqrt{\gamma} L & (\text{Dir/Dir}) \\ 2 \cosh \sqrt{\gamma} L & (\text{Dir/Neu}) \\ 2\sqrt{\gamma} \sinh \sqrt{\gamma} L & (\text{Neu/Neu}) \\ 2(\cosh \sqrt{\gamma} L - 1) & (\text{periodic}) \end{cases} \quad (46)$$

where the γ -independent prefactor is fixed by zeta-regularisation. We stress that the leading behaviour of the determinant is independent of the boundary conditions in the large L limit

$$\det(\gamma - \partial_\tau^2) \sim \exp(\sqrt{\gamma} L). \quad (47)$$

We consider a constant force $f(\tau) = f$ and the case of free (Neumann) or periodic boundary conditions (the case of fixed (Dirichlet) boundary conditions is discussed in Appendix B). The double integral in the exponential of Eq. (44) is most easily computed for Neumann and periodic boundary conditions, as the Laplacian possesses a zero mode $\psi_0(\tau) = 1/\sqrt{L}$ in this case. Using (45) with $\tilde{f}_n = \delta_{n,0} f \sqrt{L}$ shows that (minus) the argument of the exponential in (45) is

$$\frac{|\tilde{f}_0|^2}{2(w\kappa)^2(L_m^{-4} + L_w^{-4})} = \frac{f^2 L}{2(m^4 w^2 + |R''(0)|)} \quad (48)$$

The modulus of the determinant in the denominator of (44,45) is

$$|\det(L_m^{-2} + i L_w^{-2} - \partial_\tau^2)| \sim \exp [L \operatorname{Re} \sqrt{1/L_m^2 + i/L_w^2}]$$

when $L \gg L_m, L_w$. Finally we deduce

$$r_{w,m}(f) := \lim_{L \rightarrow \infty} \frac{\ln \langle \mathcal{N}_{\text{tot}}^w(f) \rangle}{L} = \Lambda(1) - \operatorname{Re} \sqrt{\frac{1}{L_m^2} + \frac{i}{L_w^2}} - \frac{f^2}{2(m^4 w^2 + |R''(0)|)} \quad (49)$$

where $\Lambda(1) = \lim_{L \rightarrow \infty} (1/L) \ln \langle |\det(L_m^{-2} - \partial_\tau^2 + U(\tau))| \rangle$ will be determined in Sections 7 and 8. In this section we only need to know that taking $L_m \rightarrow \infty$ yields the value $\Lambda(1) = C/L_c$, Eq. (10), where C is a dimensionless number of order unity and L_c the Larkin length.

The form (49) is now appropriate to consider first the limit $m^2 \rightarrow 0$ at fixed w , and second the limit $w \rightarrow \infty$ (which clearly do not commute). The first limit leads to $r_w(f) := \lim_{m^2 \rightarrow 0} r_{w,m}(f)$, with

$$r_w(f) = \frac{C}{L_c} - \frac{1}{\sqrt{2} L_w} - \frac{f^2}{2|R''(0)|} \quad (50)$$

which is valid for $L_m, L \gg L_w, L_c$. Taking now the limit $w \rightarrow \infty$, i.e. $L_w \gg L_c$, we obtain $r_{\text{tot}}(f) := \lim_{w \rightarrow \infty} r_w(f)$, with

$$r_{\text{tot}}(f) = \frac{C}{L_c} - \frac{f^2}{2|R''(0)|}. \quad (51)$$

This is one of the central results of the paper. We define the threshold $f_c^{\text{tot}} = \sqrt{2r|R''(0)|}$ as the value of f for which this rate vanishes (i.e. $\langle \mathcal{N}_{\text{tot}} \rangle \sim 1$). We get $f_c^{\text{tot}} = \sqrt{2C|R''(0)|/L_c}$, i.e.

$$f_c^{\text{tot}} = \sqrt{2C} \frac{v_p \kappa}{L_c^2} = \frac{\sqrt{2C|R''(0)|R'''(0)^{1/3}}}{\kappa^{1/3}} \quad (52)$$

as displayed in the text. It is interesting to note that it has a similar order of magnitude as the Larkin-Ovchinnikov (LO) formula [1, 2]

$$f_c^{\text{LO}} = \frac{|R''(0)|^{2/3}}{(v_p \kappa)^{1/3}} \quad (53)$$

with $R'''(0) = |R''(0)|/v_p^2$, which, however is only an order of magnitude estimate. As discussed in the text, our result (52) is an exact upper bound for the true f_c in the continuous model, or the discrete one in the limit $L_c \gg a$.

Concluding remarks —. Let us conclude by some remarks on the validity of the present calculation. Our starting formula (45) for the mean number of equilibria $\langle \mathcal{N}_{\text{tot}}^w(f) \rangle$ is exact for arbitrary m, w, L . Our strategy to obtain a robust value for f_c^{tot} (independent of details of the procedure) was to consider $m \rightarrow 0$ first, then $L \rightarrow +\infty$ and only at the end $w \rightarrow +\infty$, so that the condition $m^4 w^2 \ll |R''(0)|$ is always satisfied. With that procedure we found that the criterion $\langle \mathcal{N}_{\text{tot}}^w(f) \rangle \sim 1$ identifies f_c^{tot} unambiguously, independently of any further details of the boundary conditions. Furthermore it is independent of the type and range of correlations of the disorder, whether random field, random bond, or random periodic, i.e. independent of the precise shape of the function $R(u)$. Hence it is an upper bound on f_c in *any* type of disorder.

It is useful to recall that a similar robustness of the depinning threshold f_c with respect to boundary conditions was observed in Ref. [43] (and previous works cited there). There f_c was studied for an elastic line on a cylinder of width $W = \alpha v_p (L/L_c)^\zeta$, where ζ is the roughness exponent at depinning (and $m = 0$) and α a dimensionless constant. The latter is measured from the roughness of the last metastable configuration encountered as f is increased towards f_c . The value of f_c was found independent of the aspect ratio α of the cylinder when both L and W become large. Only finite size corrections, which are subdominant, depend on the aspect ratio and other details. These subdominant sample to sample fluctuations of the depinning threshold force were also studied in Ref. [47, 46].

Let us now comment on the respective order of limits of large L and large w . In the present calculation, a finite value of w means that any equilibrium configuration which extends beyond a width $W_L = w/\sqrt{L}$ is not counted in $\mathcal{N}_{\text{tot}}^w(f)$. If we want the upper bound argument to hold, we only need that this width be larger (or of the same order) than the typical width at depinning, i.e. $W_L \gg v_p (L/L_c)^\zeta$, equivalent to $w \gg v_p L_c^{1/2} (L/L_c)^{\zeta+1/2}$. On the other hand, our intermediate result (50) for the finite

w rate, $r_w(f)$, requires $L/L_w \gg 1$. From the definition (42) of L_w , that is equivalent to $w \ll v_p L_c^{1/2} (L/L_c)^2$. Hence whenever $\zeta < 3/2$, which is the case for most classes of disorder, both conditions can be met simultaneously: one can safely use formula (50) and the term $1/L_w$ is then negligible in the thermodynamic limit $W \sim L^\zeta \rightarrow \infty$, leading to (51) and (52). For the case of periodic depinning studied numerically in the main text, $\zeta = 3/2$ (the roughness of the Larkin model, see Appendix C). In that case $W \sim L^\zeta$ is equivalent to $L \sim L_w$ and one cannot use the second term in the asymptotic rate formula (50). Instead one must replace it by $-\frac{1}{L} \ln |\det (L_w^{-2} - \partial_\tau^2)|$. An estimate of this quantity however, shows that it is again negligible in the thermodynamic limit.

4.2.4. Interface model on arbitrary graph and dimension d

As mentioned earlier the present work establishes a connection between the pinning and localization theories. In the 1D continuum elastic line model it is best illustrated by rewriting the threshold force f_c^{tot} (52) as

$$\frac{(f_c^{\text{tot}})^2}{2|R''(0)|} = \lim_{L \rightarrow \infty} \frac{\ln \langle |\det (-\partial_\tau^2 + U(\tau))| \rangle}{L} \quad (54)$$

From (41) and following the same steps, a similar formula can be written for the discrete model (5). It can in fact be generalized further, to an interface u_i , $i \in \mathbb{Z}^d$ of internal dimension d , with an arbitrary elastic matrix $-\Delta_{ij} \rightarrow K_{ij}$, for instance $\hat{K}_q \sim |q|^a$ in Fourier representation, with $a = 2$ ($a < 2$) for short-range (long-range) elasticity - and an on-site Gaussian random potential correlated as in (5). The same method leads to a general formula for the threshold force f_c^{tot} , which is again an upper bound for the depinning threshold force, $f_c \leq f_c^{\text{tot}}$ with

$$\frac{(f_c^{\text{tot}})^2}{2|R''(0)|} = \lim_{\Omega \rightarrow \infty} \frac{\ln \langle |\det (K_{ij} + U_i \delta_{ij})| \rangle}{\Omega} \quad (55)$$

where Ω is the volume of the system and U_i a Gaussian random potential with correlator $\langle U_i U_j \rangle = (R''''(0)/\kappa^2) \delta_{ij}$. This formula further generalizes to an arbitrary graph.

4.3. Rate for the number of stable equilibria : $r_{\text{st}}(f)$

We show that the analysis for $r_{\text{tot}}(f)$ can be extended for the computation of the number of *stable* equilibria in the presence of the external force. In order to consider only stable equilibria, (15,16) must be modified as follows

$$\mathcal{N}_{\text{st}}(f) = \int_{\mathbb{R}^K} d\mathbf{u} \det (\partial_i \partial_j \mathcal{H}(\mathbf{u})) \Theta (\partial_i \partial_j \mathcal{H}(\mathbf{u})) \prod_{i=1}^K \left(e^{-u_i^2/(2w^2)} \delta (\partial_i \mathcal{H}(\mathbf{u}) - f_i) \right)$$

where $\Theta(M) = 1$ if all eigenvalues of the matrix M are positive, and 0 otherwise. Because $V'_i(u_i)$ and $V''_i(u_i)$ are independent, Eq. (18), we have the same simplification as for the calculation of the total number of equilibria :

$$\langle \mathcal{N}_{\text{st}}(f) \rangle = \langle \det (\partial_i \partial_j \mathcal{H}) \Theta (\partial_i \partial_j \mathcal{H}) \rangle \int_{\mathbb{R}^K} d\mathbf{u} \left\langle \prod_{i=1}^K \left(e^{-u_i^2/(2w^2)} \delta (\partial_i \mathcal{H}(\mathbf{u}) - f_i) \right) \right\rangle \quad (56)$$

where we have also made use of the fact that $\partial_i \partial_j \mathcal{H}$ does not depend explicitly on \mathbf{u} , but only through $V_i''(u_i)$, which are i.i.d. Gaussian random variables. Finally we can perform the same sequence of manipulations for a constant force

$$\langle \mathcal{N}_{\text{st}}(f) \rangle = \overbrace{\langle \det(\partial_i \partial_j \mathcal{H}) \Theta(\partial_i \partial_j \mathcal{H}) \rangle}^{\sim \exp[L r_{\text{st}}]} \frac{\exp \left\{ -\frac{1}{2(w\kappa)^2} \mathbf{f}^T [(L_m^{-2} \mathbf{1}_K - \Delta)^2 + L_w^{-4} \mathbf{1}_K]^{-1} \mathbf{f} \right\}}{\underbrace{|\det((L_m^{-2} + i L_w^{-2}) \mathbf{1}_K - \Delta)|}_{\sim \exp \left\{ -L \left[\text{Re} \sqrt{\frac{1}{L_m^2} + \frac{1}{L_w^2}} + \frac{f^2}{2(m^4 w^2 + |R''(0)|)} \right] \right\}}}} \quad (57)$$

where we have assumed the exponential behaviour in the absence of the external force $\langle \mathcal{N}_{\text{st}}(0) \rangle|_{w=\infty} \sim e^{L r_{\text{st}}}$. This allows us to define a new rate controlling the number of stable equilibria $\langle \mathcal{N}_{\text{st}}(f) \rangle \sim e^{L r_{\text{st}}(f)}$ and take the limits $\lim_{w \rightarrow \infty} \lim_{m^2 \rightarrow 0}$. Finally we obtain

$$r_{\text{st}}(f) = r_{\text{st}} - \frac{f^2}{2|R''(0)|}, \quad (58)$$

i.e. the same f -dependence as $r_{\text{tot}}(f)$, Eq. (51).

We have not been able to compute analytically the rate r_{st} so far, however, by dimensionless analysis, we can write that $r_{\text{st}} = C_{\text{st}}/L_c$ is another dimensionless constant, still unknown. The knowledge of C_{st} would provide another, more stringent ($C_{\text{st}} \leq C$), upper bound for the depinning threshold as the value f_c^{st} of the force such that $r_{\text{st}}(f) = 0$ which gives $f_c^{\text{st}} = \sqrt{2r_{\text{st}}|R''(0)|} \leq f_c^{\text{tot}}$ as we have obviously $\mathcal{N}_{\text{st}} \leq \mathcal{N}_{\text{tot}}$.

5. Numerical calculation of the depinning threshold

We have computed f_c numerically for a discrete elastic chain of K monomers using the algorithm developed in Ref. [42]. The energy of the chain is given by Eq. (5) with $m^2 = 0$ and $\kappa = 1$. The DP lives on a torus $(\tau, u) \in [0, L] \times [0, 2\pi/v_p]$ (i.e. we choose periodic boundary conditions in the two directions). A convenient model for the disordered force is the harmonic model

$$V_i(u) = \xi_{1,i} \cos(u/v_p) + \xi_{2,i} \sin(u/v_p), \quad (59)$$

where $\xi_{\alpha,i}$ are independent real Gaussian numbers of zero mean, $\langle \xi_{\alpha,i} \xi_{\beta,j} \rangle = \sigma^2 \delta_{\alpha,\beta} \delta_{i,j}$. This leads to the correlations (6) for the periodic correlation function

$$R(u) = \sigma^2 \cos(u/v_p). \quad (60)$$

This model provides a simple practical way to ensure that the disordered strength is translational invariant. Setting $v_p = 1$ for convenience, the variance of the disorder is $-R''(0) = R''''(0) = \sigma^2$. The presence of a stationary state is detected for a given force f . The equations of motion are (for $\kappa = 1$)

$$\dot{u}_i(\tau) = -\frac{\partial \mathcal{H}(\mathbf{u})}{\partial u_i} = u_{i+1} - 2u_i + u_{i-1} - V_i'(u_i) + f \quad \text{for } i = 1, \dots, K \quad (61)$$

(these are the Langevin equations in the zero temperature limit of vanishing Langevin noise). For a given force f we target the first metastable state by using an efficient

algorithm [42]. Monomers are considered one by one and moved from their positions to the first equilibrium point (for the model (59), the equilibrium point of each monomer can be easily found by a bisection method). The iteration stops when all monomers have a velocity smaller than a small threshold v_{\min} (here we set $v_{\min} = 10^{-6}$). The procedure is repeated by increasing the force by steps $\delta f = 0.01$. The search is ended when no stationary state are found and all monomers have moved forward of at least two periods of the disorder, giving the value of the critical force f_c . Our results are shown in Fig. 2 for DP of $K = 512$ monomers, varying the disorder strength σ^2 . When compared to the upper bound found in the paper, Eq. (11), the critical force is

$$f_c^{\text{tot}}/f_c = 1.64 \pm 0.02. \quad (62)$$

The range of disordered strength considered in the simulation corresponds to $L_c/a = \sigma^{-2/3}$ between $1/\sqrt{2}$ to 2. Thus it is quite remarkable that we do not observe any significant deviation from the behaviour $f_c \propto \sigma^{4/3}$ (Fig. 2), which is expected to hold in the continuum limit ($L_c \gg a$).

6. Equilibria configurations: spatial correlations in the annealed measure

It is interesting to ask what is the typical spatial configuration \mathbf{u} of an elastic line at a force-free stationary point (equilibrium) chosen at random. In a fixed environment, it involves a quenched measure, which is difficult to study. It is simpler, but still quite instructive, to ask the same question over the set of all stationary points in all environments, i.e. to define the annealed measure

$$\mathcal{P}_a(\mathbf{u}) := \frac{\rho(\mathbf{u})}{\langle \mathcal{N}_{\text{tot}} \rangle} \quad (63)$$

where $\rho(\mathbf{u})$ was defined in (16). We also introduce the annealed averaging of any function of the monomers positions :

$$\langle F(\mathbf{u}) \rangle_a := \left\langle \int_{\mathbb{R}^K} d\mathbf{u} \mathcal{P}_a(\mathbf{u}) F(\mathbf{u}) \right\rangle, \quad (64)$$

where K is the number of monomers and $\langle \dots \rangle$ denotes averaging over the disorder. The normalization in (63) obviously ensures that $\langle 1 \rangle_a = 1$. We thus calculate the generating function in presence of a source \mathbf{j} as

$$Z(\mathbf{j}) := \langle e^{\mathbf{j} \cdot \mathbf{u}} \rangle_a. \quad (65)$$

Its calculation is very similar, but slightly different from the one of Section 4 for an external force, see in particular the Subsection 4.2.2. We can examine Eq. (39) where we can set for now $w = +\infty$ and $\mathbf{f} = 0$ but we need to add the factor $e^{\mathbf{j} \cdot \mathbf{u}}$. Performing the integration over \mathbf{u} we now obtain

$$Z(\mathbf{j}) = \exp \left(\frac{|R''(0)|}{2} \mathbf{j} \cdot (m^2 \mathbf{1}_K - \kappa \Delta)^{-2} \cdot \mathbf{j} \right) \quad (66)$$

Hence the annealed measure $\mathcal{P}_a(\mathbf{u})$ over \mathbf{u} is centered Gaussian and its two point correlation function is

$$\langle u_i u_j \rangle_a = |R''(0)| ([m^2 \mathbf{1}_K - \kappa \Delta]^{-2})_{ij} \quad (67)$$

which is the same result as for the so-called Larkin model recalled in Appendix C. In the limit of zero mass it yields a roughness exponent⁴ $\zeta_L = 3/2$, see also Appendix C. Hence we have established here by a precise calculation, the fact (anticipated from the physics of the dimensional reduction) that the annealed measure over all equilibria (stable and unstable) and environments yields configurations with the Larkin roughness.

It is then immediate to provide a few extensions. For instance

$$\langle u_i u_j \rangle_{a,w} = |R''(0)| \left(\left[(m^2 \mathbf{1}_K - \kappa \Delta)^2 + \frac{|R''(0)|}{w^2} \mathbf{1}_K \right]^{-1} \right)_{ij} \quad (68)$$

when $\mathcal{P}_{a,w}$ is the measure where displacements are restricted, see subsection 4.2.2, defined as in (63) with $\rho(\mathbf{u}) \rightarrow \rho(\mathbf{u})\phi(\mathbf{u})$ and $\langle \mathcal{N}_{\text{tot}} \rangle \rightarrow \langle \mathcal{N}_{\text{tot}}^w \rangle$. Finally in the case $w = +\infty$ and $\mathbf{f} \neq 0$ it is immediate (in view of the remark at the end of Subsection 4.2.2) that the result (67) still holds but for the shifted deviation from disorder-free equilibrium, i.e. for $\mathbf{u} - \mathbf{u}_0$.

7. Relation with one-dimensional Anderson localization

The main outcome of Section 3 was the representation of the number of equilibria of the elastic line in terms of the determinant of a discrete random Schrödinger operator, Eq. (21), or a random differential operator (27). Such determinants are common in the problem of one-dimensional localization of a wave by a random medium. A famous example is the Herbert-Jones-Thouless relation [63, 64, 65] (see also the appendix of Ref. [66] for a discussion of the continuous case). This remark will allow us to make a precise connection with the study of the one-dimensional Schrödinger equation for a random (time-independent) potential.

7.1. From the number of equilibria to the generalized Lyapunov exponent

Although it is not essential, we find more transparent to formulate the calculation of the mean value $\langle \mathcal{N}_{\text{tot}} \rangle$ in the continuum limit, i.e. our starting point is the representation (27). As is well-known [67, 68], such ratios of functional determinants for the Schrödinger operators (25) can be evaluated by so-called Gelfand-Yaglom method as

$$\frac{\det(m^2/\kappa + H)}{\det(m^2/\kappa + H_{\text{free}})} = \frac{y(L)}{y_{\text{free}}(L)} \quad (69)$$

in terms of the solutions $y(\tau)$ of the *initial value* (Cauchy) problem for the same operators : $(m^2/\kappa + H)y(\tau) = 0$, i.e.

$$-\frac{d^2 y(\tau)}{d\tau^2} + U(\tau)y(\tau) = -\frac{m^2}{\kappa}y(\tau) \quad (70)$$

4. The roughness exponent is given by considering $\langle u(\tau)u(\tau') \rangle \sim \langle \tau |\Delta^{-2}| \tau' \rangle \sim |\tau - \tau'|^{2\zeta_L}$, as clearly the above calculation generalizes to arbitrary internal dimension and elasticity. Simple dimensional analysis gives $\zeta_L = 2 - d/2$ for an interface in (spatial) dimension d (i.e. $\tau \in \mathbb{R}^d$).

for

$$\begin{cases} y(0) = 0 \\ y'(0) = 1 \end{cases} \quad (71)$$

(see Appendix A). We have obviously $y_{\text{free}}(\tau) = L_m \sinh(\tau/L_m)$ where $L_m = \sqrt{\kappa}/m$. We deduce

$$\langle \mathcal{N}_{\text{tot}} \rangle = \frac{\langle |y(L)| \rangle}{L_m \sinh(L/L_m)}. \quad (72)$$

Cauchy problems related to products of random 2×2 matrices of various types as well as their continuum limits were under active consideration recently, with many important analytical insights, see Refs. [69, 70, 71] and references therein.

At this point it is appropriate to note that the spectral problem defined by (70) with $y(0) = y(L) = 0$ is the classical problem of one-dimensional localization for the Schrödinger equation with a Gaussian white-noise potential, studied extensively since the seminal work [72], see Refs. [73, 65] for further details. To make contact to notations used for that problem in the literature we introduce

$$E = -\frac{m^2}{\kappa} = -\frac{1}{L_m^2}, \quad (73)$$

which plays the role of the energy in the Schrödinger equation (70). As is well-known the main qualitative feature of the Cauchy problem (70,71) is the exponential growth of its solution from chosen initial conditions in every realization of the disorder [73]. It is conventional to define the localization length as the inverse of the Lyapunov exponent

$$\gamma_1 := \lim_{L \rightarrow \infty} \frac{1}{L} \langle \ln |y(L)| \rangle \geq 0 \quad (74)$$

(in principle the average is not needed as $\ln |y(L)|$ is self-averaging in the limit and it was only introduced for comparison with the definition of the GLE below). However the average $\langle |y(L)| \rangle$ depends crucially on the fluctuations, and is not given by $\exp\{\gamma_1 L\}$. To discuss the role of the fluctuations, as was done in the description of turbulence one uses the multifractal formalism developed by Paladin and Vulpiani [74, 75, 76]. In this approach one introduces the moments $\langle |y(L)|^q \rangle$, with arbitrary positive parameter q . These are known to grow exponentially at large L as $\langle |y(L)|^q \rangle \sim e^{L \Lambda(q)}$ where

$$\Lambda(q) := \lim_{L \rightarrow \infty} \frac{1}{L} \ln \langle |y(L)|^q \rangle \quad (75)$$

is the large deviation rate function, also known as the *generalized* Lyapunov exponent (GLE) [74, 75, 76].⁵ It can be written as a series

$$\Lambda(q) = \sum_{n=1}^{\infty} \frac{\gamma_n}{n!} q^n \quad (76)$$

5. The GLE has another physical interpretation : if the Schrödinger equation is solved in a scattering configuration, when the disordered potential has support $[0, L]$ and vanishes outside this interval, the transmission probability through the disordered region is related to the solution of the Cauchy problem as $T \simeq |y(L)|^{-2}$ (if the length L is larger than the localization length, the precise matching of the wave function between the disordered region and the regions free of disorder is not important). The distribution of the reflection probability $1 - T$ has been determined in Ref. [77] in the limit $E \gg D^{2/3}$. The Landauer formula relates this probability to the electric resistance (in unit $2e^2/h$) as $\rho = 1/T - 1$. We conclude that the GLE also controls the moments of the resistance $\langle \rho^\theta \rangle \sim e^{L \Lambda(2\theta)}$.

where $\gamma_n L$ is the cumulant of order n of $\ln |y(L)|$ at large L .

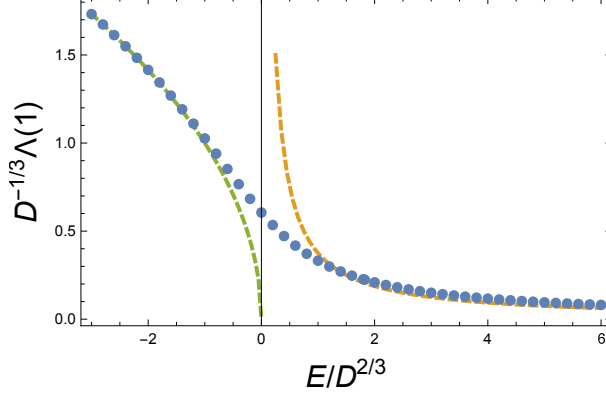


Figure 3: Generalized Lyapunov exponent $\Lambda(1)$ as a function of the energy E (blue dots). The GLE is computed thanks to the method presented in Subsection 8.1. Dashed lines are $\sqrt{-E}$ (green), Eq. (98) or (101), and $3/(8E)$ (orange), Eq. (78). The dependence in q will be discussed in Sections 7 and 10.

From Eq. (72), it is related to the rate, governing the exponential growth $\langle \mathcal{N}_{\text{tot}} \rangle \sim \exp[rL]$ for $L \rightarrow \infty$, as

$$r = \Lambda(1) - \sqrt{-E} = \Lambda(1) - 1/L_m, \quad (77)$$

defined for $E < 0$. For the study of the localization properties it is natural to consider the so-called *semiclassical regime* of large positive energy, $E \gg D^{2/3}$. In that regime the fluctuations can be considered as Gaussian with subdominant higher cumulants [78], $\Lambda(q) \simeq \gamma_1 (q + q^2/2)$, where the Lyapunov exponent can be computed perturbatively [77], $\gamma_1 \simeq D/(4E)$, thus

$$\Lambda(q) \simeq \frac{D}{4E} \left(q + \frac{1}{2} q^2 \right) \quad \text{for } E \gg D^{2/3}. \quad (78)$$

The property $\gamma_2 \simeq \gamma_1$ is known as “single parameter scaling” [79] (see also the discussion in Ref. [80]). The GLE is plotted in Fig. 3 for $q = 1$. This regime would correspond to $m^2 < 0$ with $|L_m| \ll L_c$ while here, in the elastic line counting problem, we are interested in the opposite case $m^2 \geq 0$ of negative effective energies $E < 0$. The explicit evaluation of (72) remains an outstanding and non-perturbative problem where non-Gaussian fluctuations dominate (for early works see e.g. Refs. [81, 82, 83] where it was analysed for integer value of q ; see also Section 10).

7.2. Stochastic Riccati equation

A recursive method was developed in Ref. [78] allowing to obtain integral representations for the γ_n 's in terms of multiple integrals, but they are quite complicated and not convenient to obtain limiting behaviours. An alternative way of calculating these quantities, suitable for the $E \rightarrow -\infty$ limit (large mass limit for the DP problem), was proposed in Ref. [80] for a different model. We adjust this approach here: the transformation

$$|y(L)| = \exp \left\{ \int_0^L d\tau z(\tau) \right\} \quad (79)$$

relates (70) to the stochastic Riccati equation⁶

$$\frac{dz(\tau)}{d\tau} = -E - z(\tau)^2 + U(\tau) = -\mathcal{W}'(z(\tau)) + U(\tau), \quad (80)$$

where

$$\mathcal{W}(z) = Ez + \frac{1}{3}z^3. \quad (81)$$

For $E < 0$ and $U(\tau) = 0$, $z = \sqrt{|E|}$ is a fixed point. The “noise” $U(\tau)$ thus generates fluctuations around this point.

7.2.1. A perturbative analysis of the stochastic differential equation (80)

We present first a perturbative approach to the determination of the GLE, valid for small disorder D and large negative energy E . This method provides the main q -dependence of $\Lambda(q)$ in this regime, however it will turn insufficient in order to obtain the GLE for the specific value $q = 1$, which will be shown to involve non perturbative contributions. We follow the method introduced in Ref. [80] (section 6 of this reference) in a different situation : since in the limit $E \rightarrow -\infty$ the process $z(x)$ is most of the time trapped near $z = \sqrt{-E}$, this suggests to linearize the “force”, $-\mathcal{W}'(z) = -E - z^2 \simeq -2\sqrt{|E|}(z - \sqrt{|E|})$, leading to the Ornstein-Uhlenbeck process. The method developed below is a systematic perturbative expansion around the Ornstein-Uhlenbeck process. This can be most conveniently achieved at the level of the stochastic differential equation (SDE) (80) (this is more straightforward than from the Fokker-Planck equation (FPE)). For convenience, we write

$$E = -k^2 \quad (82)$$

and rescale the coordinate and the process as

$$z(x) = k (1 + \epsilon \zeta(u)) \quad \text{with} \quad u = kx. \quad (83)$$

Eq. (80) leads to the SDE in terms of dimensionless variables

$$\zeta'(u) = -2\zeta(u) + \eta(u) - \epsilon \zeta(u)^2, \quad (84)$$

where $\eta(u)$ is a normalized Gaussian white noise, $\langle \eta(u)\eta(u') \rangle = \delta(u - u')$, and

$$\epsilon := \sqrt{\frac{2D}{k^3}} \quad (85)$$

6. Note that this equation also describes the thermally activated motion at temperature T of a particle near depinning with $-E = f - f_c$ and $D = T$

is the small perturbative parameter. We now expand the process in powers of ϵ as $\zeta = \zeta_0 + \zeta_1 + \zeta_2 + \dots$. The different terms can be found recursively

$$\zeta_0(u) = \int_0^u dt e^{-2(u-t)} \eta(t) \quad (86)$$

$$\zeta_1(u) = -\epsilon \int_0^u dt e^{-2(u-t)} \zeta_0(t)^2 \quad (87)$$

$$\zeta_2(u) = 2\epsilon^2 \int_0^u dt e^{-2(u-t)} \zeta_0(t) \int_0^t dt' e^{-2(t-t')} \zeta_0(t')^2 \quad (88)$$

$$\zeta_3(u) = -\epsilon \int_0^u dt e^{-2(u-t)} [\zeta_1(t)^2 + 2\zeta_0(t)\zeta_2(t)] \quad (89)$$

etc. Making use of the Gaussian nature of the Ornstein-Uhlenbeck process and of

$$\langle \zeta_0(u) \zeta_0(u') \rangle_{\text{stat}} = \frac{1}{4} e^{-2|u-u'|} \quad (90)$$

we can compute any correlations functions. $\langle \dots \rangle_{\text{stat}}$ denotes averaging in the stationary regime (i.e. for $u, u' \gg 1$).

We can check the method on the Lyapunov exponent: it leads to the expansion

$$\frac{\gamma_1^{(\text{pert})}}{k} = 1 + \epsilon \langle \zeta(u) \rangle_{\text{stat}} = 1 - \frac{\epsilon^2}{8} - \frac{5\epsilon^4}{128} + \mathcal{O}(\epsilon^6) \quad (91)$$

which is in perfect correspondence with the analytic part of the expansion obtained from the exact result. The complex Lyapunov exponent for $D = 1$ is [73] (see also Ref. [66])

$$\Omega = \gamma_1 - i\pi N = \frac{\text{Ai}'(-E) - i \text{Bi}'(-E)}{\text{Ai}(-E) - i \text{Bi}(-E)} \quad (92)$$

leading to

$$\frac{\gamma_1}{k} = 1 - \frac{\epsilon^2}{8} - \frac{5\epsilon^4}{128} + \mathcal{O}(\epsilon^6) - \frac{e^{-16/(3\epsilon^2)}}{2} \left[1 - \frac{\epsilon^2}{12} + \mathcal{O}(\epsilon^4) \right] \quad (93)$$

The Lyapunov exponent exhibits non-analytic contributions, $\sim \exp[-8|E|^{3/2}/(3D)]$, which are associated to the possibility of rare excursions of the process $z(x)$ to $\pm\infty$ related to the exponentially small probability current (this problem was not present in the case studied in Ref. [80] by the same method).

The variance is given by

$$\gamma_2^{(\text{pert})} = 2k\epsilon^2 \lim_{u \rightarrow \infty} \langle \zeta(u) \int_0^u dv \zeta(v) \rangle_c \quad (94)$$

where $\langle XY \rangle_c = \langle XY \rangle - \langle X \rangle \langle Y \rangle$. The limit $u \rightarrow \infty$ ensures that the correlator is computed in the stationary regime. Using the expressions (86,87,88), some lengthy algebra gives

$$\frac{\gamma_2^{(\text{pert})}}{k} = \frac{\epsilon^2}{4} + \frac{9\epsilon^4}{64} + \mathcal{O}(\epsilon^6) \quad (95)$$

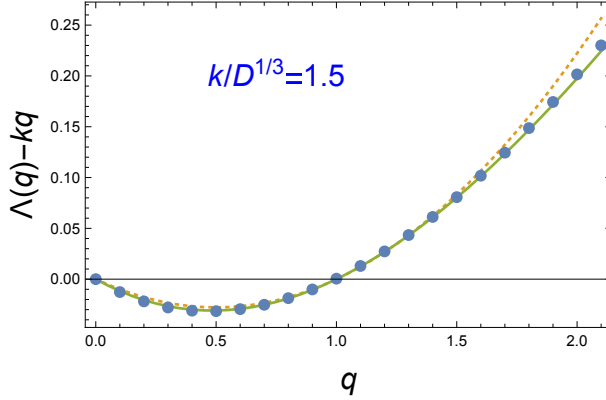


Figure 4: Generalized Lyapunov exponent obtained numerically (dots) according to the method of Subsection 8.1. Dotted line is $-q(1-q)D/(4k^2)$ and continuous line corresponds to (98). We have set $D = 1$.

The leading term to the third cumulant is more easy to compute

$$\begin{aligned}\gamma_3^{(\text{pert})} &= k \epsilon^3 \lim_{u \rightarrow \infty} \frac{1}{u} \left\langle \left(\int^u (\zeta - \langle \zeta \rangle) \right)^3 \right\rangle \\ &= 3k \epsilon^3 \lim_{u \rightarrow \infty} \frac{1}{u} \left\langle \left(\int^u \zeta_0 \right)^2 \int^u (\zeta_1 - \langle \zeta_1 \rangle) \right\rangle + \dots\end{aligned}\quad (96)$$

hence

$$\frac{\gamma_3^{(\text{pert})}}{k} = -\frac{3\epsilon^4}{16} + \mathcal{O}(\epsilon^6). \quad (97)$$

One can check that $\gamma_4 = \mathcal{O}(\epsilon^6)$, hence gathering (93,95,97) leads the perturbative result $\Lambda(q) \simeq \Lambda_{\text{pert}}(q)$ with

$$\Lambda_{\text{pert}}(q) = kq - \frac{D}{4k^2} q(1-q) - \frac{D^2}{32k^5} q(1-q)(5-4q) + \mathcal{O}(D^3/k^8). \quad (98)$$

This approximate expression of the GLE is compared with numerics of Section 8 in Fig. 4 : the agreement is excellent. Quite remarkably, Eq. (98) shows that the rate r vanishes up to third order in $s \ll 1$ (large mass limit). We conjecture that this remains true at all orders in D , i.e.

$$\Lambda_{\text{pert}}(1) - k = 0 \quad (99)$$

which is confirmed by numerics (see Figs. 4 and 6, and discussion below).

7.2.2. The need of a non perturbative analysis and a first estimate

For $E < 0$, the potential (81) is not confining, thus the noise is not only responsible for small fluctuations around $+\sqrt{|E|}$, characterized by (98), but can also produce large excursions of the process at $\pm\infty$: if the process overcomes the potential barrier at $-\sqrt{|E|}$, it is rapidly driven towards $-\infty$, reinjected at $+\infty$, from which it eventually goes back to

$+\sqrt{|E|}$. The rare jumps are separated by time intervals exponentially distributed [84]. The probability rate for a jump is exponentially small :

$$N(E) \simeq \frac{\sqrt{|E|}}{\pi} \exp \left[-4|E|^{3/2}/(3D) \right] \quad (100)$$

(this is the integrated density of states of the disordered model (25), cf. Ref. [72]). This picture suggests to split the process into two parts, describing the small fluctuations around $z = \sqrt{|E|}$ and the rare jumps: $z(\tau) = z_{\text{trapped}}(\tau) + z_{\text{jump}}(\tau)$. Because the two processes involve different time scales, they can be assumed independent and the GLE splits in two parts: $\Lambda(q) \simeq \Lambda_{\text{pert}}(q) + \Lambda_{\text{jump}}(q)$. The contribution of the jumps is estimated by writing $z_{\text{jump}}(\tau) = \sum_n h_n(\tau - \tau_n)$ where $h_n(\tau)$ is a narrow function describing the jump at time τ_n . Over large scale, $\int_0^L d\tau z_{\text{jump}}(\tau)$ is equivalent to a Compound Poisson process with Lévy exponent $\Lambda_{\text{jump}}(q) \simeq N(E) (\langle e^{qv_n} \rangle - 1)$ where $v_n = \int d\tau h_n(\tau)$ (see Ref. [66] and references therein). This simple argument shows that the strongest dependence of the rate in E is mostly controlled by $N(E)$, hence presents the non-analytic behaviour

$$r = \Lambda(1) - \sqrt{-E} \simeq \Lambda_{\text{jump}}(1) \sim N(E) \sim \exp \left[-4|E|^{3/2}/(3D) \right]. \quad (101)$$

We stress an important point : as noticed above, the Lyapunov exponent γ_1 provides a non-analytic contribution to the GLE $\Lambda(q) = \gamma_1 q + \gamma_2 q^2/2 + \dots$. This contribution, $\sim \exp \left[-8|E|^{3/2}/(3D) \right]$, cf. Eq. (93), is however much smaller than (101), which is therefore fully controlled by *fluctuations*. In the next section, we confirm the behaviour (101) by a more detailed analysis and provide the pre-exponential function.

8. Generalized Lyapunov exponent and spectral analysis

The study of the non-analytic contribution to the GLE requires powerful methods. In this section we use the relation with a spectral problem to develop some accurate numerical methods. The diffusion (80) is characterized by the (“backward”) generator \mathcal{G} and its adjoint \mathcal{G}^\dagger (“forward generator”)

$$\mathcal{G} = D \frac{d^2}{dz^2} - (E + z^2) \frac{d}{dz}, \quad \text{and} \quad \mathcal{G}^\dagger = D \frac{d^2}{dz^2} + \frac{d}{dz} (E + z^2) \quad (102)$$

governing the conditional probability density $\mathcal{P}_\tau(z|z_0) = \langle z | \exp(\tau \mathcal{G}^\dagger) | z_0 \rangle$, solution of the Fokker-Planck equation (we recall that $(d/dz)^\dagger = -d/dz$). The moments

$$\langle |y(L)|^q \rangle = \left\langle e^{q \int_0^L d\tau z(\tau)} \right\rangle = \int dz \langle z | e^{L \mathcal{O}_q} | z_0 \rangle \quad (103)$$

are controlled by the operator

$$\mathcal{O}_q = \mathcal{G}^\dagger + qz, \quad (104)$$

where the initial condition is $z_0 = \infty$ for Dirichlet boundary condition $y(0) = 0$. We introduce the biorthogonal set of right and left eigenvectors

$$(\mathcal{G}^\dagger + qz) \Phi_n^R(z; q) = -\mathcal{E}_n(q) \Phi_n^R(z; q) \quad (105)$$

$$(\mathcal{G} + qz) \Phi_n^L(z; q) = -\mathcal{E}_n(q) \Phi_n^L(z; q) \quad (106)$$

where $n \in \mathbb{N}$ and $\mathcal{E}_0 < \mathcal{E}_1 < \dots$, with normalization condition

$$\int dz \Phi_n^L(z; q) \Phi_m^R(z; q) = \delta_{n,m} \quad (107)$$

(in Appendix D, we show that the spectrum of \mathcal{O}_q is discrete). The representation (103) shows that the moments present the exponential behaviour with the length $\langle |y(L)|^q \rangle \sim e^{-L\mathcal{E}_0(q)}$, and thus the GLE is the *largest* eigenvalue

$$\Lambda(q) = -\mathcal{E}_0(q) \quad (108)$$

of the operator \mathcal{O}_q [74]. To make connection with the study of elastic line, we can rewrite the number of equilibria as

$$\langle \mathcal{N}_{\text{tot}} \rangle = \frac{\sqrt{-E}}{\sinh(\sqrt{-E}L)} \sum_{n=0}^{\infty} e^{-L\mathcal{E}_n(1)} \int dz \Phi_n^R(z; 1) \Phi_n^L(z_0; 1) \Big|_{z_0 \rightarrow \infty} . \quad (109)$$

We now study the spectral problem with two complementary methods to determined $\Lambda(q)$: In Subsection 8.1, we discretize the operator $\mathcal{O}_q = \mathcal{G}^\dagger + qz$ and perform a direct diagonalisation. In Subsection 8.2, we use a more precise method based on a neat analysis of the differential equation for $\Phi_0^R(z; q)$.

8.1. Continuous time random walk with drift

The FPE $\partial_\tau \mathcal{P}_\tau(z) = \mathcal{G}^\dagger \mathcal{P}_\tau(z)$ can be discretized in space as follows : we write $z = nb$ and introduce the transition rate from site m to site $n = m \pm 1$

$$t_{n,m} = \frac{1}{b^2} e^{(\mathcal{U}_m - \mathcal{U}_n)/2} \quad (110)$$

where $\mathcal{U}_n = \mathcal{U}(nb)$. The continuous time random walk is thus described by the master equation

$$\partial_\tau P_\tau(n) = t_{n,n+1} P_\tau(n+1) + t_{n,n-1} P_\tau(n-1) - (t_{n+1,n} + t_{n-1,n}) P_\tau(n) \quad (111)$$

(in the limit $b \rightarrow 0$ we recover the continuous diffusion for $D = 1$; cf. Ref. [85] for example). The boundaries must be discussed in detail. In order to mimic the absorption at $z = -\infty$ with reinjection at $z = +\infty$, we consider a finite lattice $n \in \{-M, -M+1, \dots, +M\}$ and choose the following transition rates connecting the two boundaries

$$t_{M,-M} = \frac{1}{b^2} p_{\text{inj}} \quad \text{and} \quad t_{-M,M} = 0 \quad (112)$$

where p_{inj} is a positive parameter. Eq. (111) must be supplemented by

$$\partial_\tau P_\tau(-M) = t_{-M,-M+1} P_\tau(-M+1) - (t_{-M+1,-M} + t_{M,-M}) P_\tau(-M) \quad (113)$$

$$\partial_\tau P_\tau(M) = t_{M,M-1} P_\tau(M-1) + t_{M,-M} P_\tau(-M) - t_{M-1,M} P_\tau(M) . \quad (114)$$

These equations define the $(2M+1) \times (2M+1)$ matrix $(\mathcal{G}^\dagger)_{n,m}$. Adding $(qnb)\delta_{n,m}$ we obtain the matrix $(\mathcal{O}_q)_{n,m}$ and perform exact diagonalization.

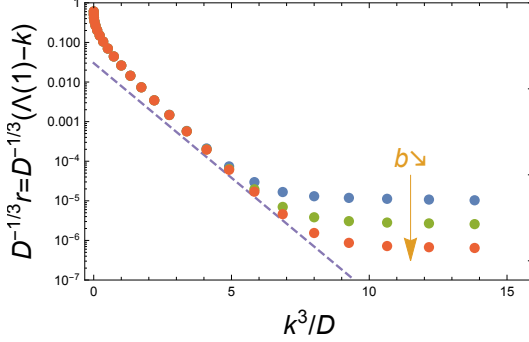


Figure 5: Rate $r = -\mathcal{E}_0(1) - k = \Lambda(1) - k$, where $E = -k^2$, obtained by diagonalization of $(2M + 1) \times (2M + 1)$ matrix $(\mathcal{O}_q)_{n,m}$. Lattice spacing is $b = 0.02, 0.01$ and 0.005 , with $M \times b = 5$ fixed ($0 \leq k \leq 2.4$). The line corresponds to $\propto \exp[-4|E|^{3/2}/(3D)]$.

For $E = -k^2$, we first check the method in the small D/k^3 (perturbative) limit for $q \neq 1$: Fig. 4 shows that the agreement with the perturbative result is excellent already for $D/k^3 = 2/3$ (for lattice spacing $b = 0.005$ and $2M + 1 = 2001$ sites). The study of the case $q = 1$ is more tricky as it requires to identify an exponentially small non-analytic correction. First we have checked that the finite size effect is negligible (provided $M \times b \gg k$), as well as the role of the parameter p_{inj} (it can be changed by several orders of magnitude without modifying significantly the result). The most important parameter is the lattice spacing b . Fig. 5 shows the different data obtained by diminishing b while keeping $M \times b$ constant. This confirms :

- (i) that $r = \Lambda(1) - k$ is non-analytic in the small parameter D/k^3 ,
- (ii) its main exponential behaviour is $\sim \exp[-4k^3/(3D)]$, corresponding to (101).
- (iii) We find the value $r = \Lambda(1) \simeq 0.59 D^{1/3}$ for $E = 0$ (i.e. $m^2 = 0$).

8.2. Analysis of the differential equation $\mathcal{O}_q \Phi_0^R = \Lambda(q) \Phi_0^R$

The numerical study of the rate (77) at large $k = \sqrt{-E}$ requires to determine the eigenvalue $\mathcal{E}_0(q) = -\Lambda(q)$ with extreme precision. For Hermitian one-dimensional operators, such as Schrödinger operators, a well-known algorithm, based on the Sturm-Liouville theorem stating that the n -th excited state has n nodes, provides the spectrum with high accuracy. The method cannot be used for the problem of interest here because the two first eigenfunctions of the operator \mathcal{O}_q , denoted $\Phi_0^R(z; q)$ and $\Phi_1^R(z; q)$ above, are both strictly positive. The nature of these eigenvectors is discussed in Appendix D.

We have found a criterion allowing to determine $\Lambda(q) = -\mathcal{E}_0(q)$ by a careful study of the function $\Phi_0^R(z; q)$ obtained numerically (Fig. D.15). The starting point is the differential equation

$$\varphi''(z) + (E + z^2)\varphi'(z) + [(2 + q)z - \lambda]\varphi(z) = 0 \quad (115)$$

corresponding to $\mathcal{O}_q \Phi_0^R(z; q) = \Lambda(q) \Phi_0^R(z; q)$ with $\Phi_0^R(z; q) \rightarrow \varphi(z)$ and for arbitrary value of the spectral parameter $\Lambda(q) \rightarrow \lambda$ (and for $D = 1$). A spectral problem is defined by specifying boundary conditions (or asymptotic behaviours). Here, it is easy to see

that the two linearly independent asymptotic behaviours of the solution of (115) are

$$|z|^{-2-q} \quad \text{and} \quad |z|^q e^{-\mathcal{W}(z)}.$$

As argued in Appendix D, the first eigenvector $\Phi_0^R(z; q)$ is the only one which behaves algebraically at infinity on both sides, so that we must select the solution with asymptotic behaviours :

$$\varphi(z) \simeq A_{\pm}(\lambda) |z|^{-2-q} \quad \text{for} \quad z \rightarrow \pm\infty. \quad (116)$$

For $q = 0$, when $\Lambda(0) = 0$, we have shown that the two coefficients are equal, $A_+(0) = A_-(0)$, cf. Eq. (D.9). We have verified numerically that this property remains true for $q > 0$, see an example of solution in Fig. D.15. This key observation has led us to propose the following method for the determination of the lowest eigenvalue $\mathcal{E}_0(q) = -\Lambda(q)$: we solve (115) and choose λ large enough to get the power law behaviours $\varphi(z) \sim |z|^{-2-q}$. Then, decreasing progressively λ , the eigenvalue is given when the two coefficients match exactly :

$$A_-(\lambda) = A_+(\lambda) \quad \text{for} \quad \lambda = \Lambda(q) = -\mathcal{E}_0(q). \quad (117)$$

We have compared the numerical values obtained in this way with the one deduced by direct diagonalization of the matrix $(\mathcal{O}_q)_{n,m}$ (previous Subsection): we have obtained a perfect agreement for the smallest values of the parameter k (Fig. 6), when diagonalization is reliable (cf Fig. 5). The method is sufficiently accurate to make accessible relatively large k (up to $k = 2.5$) leading to the precision on the eigenvalue, and thus the rate $r = \Lambda(1) - k$, up to $\sim 10^{-11}$.

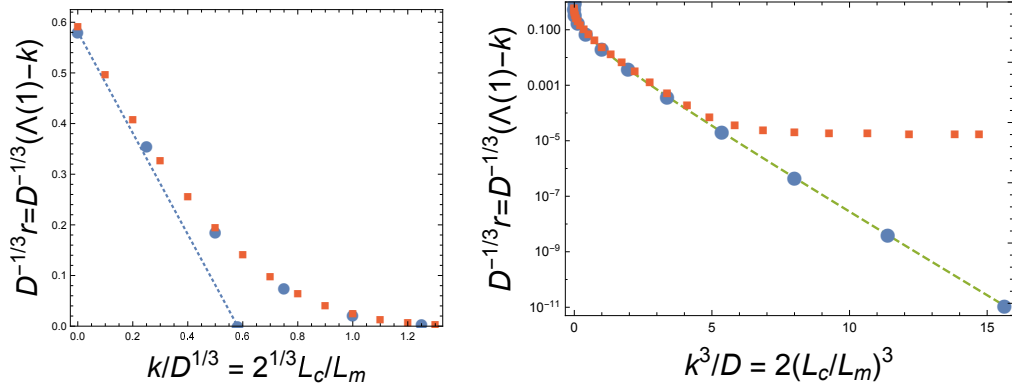


Figure 6: Generalized Lyapunov exponent $\Lambda(1)$.— Left : the rate $r = \Lambda(1) - k$ is plotted as a function of k (with $E = -k^2$) in linear scale (dotted blue line is $C (2D)^{1/3} - k$). Right : the rate $r = \Lambda(1) - k$ is plotted as a function of k^3 in log-linear scale. The GLE is obtained numerically by two methods : diagonalization of the discretised operator \mathcal{O}_q , Subsection 8.1, (red squares) and analysis of the differential equation (blue dots), Subsection 8.2 ; in the first case (red squares), we recall that the saturation of the data at large k is a lattice effect. The dashed green line is $0.08D|E|^{-1} \exp[-4|E|^{3/2}/(3D)]$.

We obtain the value of the GLE in the limit $E \rightarrow 0^-$ (i.e. $m^2 \rightarrow 0^+$) :

$$r = \Lambda(1) \simeq 0.58 D^{1/3} \simeq 0.46/L_c, \quad (118)$$

i.e. a value close to the one obtained by the diagonalisation (§ 8.1). This value corresponds to the limiting behaviour (8) for $x \rightarrow \infty$. The result also agrees with the one

deduced from the first 8 cumulants for $E = 0$, given in Table 1 of Ref. [78]. Fig. 6 shows the agreement of the two numerical methods in the small $k = \sqrt{|E|}$ regime. The $E \rightarrow 0$ behaviour will also be needed later. As the parameter E enters the spectral problem $\mathcal{O}_q \Phi_0^R = \Lambda(q) \Phi_0^R$ as an additive constant in the drift of the diffusion operator, we expect that $\Lambda(q)$ is an analytic function of E at $E = 0$; moreover, in the localization problem, the value of the energy $E = 0$ does not play any special role in the presence of the disorder. This is supported by the study of Ref. [80] (cf. Appendix 3 of this article). As a consequence, the GLE presents the behaviour

$$\Lambda(1) = C (2D)^{1/3} - a_1 (2D)^{-1/3} E + \mathcal{O}(E^2) \quad \text{as } E \rightarrow 0 \quad (119)$$

where we have obtained numerically $a_1 \simeq 0.47$ (cf. Fig. 3). Correspondingly, we get

$$r = C (2D)^{1/3} - \sqrt{-E} - a_1 (2D)^{-1/3} E + \mathcal{O}(E^2) \quad \text{as } E \rightarrow 0^- \quad (120)$$

(cf. Fig. 6).

In the limit $E \rightarrow -\infty$ (i.e. $m^2 \rightarrow +\infty$), we confirm once again the main exponential behaviour (101). Moreover, the method allows to extract unambiguously the behaviour of the pre-exponential function : cf. Fig. 8. The results of the numerical calculation are compatible with

$$\Lambda(1) = -\mathcal{E}_0(1) \simeq \sqrt{|E|} + \frac{0.08 D}{|E|} e^{-4|E|^{3/2}/(3D)} \quad \text{for } |E|^{3/2} \gg D. \quad (121)$$

This asymptotic behaviour corresponds to the limiting behaviour (8) for $x \rightarrow 0$. In Appendix E, written by D. Saykin, it is demonstrated that the above coefficient 0.08 is actually $1/(4\pi)$.

8.3. Higher eigenvalues

The other eigenvalues of the operator \mathcal{O}_q , $\mathcal{E}_n(q)$ for $n > 0$, are also of interest as they control the relaxation towards equilibrium. We have obtained it by a direct diagonalization of the discretized operator $(\mathcal{O}_q)_{n,m}$: we have plotted the three first energies in Fig. 7 (we have also checked that the diagonalization of the discretized operator $(\mathcal{H}_q)_{n,m}$ gives the same result). Interestingly, we see that the two lowest energy levels become exponentially close in the large $k/D^{1/3}$ limit (cf. Fig. 7). The higher excited eigenvalues are well separated.

A more precise method is to study neatly the differential equation (115) : the first node in the solution $\varphi(z)$ appears when $\lambda \leq -\mathcal{E}_1(q)$. This allows to determine the non-analytic contribution to $\mathcal{E}_1(q)$ for relatively large $|E|^{3/2}/D$. Such a precise analysis of $\mathcal{E}_1(1)$ shows that the non-analytic contribution to $\mathcal{E}_1(1)$ is *half* of the correction to $\mathcal{E}_0(1)$:

$$\mathcal{E}_1(1) \simeq -\sqrt{|E|} - \frac{0.04 D}{|E|} e^{-4|E|^{3/2}/(3D)} \quad \text{for } |E|^{3/2} \gg D, \quad (122)$$

compare with Eq. (121). See Fig. 8 : the left plot shows the $1/|E|$ behaviour of the pre-exponential factor and the right plot exhibits the ratio 1/2 in the large $|E|/D^{2/3}$ limit (we attribute the deviation of the last point to some numerical error). In Section 9, it will be shown that such non-analytic contribution to $\mathcal{E}_1(1)$ can indeed be obtained by a judicious extension of the classical WKB analysis. Furthermore, we will demonstrate that the dimensional factor is $1/(8\pi) \simeq 0.04$.

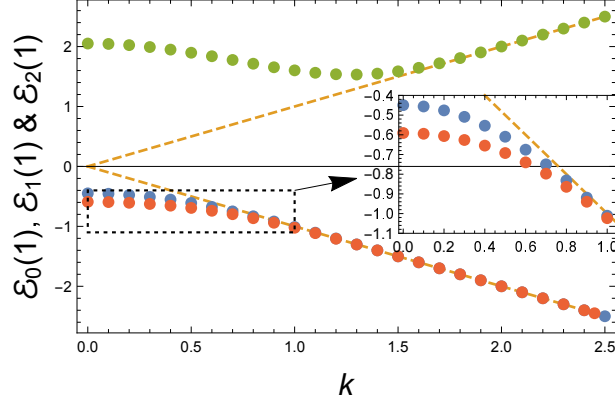


Figure 7: The three first energies obtained by diagonalization for $q = 1$. Straight dashed lines are $\pm k$. We have set $D = 1$.

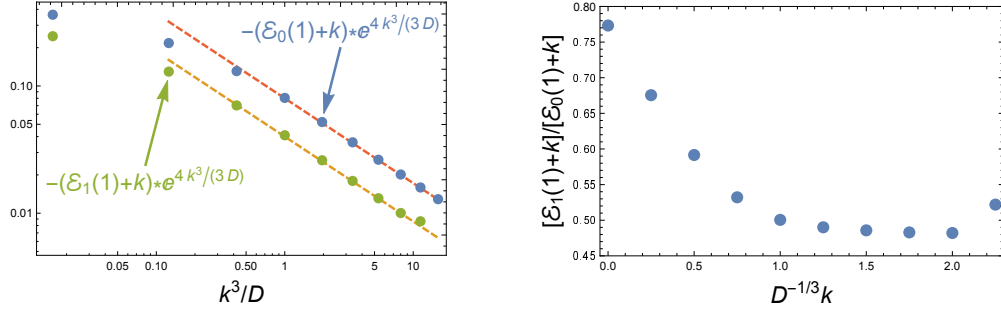


Figure 8: The two non-analytic corrections to $\mathcal{E}_0(1)$ and $\mathcal{E}_1(1)$. The two dashed lines correspond to $0.08D/|E|$ and $0.04D/|E|$ (where $E = -k^2$). Right : ratio of the two corrections.

We have also checked numerically that, not only for $q = 1$ but for arbitrary values of q , the two eigenvalues become exponentially close in the large $|E|/D^{2/3}$ limit. From the analysis of Sections 9, we conclude that the gap is $\mathcal{E}_1(q) - \mathcal{E}_0(q) = \mathcal{O}(e^{-4|E|^{3/2}/(3D)})$ where only the pre-exponential function carries the q -dependence.

We can connect this spectral analysis with the study of equilibria for the elastic line : Fig. 7 shows that only the two lowest energies are positive and lead to exponentially growing contributions in Eq. (109) :

$$\langle \mathcal{N}_{\text{tot}} \rangle \simeq A_0 e^{r L} + A_1 e^{r_1 L} + \mathcal{O}(e^{-c_2 L}) \quad (123)$$

where $r_1 = -\mathcal{E}_1(1) - \sqrt{|E|} < r$ and $c_2 = \mathcal{E}_2(1) + \sqrt{|E|} > 0$. Moreover, in the limit $|E|^{3/2} \gg D$ ($L_m \ll L_c$), Eqs. (121,122) show that $r_1 \simeq r/2$.

9. WKB analysis of $\mathcal{E}_1(q)$

In this section we study the eigenvalue $\mathcal{E}_1(q)$, which controls finite size effect (elastic line of finite length L), Eq. (123), and also provides a lower bound for the rate r . The

calculation confirms the $D \rightarrow 0$ behaviour obtained numerically in the previous section, Eq. (122).

9.1. The double well effective potential

In the previous section, we have shown that the largest eigenvalue of the operator \mathcal{O}_q defined by (104) coincides with the GLE. It is convenient to perform a non-unitary transformation in order to relate \mathcal{O}_q to a Hermitian operator \mathcal{H}_q , which can be interpreted as the quantum Hamiltonian for a particle in a one-dimensional double well potential, as we will see below (cf. details in Appendix D and more precisely Eq. (D.14)). Here, we analyse the ground state energy $\mathcal{E}_1(q)$ of the Hamiltonian \mathcal{H}_q , which coincides with the second eigenvalue of the operator \mathcal{O}_q . We find convenient to rescale the coordinate as $\zeta = |E|^{-1/2} z$ and the energy as $\mathcal{H}_q = |E|^{-1/2} \mathcal{H}_q$, hence we denote $\mathcal{E}_n(q) = |E|^{-1/2} \mathcal{E}_n(q) = L_m \mathcal{E}_n(q)$ ($n \in \mathbb{N}^*$) the spectrum of the new Hamiltonian

$$\mathcal{H}_q = -s \frac{d^2}{d\zeta^2} + V_q(\zeta) \quad (124)$$

where

$$V_q(\zeta) = \frac{1}{4s} (\zeta^2 - 1)^2 - (q+1)\zeta \quad \text{and} \quad s = \frac{D}{|E|^{3/2}} \quad (125)$$

(see Fig. 9). One can show that the eigenvalues of \mathcal{H}_q are $\mathcal{E}_n(q)$ with $n \in \mathbb{N}^*$. Note that the spectra of $-\mathcal{O}_q$ and \mathcal{H}_q coincide apart from the eigenvalue $\mathcal{E}_0(q)$, which is in the spectrum of \mathcal{O}_q but not of \mathcal{H}_q , as discussed in the previous Section. Note that for $q = 0$, the Hamiltonian (124) has the correct expected exact non-normalizable eigenstate at zero energy.

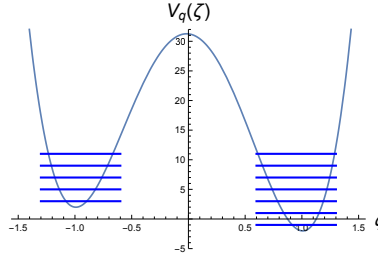


Figure 9: The effective potential for $q = 1$. The two spectra associated with the two harmonic wells are in correspondence for integer q (apart for the $q+1$ lowest levels ; $q+1 = 2$ on the plot).

As we have seen in the article, the results seem to give a strong evidence in favour of very fast, hence non-perturbative vanishing of the $\Lambda(1) = -|E|^{1/2} \mathcal{E}_0(1)$ in this regime. Although $\Lambda(1)$ is given by an eigenvalue which does not belong to the spectrum of \mathcal{H}_q , we still can analyse semiclassically the ground state energy $\mathcal{E}_1(q)$ of the latter Hamiltonian, which provides a lower bound for $\Lambda(q) = -\mathcal{E}_0(q) > -\mathcal{E}_1(q)$ (moreover the numerics has showed that the non-analytic corrections to $\mathcal{E}_0(1)$ and $\mathcal{E}_1(1)$ only differ by a factor 1/2 in the $s \rightarrow 0$ limit ; cf. Section D). The only way the energy $\mathcal{E}_1(q)$ of the ground state (located semiclassically in the right well around $\zeta \approx 1$) can get such a non-perturbative shift is by a tunnelling admixture from the lowest-level eigenstate located semiclassically in the higher (left) potential well.

We now develop an improved WKB procedure in order to analyse the ground state of the Schrödinger equation

$$\mathcal{H}_q \Psi(\zeta) = \mathcal{E} \Psi(\zeta) \quad (126)$$

as $s \rightarrow 0$. The potential $V_q(\zeta)$ has two deep minima around $\zeta = \pm 1$ separated by a big barrier around $\zeta = 0$ (Fig. 9). The potential is well approximated by two quadratic wells near these two points

$$V_q(\zeta) \simeq -q + 1 + \frac{1}{s}(\zeta + 1)^2 \quad \text{for } \zeta \sim -1 \quad (127)$$

$$\simeq -(q + 1) + \frac{1}{s}(\zeta - 1)^2 \quad \text{for } \zeta \sim +1. \quad (128)$$

Before starting the presentation of the WKB method, it is useful to have in mind the correspondence with the standard formulae in quantum mechanics. This is done by identifying $s = \hbar^2/2m$: we can set $\hbar = 1$ and $m = 1/(2s)$. We see that the classical oscillator frequency in each well in our problem is given by $\omega = 2$. The spectra related to the two harmonic wells (127,128) are :

$$\begin{cases} \mathcal{E}_n^R = 2n - q \\ \mathcal{E}_n^L = 2n + 2 + q \end{cases} \quad \text{with } n \in \mathbb{N} \quad (129)$$

which shows that the two spectra are in correspondence for integer q , apart for the $q + 1$ lowest levels (Fig. 9).

9.2. Weakly asymmetric double well ($|q + 1| \ll 1$)

For $q = -1$ the double well potential is symmetric and it is possible to use known results to express the energy of the ground state [86, 87, 88]. The analysis of the bottom of the spectrum can be mapped onto a simple two level problem

$$\begin{pmatrix} \mathcal{E}_0^R & -\Delta/2 \\ -\Delta/2 & \mathcal{E}_0^L \end{pmatrix} \quad (130)$$

For $q = -1$, we have $\mathcal{E}_0^R = \mathcal{E}_0^L$ and the two eigenvalues are $\pm\Delta/2$. Going back to standard notations, the semiclassical calculation of the splitting for the Hamiltonian $H = -[\hbar^2/(2m)]\partial_x^2 + V(x)$, with $V(x) = (1/8)ma^2\omega^2[(x/a)^2 - 1]^2$, is [87] $\Delta = 4\sqrt{3}\hbar\omega \sqrt{S/(2\pi\hbar)} \exp[-S/\hbar]$ where $S = \int_{-a}^a dx \sqrt{2mV(x)}$ (the formula given in § 50 of Ref. [86] must be corrected by a factor $\sqrt{\pi/e}$ [87]), which gives the ground state energy

$$\mathcal{E}_1(-1) \simeq 1 - \frac{\Delta}{2} \simeq 1 - \frac{4}{\sqrt{\pi s}} e^{-2/(3s)}. \quad (131)$$

If q is still close to -1 but slightly deviates such that $|\mathcal{E}_0^L - \mathcal{E}_0^R| = 2|q + 1| \gg \Delta \sim \exp[-2/(3s)]$, we can assume that the coupling is still described by the same formula and use second order perturbation formula [89]. As a consequence the shift of energy levels is now much smaller : whereas it was proportional to the tunnelling amplitude $\sim \exp[-S/\hbar]$ in the degenerate case, it is now proportional to the tunnelling probability $\sim \exp[-2S/\hbar] \sim \exp[-4/(3s)]$:

$$\mathcal{E}_1(q) \simeq \mathcal{E}_0^R - \frac{|\Delta/2|^2}{\mathcal{E}_0^L - \mathcal{E}_0^R} \underset{q \simeq -1}{\simeq} -q - \frac{2}{\pi(q + 1)s} e^{-4/(3s)}. \quad (132)$$

Additionally to the non-analytic contributions (131) and (132), there exist also some analytic contributions due to the anharmonicity of the potential, which are not studied here (such corrections have the same origin as the contribution $-\Lambda_{\text{pert}}(q)$ to $\mathcal{E}_0(q)$ obtained above in § 7.2.1).⁷

9.3. Strongly asymmetric double well ($|q+1| \gtrsim 1$)

In the “strongly” asymmetric potential limit, i.e. for $|q+1| \gtrsim 1$, it is not anymore possible to restrict the problem to a two level problem. We have to develop a different strategy involving two different approximation schemes : in the neighbourhood of each potential well ($\zeta \sim \pm 1$), the potential is replaced by parabolas, which allows to express the exact solution of the approximated Schrödinger equation locally. In between, inside the potential barrier, we write the approximate WKB solution of the (exact) Schrödinger equation and match the three expressions. This strategy is borrowed from Ref. [88].

9.3.1. Step 1: wave function for $\zeta \sim +1$

In the neighbourhood of the right well, the Schrödinger equation (126) takes the form

$$\left[-s \frac{d^2}{d\zeta^2} - q - 1 + \frac{1}{s}(\zeta - 1)^2 \right] \Psi(\zeta) \simeq \mathcal{E} \Psi(\zeta) . \quad (133)$$

It will be convenient to introduce the variable $\xi = (\zeta - 1)/\sqrt{s}$ and parametrize the energy as

$$\mathcal{E} = \mathcal{E}_0^R + 2\epsilon = -q + 2\epsilon ,$$

where ϵ is a small (negative) shift to the ground state energy of the right well. Extracting the Gaussian function $\Psi(\zeta) = y(\xi) \exp[-(1/2)\xi^2]$ we obtain that the function $y(\xi)$ obeys the Hermite equation $y''(\xi) - 2\xi y'(\xi) + 2\epsilon y(\xi) = 0$, whose solution can be expressed in terms of the Hermite function [90] with integral representation (for $\epsilon < 0$)

$$H_\epsilon(\xi) = \frac{1}{\Gamma(-\epsilon)} \int_0^\infty dt t^{-1-\epsilon} e^{-t^2-2\xi t} . \quad (134)$$

This integral representation is suitable to extract the asymptotic behaviour

$$H_\epsilon(\xi) \simeq (2\xi)^\epsilon \quad \text{for } \xi \rightarrow +\infty \quad (135)$$

and, splitting the integral in (134) as $\int_0^\infty = \int_{-\infty}^{+\infty} - \int_{-\infty}^0$:

$$H_\epsilon(\xi) \simeq -(-2\xi)^\epsilon + \frac{\sqrt{\pi}}{\Gamma(-\epsilon)} (-\xi)^{-\epsilon-1} e^{+\xi^2} \quad \text{for } \xi \rightarrow -\infty . \quad (136)$$

This shows that the solution of (133),

$$\Psi(\zeta) \simeq C_R H_\epsilon \left(\frac{\zeta - 1}{\sqrt{s}} \right) e^{-(\zeta-1)^2/(2s)} , \quad (137)$$

7. We have also been able to obtain the $\mathcal{O}(s)$ correction to \mathcal{E}_0^R by a perturbative treatment of the non-anharmonic terms describing the deviation from the quadratic potential at $\zeta = +1$ in the Hamiltonian \mathcal{H}_q .

decays exponentially for $\xi = (\zeta - 1)/\sqrt{s} \rightarrow +\infty$ and grows exponentially for $\xi = (\zeta - 1)/\sqrt{s} \rightarrow -\infty$. Keeping the variable ξ , we write :

$$\Psi(\zeta) \simeq C_R \times \begin{cases} -(-2\xi)^\epsilon e^{-\xi^2/2} + \frac{\sqrt{\pi}}{\Gamma(-\epsilon)} (-\xi)^{-\epsilon-1} e^{+\xi^2/2} & \text{as } \xi \rightarrow -\infty \\ (2\xi)^\epsilon e^{-\xi^2/2} & \text{as } \xi \rightarrow +\infty \end{cases} \quad (138)$$

9.3.2. Step 2: wave function for $\zeta \sim -1$

In the neighbourhood of the left harmonic well, the Schrödinger equation (126) takes the form

$$\left[-s \frac{d^2}{d\zeta^2} + q + 1 + \frac{1}{s}(\zeta + 1)^2 \right] \Psi(\zeta) \simeq \mathcal{E} \Psi(\zeta). \quad (139)$$

It is now convenient to write the energy as $\mathcal{E} = \mathcal{E}_0^L + 2\tilde{\epsilon} = q + 2 + 2\tilde{\epsilon}$ so that $\tilde{\epsilon} = -(q + 1) + \epsilon \simeq -(q + 1)$, as we expect that ϵ is exponentially small. We choose the solution

$$\Psi(\zeta) \simeq C_L H_{\tilde{\epsilon}} \left(-\frac{\zeta + 1}{\sqrt{s}} \right) e^{-(\zeta+1)^2/(2s)}, \quad (140)$$

which now decays in the negative direction and grows in the positive direction :

$$\Psi(\zeta) \simeq C_L \times \begin{cases} (-2\xi)^{\tilde{\epsilon}} e^{-\xi^2/2} & \text{as } \xi \rightarrow -\infty \\ -(-2\xi)^{\tilde{\epsilon}} e^{-\xi^2/2} + \frac{\sqrt{\pi}}{\Gamma(-\tilde{\epsilon})} \xi^{-\tilde{\epsilon}-1} e^{+\xi^2/2} & \text{as } \xi \rightarrow +\infty \end{cases} \quad (141)$$

where now $\xi = (\zeta + 1)/\sqrt{s}$.

9.3.3. Step 3: WKB solution inside the barrier

Inside the potential barrier, the solution of (126) is well approximated by the WKB wave function

$$\Psi(\zeta) \simeq \Psi^{\text{WKB}}(\zeta) = \left(\frac{\sqrt{s(2q+1)}}{2s p(\zeta)} \right)^{1/2} \left[A e^{\int_{-1}^{\zeta} d\zeta' p(\zeta')} + B e^{-\int_{-1}^{\zeta} d\zeta' p(\zeta')} \right] \quad (142)$$

where

$$p(\zeta) = \sqrt{\frac{1}{s}(V_q(\zeta) - \mathcal{E})}. \quad (143)$$

The validity of the WKB expression (142) extends to the domain at the left of the turning point ζ_0 where $\mathcal{E} = V_q(\zeta_0)$. Using the approximate form (128) we find $\zeta_0 = 1 - \sqrt{s}[1 + \epsilon + \mathcal{O}(\epsilon^2)]$. We expect that ϵ is exponentially small $\sim e^{-4/(3s)}$, as is indeed confirmed below, thus

$$\zeta_0 = 1 - \sqrt{s} + \mathcal{O}(e^{-4/(3s)}). \quad (144)$$

9.3.4. Step 4: matching

In order to match the WKB solution (142) with (137) and (140), it is convenient to introduce a specific notation for the action : we define

$$\Phi_L(\zeta) = \int_{-1}^{\zeta} p(\zeta') d\zeta' \quad \text{and} \quad \Phi_R(\zeta) = \int_{\zeta}^{\zeta_0} p(\zeta') d\zeta'. \quad (145)$$

The total action associated to the trajectory going from $\zeta = -1$ to the turning point is denoted

$$S_q = \int_{-1}^{\zeta_0} p(\zeta') d\zeta' \quad (146)$$

thus $S_q = \Phi_L(\zeta) + \Phi_R(\zeta)$, obviously.

Matching of (137) with (142) —. In the vicinity of the right harmonic well at $\zeta = +1$, the asymptotic form (138) for $\xi \rightarrow -\infty$ should match with the WKB solution (142), which provides a first constraint on the two coefficients A and B . We must therefore consider ζ sufficiently far from the turning point, i.e. $(\zeta_0 - \zeta) \gg \sqrt{s}$, so that the asymptotic behaviour (138) holds. ζ must however be sufficiently close to the turning point so that the parabolic approximation (for the potential) is still justified. This last observation allows us to simplify the action $\Phi_R(\zeta)$: the parameter $t_* = (1 - \zeta)/(1 - \zeta_0) \gg 1$ will be treated as a large parameter. Using $V_q(\zeta_0) = \mathcal{E}$ we have $p(\zeta) = (1/s)\sqrt{(1 - \zeta)^2 - (1 - \zeta_0)^2}$. Introducing the variable $t = (1 - \zeta)/(1 - \zeta_0)$ we find in this approximation:

$$\begin{aligned} \Phi_R(\zeta) &= \frac{1}{s} \int_{\zeta}^{\zeta_0} \sqrt{(\zeta' - 1)^2 - (\zeta_0 - 1)^2} d\zeta' \\ &= \frac{(1 - \zeta_0)^2}{s} \int_1^{t_*} \sqrt{t^2 - 1} dt = \frac{(1 - \zeta_0)^2}{s} \frac{1}{2} \left(t_* \sqrt{t_*^2 - 1} - \operatorname{arccosh}(t_*) \right) \end{aligned} \quad (147)$$

and finally using $t_* \sqrt{t_*^2 - 1} \approx t_*^2 - 1/2$ and $\operatorname{arccosh}(t_*) \approx \ln(2t_*)$, we get

$$\Phi_R(\zeta) \simeq \frac{(1 - \zeta_0)^2}{2s} \left[t_*^2 - \ln(2t_*) - \frac{1}{2} \right].$$

We now find convenient to express $\Phi_R(\zeta)$ in terms of the variable $\xi = (\zeta - 1)/\sqrt{s} = -[(1 - \zeta_0)/\sqrt{s}] t_*$ introduced above :

$$\Phi_R(\zeta) \simeq \frac{1}{2} \xi^2 - \frac{1 + 2\epsilon}{2} \ln \left(\frac{-2\xi}{\sqrt{1 + 2\epsilon}} \right) - \frac{1 + 2\epsilon}{4} \quad (148)$$

from which we write the WKB wave function as

$$\begin{aligned} \Psi^{\text{WKB}}(\zeta) &\simeq A (2q + 1)^{1/4} e^{S_q + 1/4} (-2\xi)^\epsilon e^{-\xi^2/2} \\ &\quad + B (2q + 1)^{1/4} e^{-S_q - 1/4} (-2\xi)^{-1-\epsilon} e^{+\xi^2/2}, \end{aligned} \quad (149)$$

where we made use that $\epsilon \ll 1$. Matching with (138) for $\xi \rightarrow -\infty$ gives

$$A = -e^{-S_q - 1/4} C_R \quad (150)$$

$$B = -2\epsilon\sqrt{\pi} e^{S_q + 1/4} C_R \quad (151)$$

where we have used $\Gamma(-\epsilon) \simeq -1/\epsilon$. We get the first condition

$$\frac{A}{B} = \frac{e^{-1/2}}{2\epsilon\sqrt{\pi}} e^{-2S_q}. \quad (152)$$

Matching of (140) with (142) —. We proceed the same way in the neighbourhood of the left harmonic well and match the asymptotic behaviour (141) for $\xi \rightarrow +\infty$ with the WKB approximation (142). In the region where the two expressions of the wave function match, we can use the parabolic approximation for the potential :

$$\Phi_L(\zeta) = \frac{1}{s} \int_{-1}^{\zeta} \sqrt{(2q+1)s + (\zeta' + 1)^2} d\zeta' \quad (153)$$

(we recall that we can neglect ϵ there). Introducing the variable $t = (\zeta' + 1)/\sqrt{s(2q+1)}$, this rewrites

$$\Phi_L(\zeta) = (2q+1) \int_0^{t_*} \sqrt{1+t^2} dt = (2q+1) \frac{1}{2} \left(t_* \sqrt{1+t_*^2} + \operatorname{arcsinh}(t_*) \right) \quad (154)$$

(142) and (141) match in the regime where $t_* = (\zeta + 1)/\sqrt{s(2q+1)} \gg 1$, thus, using $t_* \sqrt{1+t_*^2} \approx t_*^2 + 1/2$ and $\operatorname{arcsinh}(t_*) \approx \ln(2t_*)$, we find

$$\Phi_L(\zeta) \simeq \left(q + \frac{1}{2} \right) \left(t_*^2 + \ln(2t_*) + \frac{1}{2} \right). \quad (155)$$

At this stage it is convenient to use the variable $\xi = (\zeta + 1)/\sqrt{s} = \sqrt{(2q+1)} t_*$ introduced above :

$$\Psi^{\text{WKB}}(\zeta) \simeq A e^{(2q+1)/4} \left(\frac{2\xi}{\sqrt{(2q+1)}} \right)^q e^{+\xi^2/2} + B e^{-(2q+1)/4} \left(\frac{2\xi}{\sqrt{(2q+1)}} \right)^{-q-1} e^{-\xi^2/2} \quad (156)$$

which matches with (141) for $\xi \rightarrow +\infty$ (we recall that $\tilde{\epsilon} \simeq -q-1$) if

$$A = \frac{2^{-q} \sqrt{\pi}}{\Gamma(q+1)} (2q+1)^{q/2} e^{-(2q+1)/4} C_L \quad (157)$$

$$B = -(2q+1)^{-(q+1)/2} e^{(2q+1)/4} C_L \quad (158)$$

We deduce the second condition

$$\frac{A}{B} = -\frac{2^{-q} \sqrt{\pi}}{\Gamma(q+1)} (2q+1)^{q+1/2} e^{-(2q+1)/2}. \quad (159)$$

It is worth emphasizing the result $A \sim B$, obtained from the improved WKB method developed here. The naive (standard) WKB method would have given $B|_{\text{naive WKB}} = 0$, since the only term of (142) which is vanishing as $\zeta \rightarrow -\infty$, in the classically forbidden region, is the term with coefficient A .

9.3.5. Ground state energy

Comparing (152) and (159) finally provides the expression of the shift of the ground state energy

$$\epsilon \simeq -\frac{\Gamma(q+1) e^q}{2\pi\sqrt{2}(q+1/2)^{q+1/2}} e^{-2S_q} \quad (160)$$

Making use of (144), we can write the action (146) as

$$S_q = \frac{1}{2s} \int_{-1}^{1-\sqrt{s}} d\zeta \sqrt{(1-\zeta^2)^2 - 4s(q+1)\zeta + 4sq(1-\sqrt{s}) - s^2}. \quad (161)$$

In Appendix F, we show that it presents the limiting behaviour

$$S_q \underset{s \rightarrow 0}{\simeq} \frac{2}{3s} - \frac{q}{2} \ln s + c_q + \mathcal{O}(s^{1/2} \ln s), \quad (162)$$

where

$$2c_q = q + 4q \ln 2 - \left(q + \frac{1}{2}\right) \ln(2q+1). \quad (163)$$

We conclude that the ground state energy of the Schrödinger operator \mathcal{H}_q is given by

$$\mathcal{E}_1(q) = -q + 2\epsilon \simeq -q - \frac{\Gamma(q+1) e^{-2c_q+q}}{\pi\sqrt{2}(q+1/2)^{q+1/2}} s^q e^{-4/(3s)} \quad (164)$$

which presents a different pre-exponential dependence, compared to (132) obtained for weakly asymmetric double-well. Going back to the initial notation

$$\mathcal{E}_1(q) \simeq -q\sqrt{|E|} - \frac{\Gamma(q+1) D^q}{2^{3q}\pi |E|^{(3q-1)/2}} e^{-4|E|^{3/2}/(3D)}. \quad (165)$$

It is however important to remember that (164,165) are *not* the full result, but only the *non-analytic* contribution to the ground state energy (which is not expected to be the dominant correction). As discussed at length in the main text and in Section 8, the ground state energy is also shifted by analytic contributions (in s) related to the non-harmonicity of the potential. As explained above, the analytic terms are also given by (98) :

$$\mathcal{E}_1(q) \simeq -\Lambda_{\text{pert}}(q) + \mathcal{O}(e^{-4|E|^{3/2}/(3D)}). \quad (166)$$

For $q = 1$, we have demonstrated that the first analytic contributions vanish (up to $\mathcal{O}(s^2)$) and observed numerically that this is true at all orders in s . Hence the final result for $q = 1$ is expected to be

$$\mathcal{E}_1(1) + \sqrt{|E|} \simeq -\frac{D}{8\pi|E|} e^{-4|E|^{3/2}/(3D)}. \quad (167)$$

Note that not only the power law of the pre-exponential term perfectly agrees with the numerical result, cf. Eq. (122), but moreover the dimensionless factor $1/(8\pi) \simeq 0.0397887$ coincides with the value extracted numerically in Subsection 8.3.

10. The generalized Lyapunov exponent for even integer argument

A central quantity of the paper is the generalized Lyapunov exponent $\Lambda(q)$ for a particular value of its argument, $q = 1$. In this section, we show that when its argument is an even integer, $q = 2n$ with $n \in \mathbb{N}^*$, the analysis can be greatly simplified. The main idea is to consider $\langle y(\tau)^q \rangle$ instead of $\langle |y(\tau)|^q \rangle$, which obviously coincide for $q = 2n$.

The method presented in this section is based on the observation that the correlation functions of the form $\langle y(\tau)^n y'(\tau)^m \rangle$ with $n+m > 0$ can be analysed through a closed set of $n+m+1$ coupled linear stochastic differential equations. In relation with the functional determinants of stochastic operators, this means that, in the present Section, we consider $\langle y(L)^q \rangle = \langle \det(-E - \partial_\tau^2 + U(\tau))^q \rangle$ instead of $\langle |y(L)|^q \rangle = \langle |\det(-E - \partial_\tau^2 + U(\tau))|^q \rangle$.

To be concrete we introduce

$$\widehat{\Lambda}(q) := \lim_{L \rightarrow \infty} \frac{1}{L} \ln \langle y(L)^q \rangle \quad (168)$$

with $q \in \mathbb{N}^*$, to be compared with (75). The case $q = 1$ already emphasizes the difference between $\Lambda(q)$ and $\widehat{\Lambda}(q)$: by using the technique exposed below, it is rather easy to verify that $\langle y(L) \rangle = \sinh(\sqrt{-E}L)/\sqrt{-E}$ is independent of the presence of the disorder. Note that a simple explanation of the fact that $\langle y(L) \rangle = \langle \det(-E - \partial_\tau^2 + U(\tau)) \rangle = \det(-E - \partial_\tau^2)$ is independent of the disorder was given above for the discrete model, cf. Eq. (24). We deduce

$$\widehat{\Lambda}(1) = \sqrt{-E} \quad \text{for } E < 0, \quad (169)$$

whereas $\Lambda(1) = \sqrt{-E} + \mathcal{O}(e^{-4|E|^{3/2}/(3D)})$, Eq. (121). For $E = 0$, the difference is more striking since $\widehat{\Lambda}(1) = 0$ whereas the GLE is finite $\Lambda(1) \simeq 0.58 D^{1/3}$. The non-analytic part in $\Lambda(1)$ is therefore related to the presence of the absolute value in the average $\langle |y(\tau)| \rangle$.

10.1. Warming up : exact calculation of $\Lambda(2) = \widehat{\Lambda}(2)$

We recall that the starting point is the Schrödinger equation

$$-y''(\tau) + U(\tau)y(\tau) = E y(\tau). \quad (170)$$

Let us start from the simplest non trivial case $q = 2$ which requires to analyse $\langle y(\tau)^2 \rangle$. Differentiating y^2 leads to consider the set of three coupled SDEs

$$\begin{cases} \frac{d}{d\tau} y(\tau)^2 &= 2y(\tau) y'(\tau) \\ \frac{d}{d\tau} y(\tau) y'(\tau) &= (U(\tau) - E) y(\tau)^2 + y'(\tau)^2 \\ \frac{d}{d\tau} y'(\tau)^2 &= 2(U(\tau) - E) y(\tau) y'(\tau) \end{cases} \quad (\text{Stratonovich}) \quad (171)$$

which are interpreted in the Stratonovich convention, as usual in physics when Gaussian white noises arise in order to model regular physical noises [91]. The SDEs can be rewritten in the Itô convention as

$$\begin{cases} \frac{d}{d\tau} y(\tau)^2 &= 2y(\tau) y'(\tau) \\ \frac{d}{d\tau} y(\tau) y'(\tau) &= (U(\tau) - E) y(\tau)^2 + y'(\tau)^2 \\ \frac{d}{d\tau} y'(\tau)^2 &= 2(U(\tau) - E) y(\tau) y'(\tau) + 2D y(\tau)^2 \end{cases} \quad (\text{Itô}) \quad (172)$$

leading to

$$\frac{d}{d\tau} \begin{pmatrix} \langle y^2 \rangle \\ \langle y y' \rangle \\ \langle y'^2 \rangle \end{pmatrix} = \begin{pmatrix} 0 & 2 & 0 \\ -E & 0 & 1 \\ 2D & -2E & 0 \end{pmatrix} \begin{pmatrix} \langle y^2 \rangle \\ \langle y y' \rangle \\ \langle y'^2 \rangle \end{pmatrix} =: M_2 \begin{pmatrix} \langle y^2 \rangle \\ \langle y y' \rangle \\ \langle y'^2 \rangle \end{pmatrix} \quad (173)$$

The largest eigenvalue of the matrix M_2 controls the exponential growth of $\langle y(\tau)^2 \rangle$ and therefore coincides with $\hat{\Lambda}(2) = \Lambda(2)$. The characteristic polynomial is $P_2(\lambda) = \det(M_2 - \lambda \mathbf{1}_3) = -\lambda^3 - 4E\lambda + 4D$, whose appropriate root is (for $E = -k^2 < 0$)

$$\Lambda(2) = k \left[\left(2s + 2\sqrt{s^2 - 16/27} \right)^{1/3} + \frac{4/3}{\left(2s + 2\sqrt{s^2 - 16/27} \right)^{1/3}} \right] \text{ with } s = \frac{D}{k^3}, \quad (174)$$

$$= D^{1/3} \left[\left(2 + 2\sqrt{1 + 16E^3/(27D^2)} \right)^{1/3} - \frac{4E/(3D^{2/3})}{\left(2 + 2\sqrt{1 + 16E^3/(27D^2)} \right)^{1/3}} \right] \quad (175)$$

We thus have recovered a result of [92]. For $D = 0$ we have $\Lambda(2) = 2k$ as it should, and for $E = 0$, one gets $\Lambda(2) = (4D)^{1/3}$. One can also check that the $s \rightarrow 0$ expansion coincides with (98) for $q = 2$, which corresponds to the limit $E \rightarrow -\infty$. For large positive energy $E \gg D^{2/3}$, we have $\Lambda(q) \simeq (q + q^2/2) \gamma_1 \simeq (q + q^2/2) D/(4E)$ (cf. Section 7.1) : we can check that the expansion of (175) for $E \rightarrow +\infty$ gives $\Lambda(2) \simeq D/E$, as it should. The GLE is plotted in Fig. 10 for $q = 1$ and $q = 2$: in order to match the asymptotic behaviours, $\Lambda(q) \simeq q\sqrt{-E}$ for $E \rightarrow -\infty$, we choose to plot $\Lambda(q)/q$.

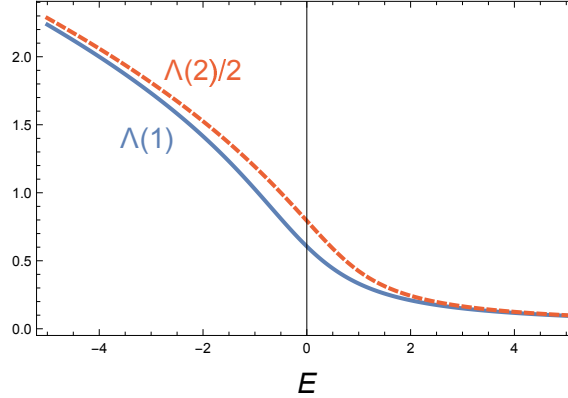


Figure 10: Comparison between $\Lambda(1)$, obtained numerically (Subsection 8.1), and $\Lambda(2)/2$, given by Eq. (175) ; we set $D = 1$.

10.2. Analysis of $\hat{\Lambda}(q)$ with $q \in \mathbb{N}^*$

We can generalise the above calculation to the case $q \in \mathbb{N}^*$. Clearly, this leads to consider a linear system with $q + 1$ equations, controlled by a $(q + 1) \times (q + 1)$ matrix M_q , given below, whose largest eigenvalue coincides with $\hat{\Lambda}(q)$. When $q = 2n$ is an **even** integer, we have furthermore $\Lambda(2n) = \hat{\Lambda}(2n)$. Because the eigenvalue $\hat{\Lambda}(q)$ is the root of a polynomial of degree $q + 1$, it is necessarily analytic in the disorder parameter D , which appears in the coefficients of the matrix. Hence, throughout the paper, we have made the two remarkable observations :

- for $q = 1$, the analytic part of $\Lambda(q) - kq$ vanishes and $\Lambda(1)$ is a purely non-analytic function of $s = D/|E|^{3/2}$ (Section 8).

- For $q = 2n$, the non-analytic contributions to $\Lambda(q)$ vanish and the GLE is analytic in $s = D/|E|^{3/2}$.

In particular, this shows that the replica trick must be used with caution as it is not possible to deduce $\langle |y(\tau)|^q \rangle$ for arbitrary real q from $\langle y(\tau)^{2n} \rangle$.

10.2.1. Linear system of SDEs

Let us now discuss systematically the calculation of $\Lambda(2n)$. For $q = 2n$, one has to consider the $q + 1$ equations

$$\begin{aligned} \frac{d}{d\tau} y(\tau)^{q-m} y'(\tau)^m &= m(U(\tau) - E) y(\tau)^{q-m+1} y'(\tau)^{m-1} \\ &+ (q-m) y(\tau)^{q-m-1} y'(\tau)^{m+1} \quad (\text{Stratonovich}) \end{aligned} \quad (176)$$

for $m = 0, 1, \dots, q$. The stochastic differential equation can be rewritten in the Itô convention :

$$\begin{aligned} \frac{d}{d\tau} y(\tau)^{q-m} y'(\tau)^m &= m(U(\tau) - E) y(\tau)^{q-m+1} y'(\tau)^{m-1} \\ &+ (q-m) y(\tau)^{q-m-1} y'(\tau)^{m+1} + m(m-1) D y(\tau)^{q-m+2} y'(\tau)^{m-2} \quad (\text{Itô}) \end{aligned} \quad (177)$$

This leads to consider the linear system

$$\frac{d}{d\tau} \begin{pmatrix} \langle y^q \rangle \\ \langle y^{q-1} y' \rangle \\ \langle y^{q-2} y'^2 \rangle \\ \vdots \\ \langle y'^q \rangle \end{pmatrix} = M_q \begin{pmatrix} \langle y^q \rangle \\ \langle y^{q-1} y' \rangle \\ \langle y^{q-2} y'^2 \rangle \\ \vdots \\ \langle y'^q \rangle \end{pmatrix} \quad (178)$$

where the $(q+1) \times (q+1)$ matrix is

$$M_q = \begin{pmatrix} 0 & q & 0 & 0 & 0 & \dots & 0 \\ -E & 0 & q-1 & 0 & 0 & \dots & 0 \\ 2D & -2E & 0 & q-2 & 0 & \dots & 0 \\ 0 & 6D & -3E & 0 & \ddots & \dots & \vdots \\ 0 & 0 & 12D & -4E & \ddots & & \\ \vdots & \vdots & \ddots & \ddots & \ddots & \ddots & \\ 0 & 0 & \dots & & & 0 & 1 \\ 0 & 0 & \dots & & q(q-1)D & -qE & 0 \end{pmatrix}. \quad (179)$$

The idea that the case of integer q leads to consider a closed system of equations for correlators of y and y' has been used earlier [93, 78, 92] (the matrix M_q was obtained in Refs. [78, 92]).

10.2.2. Perturbative analysis ($D/k^3 \ll 1$)

As a check, let us recover the perturbative result (98). For $E = -k^2$ and in the absence of disorder, the matrix M_q has the spectrum

$$\text{Spec}(M_q) = \{-qk, (-q+2)k, \dots, -2k, 0, 2k, \dots, +qk\} \quad \text{for } D = 0.$$

The largest eigenvalue $\hat{\Lambda}(q) = +qk$ is associated with the right and left eigenvectors

$$R = 2^{-q} \begin{pmatrix} k^{-q} \\ k^{-q+1} \\ \vdots \\ k^{-1} \\ 1 \end{pmatrix} \quad \text{and} \quad L = \begin{pmatrix} C_q^0 k^q \\ C_q^1 k^{q-1} \\ \vdots \\ C_q^{q-1} k \\ C_q^q \end{pmatrix} \quad (180)$$

with obviously $L^T \cdot R = 1$. Perturbation theory allows to get the $\mathcal{O}(D)$ correction to the eigenvalue : we write the perturbation to $M_q^{(0)} = M_q|_{D=0}$ as $W_{n,m} = \delta_{n,m+2} (n-1)(n-2) D$. Then

$$\begin{aligned} \hat{\Lambda}(q) &= qk + L^T \cdot W \cdot R + \mathcal{O}(D^2) \\ &= qk + \frac{D}{k^2} 2^{-q} \sum_{n=2}^q n(n-1) C_q^n + \mathcal{O}(D^2) = qk + \frac{D}{4k^2} q(q-1) + \mathcal{O}(D^2). \end{aligned} \quad (181)$$

The result is in perfect agreement with (98). We emphasize that only for even integer $q = 2n$ does the systematic perturbative expansion provide the exact result, without any additional non-analytic contribution in D/k^3 : according to the notation of Section 7 we can write

$$\Lambda(2n) = \hat{\Lambda}(2n) = \Lambda_{\text{pert}}(2n). \quad (182)$$

10.2.3. Zero energy $E = -k^2 = 0$

The determination of $\hat{\Lambda}(q)$ reduces to analyse the largest eigenvalue of a $(q+1) \times (q+1)$ matrix M_q , which is easy to implement. For $E = 0$, we can find the analytic expression of $\hat{\Lambda}(q)$ up to $q = 6$ (see Table 1).

q	$\hat{\Lambda}(q)$ for $E = 0$		
1	0		
2	$(4D)^{1/3}$	$= \Lambda(2)$	
3	$(24D)^{1/3}$		
4	$(84D)^{1/3}$	$= \Lambda(4)$	
5	$(112 + 24\sqrt{19})^{1/3} D^{1/3}$		
6	$(252 + 24\sqrt{79})^{1/3} D^{1/3}$	$= \Lambda(6)$	
\vdots	\vdots	\vdots	\vdots
$\gg 1$	$\simeq (3/4) q^{4/3} D^{1/3}$	$\simeq \Lambda(q)$	

Table 1: Generalized Lyapunov exponent $\Lambda(q)$ for even integer argument.

This simple method also allows us to study the large q behaviour. We obtain numerically (Fig. 11)

$$\Lambda(q) \simeq \frac{3}{4} q^{4/3} D^{1/3} - c_{\text{even}} (2q D)^{1/3} \quad (183)$$

with $c_{\text{even}} \simeq 0.18$ (cf. Fig. 11). Although this behaviour was obtained here for even integer arguments, we expect a smooth dependence as a function of q (as it was observed for large negative energy, Fig. 4). This is supported by comparing $\mathcal{E}_0(q) = -\Lambda(q)$ with the ground state energy $\mathcal{E}_1(q)$ of the Hamiltonian (D.14) (or (124), up to a rescaling), which provides a lower bound for the GLE. A simple harmonic approximation around the minimum of the double well potential, at $z \simeq (Dq)^{1/3}$, gives

$$\mathcal{E}_1(q) \simeq -\frac{3}{4} q^{4/3} D^{1/3} + c_{\mathcal{H}} (2qD)^{1/3} \quad (184)$$

with $c_{\mathcal{H}} = 2^{-4/3} \sqrt{6} \simeq 0.97$. As was expected, only the subleading terms of the two eigenvalues differ. We have $c_{\mathcal{H}} > c_{\text{even}}$ as it should, since $\mathcal{E}_1(q) > \mathcal{E}_0(q) = -\Lambda(q)$.

Finally, we note that the main behaviour $\Lambda(q) \sim D^{1/3} q^{4/3}$ was obtained for integer q in the conference's proceedings [82]. It is also in agreement with the numerical calculations of $L(q) = \Lambda(q)/q \sim q^{\alpha-1}$ of Zillmer & Pikovsky [92], who obtained the exponents $\alpha \simeq 1.28$ and $\alpha \simeq 1.38$ for two different values of the energy.

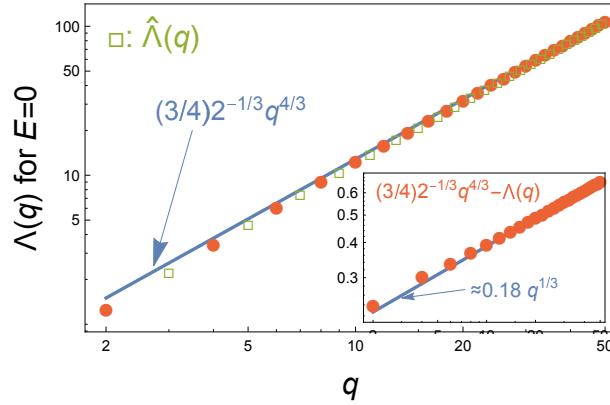


Figure 11: Generalized Lyapunov exponent $\Lambda(q)$ for integer $q = 2n$ (red dots) obtained numerically by finding the largest eigenvalue of the matrix M_q (squares correspond to even integers). Green squares correspond to $\hat{\Lambda}(q)$ for positive odd integers. Line is the asymptotic behaviour $\sim q^{4/3}$ given in the text. Inset : Subleading term (straight line is $0.18 q^{1/3}$). We set $2D = 1$.

10.3. Large deviations for the wave function amplitude

As it is clear from its definition (75), the generalized Lyapunov exponent is the generating function of the cumulants of the logarithm of the wave function $\ln |y(x)|$ [more precisely, $y(x)$ is the solution of the Cauchy initial value problem (71,70)]. As such, the GLE can be related to the large deviation function $\Phi(u)$ controlling the distribution

$$\mathcal{Q}_L(\Upsilon) = \langle \delta(\Upsilon - \ln |y(L)|) \rangle \underset{L \rightarrow \infty}{\sim} \exp \{ -L \Phi(\Upsilon/L) \} . \quad (185)$$

$\Lambda(q)$ and $\Phi(u)$ are related by a Legendre transform

$$\Phi(u) = q_* u - \Lambda(q_*) \quad \text{where } u = \Lambda'(q_*) . \quad (186)$$

We can therefore relate the behaviour (183) for $q \rightarrow +\infty$ to the asymptotic behaviour of the large deviation function

$$\Phi(u) \simeq \frac{1}{4D} u^4 \quad \text{for } u \rightarrow +\infty \quad (187)$$

characterizing the tail of the distribution of $\ln |y(L)|$, i.e. for $|y(L)| \rightarrow \infty$ (the tail for $\ln |y(L)| \rightarrow -\infty$, i.e. $|y(L)| \rightarrow 0$, should be related to $\Lambda(q)$ for $q \rightarrow -\infty$, which we have not studied). To conclude, we comment on the scaling of the fluctuations with the length L . The typical fluctuations, encoded in the variance of $\ln |y(L)|$, display the standard behaviour $[\ln |y(L)| - \gamma_1 L]_{\text{typ}} \sim (\gamma_2 L)^{1/2} \sim (D^{1/3} L)^{1/2}$, characteristic of the central limit theorem (which can be applied to $\ln |y(L)| = \int_0^L dt z(t)$ because $z(t)$ decorrelates over a finite length scale). On the other hand, the behaviour (187) shows that some rare events are responsible for atypically large fluctuations characterized by a different scaling $[\ln |y(L)|]_{\text{atyp}} \sim (D^{1/3} L)^{3/4}$.

11. Mean number of equilibria at fixed value of the energy and annealed distribution of the energy of the line over the set of equilibria

11.1. Definitions and determinant formulae for Laplace transforms

Here we show how our method can be extended to study the mean number of equilibria at fixed values of the energy, defined, for our discrete model of an elastic line, as

$$\langle \mathcal{N}_{\text{tot}}(H) \rangle = \int_{\mathbb{R}^K} d\mathbf{u} \left\langle \delta(H - \mathcal{H}(\mathbf{u})) |\det(\partial_i \partial_j \mathcal{H})| \prod_{i=1}^K \delta(\partial_i \mathcal{H}) \right\rangle \quad (188)$$

It is in fact convenient to split the total energy (5) into an elastic part and a disorder part as follows

$$\mathcal{H}(\mathbf{u}) = \mathcal{H}_{\text{ela}}(\mathbf{u}) + \mathcal{H}_{\text{dis}}(\mathbf{u}) \quad \text{with} \quad \begin{cases} \mathcal{H}_{\text{ela}}(\mathbf{u}) = \frac{1}{2} \mathbf{u}^T (-\kappa \Delta + m^2) \mathbf{u} \\ \mathcal{H}_{\text{dis}}(\mathbf{u}) = \sum_{i=1}^K V_i(u_i) \end{cases} \quad (189)$$

(Δ is here the discrete Laplacian) and define the mean number of equilibria at fixed elastic energy H_e and disorder energy H_d as

$$\langle \mathcal{N}_{\text{tot}}(H_e, H_d) \rangle = \int_{\mathbb{R}^K} d\mathbf{u} \left\langle \delta(H_e - \mathcal{H}_{\text{ela}}(\mathbf{u})) \delta(H_d - \mathcal{H}_{\text{dis}}(\mathbf{u})) |\det(\partial_i \partial_j \mathcal{H})| \prod_{i=1}^K \delta(\partial_i \mathcal{H}) \right\rangle \quad (190)$$

The easiest observable to study is the Laplace transform

$$\tilde{N}(s_e, s_d) = \int_0^{+\infty} dH_e \int_{-\infty}^{+\infty} dH_d e^{-s_e H_e - s_d H_d} \langle \mathcal{N}_{\text{tot}}(H_e, H_d) \rangle \quad (191)$$

from which we can deduce (188) from

$$\tilde{N}(s, s) = \int_{-\infty}^{+\infty} dH e^{-sH} \langle \mathcal{N}_{\text{tot}}(H) \rangle \quad (192)$$

using that the total energy is $H = H_e + H_d$. Note that the elastic energy is always positive, while the disorder part can be of either sign (hence the s_d dependence really involves a double-sided Laplace transform).

We now use that $V_i(u_i)$ and $V_i''(u_i)$ are correlated Gaussian variables, described by the covariance matrix

$$\begin{pmatrix} R(0) & R''(0) \\ R''(0) & R''''(0) \end{pmatrix}. \quad (193)$$

and independent from $V_i'(u_i)$. We also use, for each monomer, the following property of Gaussian variables (the "complete the square" trick)

$$\left\langle e^{-s_d V_i(u_i)} F(V_i''(u_i)) \right\rangle = e^{\frac{1}{2} R(0) s_d^2} \langle F(V_i''(u_i) - s_d R''(0)) \rangle, \quad (194)$$

for any function $F(x)$, where the second average runs over the marginal distribution of $V_i''(u_i)$. Equivalently one can write for any constant V

$$\langle \delta(V_i(u_i) - V) F(V_i''(u_i)) \rangle = \langle F(V_i''(u_i) - R''(0)\chi) \rangle \quad (195)$$

where χ is a Gaussian random variable of variance $R(0)$ and of mean $V/R(0)$, independent of $V''(u_i)$. So imposing the value of $V_i(u_i)$ amounts to shift the random potential by an independent Gaussian random variable. This leads to the following decoupling

$$\langle \mathcal{N}_{\text{tot}}(H_e, H_d) \rangle = J(m^2, H_e) G(m^2, H_d) \quad , \quad \tilde{N}(s_e, s_d) = \tilde{J}(m^2, s_e) \tilde{G}(m^2, s_d) \quad (196)$$

with

$$\tilde{J}(m^2, s_e) = \int \frac{d\mathbf{u}}{(2\pi |R''(0)|)^{K/2}} \exp \left\{ -\frac{[(m^2 \mathbf{1}_K - \kappa \Delta) \mathbf{u}]^2}{2 |R''(0)|} - \frac{s_e}{2} \mathbf{u}^T (m^2 \mathbf{1}_K - \kappa \Delta) \mathbf{u} \right\} \quad (197)$$

which can be evaluated to be

$$\tilde{J}(m^2, s_e) = \frac{1}{\sqrt{\det(m^2 \mathbf{1}_K - \kappa \Delta) \det((m^2 + s_e |R''(0)|) \mathbf{1}_K - \kappa \Delta)}}. \quad (198)$$

The second factor is

$$\tilde{G}(m^2, s_d) = \left\langle \left| \det(m^2 \delta_{ij} - \kappa \Delta_{ij} + V_i''(u_i) \delta_{ij}) \right| e^{-s_d \sum_{i=1}^K V_i(u_i)} \right\rangle. \quad (199)$$

Using the property (194) we obtain

$$\tilde{G}(m^2, s_d) = \left\langle \left| \det((m^2 + |R''(0)| s_d) \delta_{ij} - \Delta_{ij} + U_i \delta_{ij}) \right| \right\rangle e^{\frac{1}{2} R(0) s_d^2 K} \quad (200)$$

where the average is over centered independent Gaussian random variables U_i with correlator $\langle U_i U_j \rangle = [R''''(0)/\kappa^2] \delta_{ij}$. Hence, $\tilde{G}(m^2, s_d)$ is equal to the average of the absolute

value of the determinant studied in this paper, i.e. the numerator of (21), up to the simple shift $m^2 \rightarrow m^2 + |R''(0)|s_d$.

As a result, the Laplace transforms $\tilde{N}(s_e, s_d)$ and $\tilde{N}(s, s)$, defined in (191) are expressed very simply in terms of the determinants studied in this paper

$$\tilde{N}(s_e, s_d) = \frac{\langle |\det((m^2 + s_d |R''(0)|/\kappa) \delta_{ij} - \Delta_{ij} + U_i \delta_{ij})| \rangle e^{\frac{1}{2} R(0) s_d^2 K}}{\sqrt{\det((m^2/\kappa) \delta_{ij} - \Delta_{ij}) \det((m^2 + s_e |R''(0)|/\kappa) \delta_{ij} - \Delta_{ij})}}. \quad (201)$$

Note that since the right hand side is well defined for $s_e, s_d > -m^2/|R''(0)|$ we conclude that these Laplace transforms exist (their defining integrals are convergent in that domain). One trivially checks that in the absence of disorder one has $\tilde{N}(s_e, s_d) = 1$, i.e. $\langle \mathcal{N}_{\text{tot}}(H_e, H_d) \rangle = \delta(H_e) \delta(H_d)$ since there is then a single equilibrium with $u_i = 0$ and zero elastic energy.

The formula (21) can be similarly written for the continuum model, for which the elastic and disorder energies are defined respectively as

$$\mathcal{H}_{\text{ela}}[u] = \int_0^L d\tau \left[\frac{\kappa}{2} (\partial_\tau u(\tau))^2 + \frac{m^2}{2} u(\tau)^2 \right], \quad (202)$$

$$\mathcal{H}_{\text{dis}}[u] = \int_0^L d\tau V(u(\tau), \tau). \quad (203)$$

The joint Laplace transform (defined in the same way as for the discrete model) now reads

$$\tilde{N}(s_e, s_d) = \frac{\langle |\det((m^2 + |R''(0)|s_d)/\kappa - \partial_\tau^2 + U(\tau))| \rangle e^{\frac{1}{2} R(0) s_d^2 L}}{\sqrt{\det(m^2/\kappa - \partial_\tau^2) \det((m^2 + |R''(0)|s_e)/\kappa - \partial_\tau^2)}}, \quad (204)$$

where we recall that $\langle U(\tau)U(\tau') \rangle = 2D \delta(\tau - \tau')$ with $D = R''''(0)/(2\kappa^2) = 1/(2L_c^3)$. The above product form shows the *statistical independence of the elastic and the disorder energy at a force-free point*.

Let us now study some implications of this formula. We first review some of our previous results needed here

- (i) The determinants in (204) not containing $U(\tau)$ can be read from Eqs. (46) for various boundary conditions, all having the same leading behaviour in the large L limit $\det(\gamma - \partial_\tau^2) \sim \exp(\sqrt{\gamma}L)$.
- (ii) The following ratio of determinants was studied for large L

$$\langle \mathcal{N}_{\text{tot}} \rangle = \frac{\langle |\det(m^2/\kappa - \partial_\tau^2 + U(\tau))| \rangle}{|\det(m^2/\kappa - \partial_\tau^2)|} \sim e^{r(m^2)L} \quad (205)$$

and its rate of growth $r(m^2)$ as a function of m^2 was shown to be [see Eq. (8)]

$$r(m^2) \simeq \begin{cases} C/L_c - 1/L_m & \text{for } L_m \rightarrow \infty \\ \frac{L_m^2}{8\pi L_c^3} \exp\left\{-\frac{8}{3}(L_c/L_m)^3\right\} & \text{for } L_m \rightarrow 0 \end{cases} \quad (206)$$

where $C \simeq 0.46$ and we recall that $L_m = \sqrt{\kappa}/m$ and $L_c = \kappa^{2/3} R''''(0)^{-1/3}$ [the first limiting behaviour was given in Eq. (120), recalling the correspondence of notations $E = -m^2/\kappa$ and $(2D)^{1/3} = 1/L_c$].

In view of (i) and (ii) there are thus two main applications, studied respectively in the two subsections below :

- (a) we use the information that we know only in the large L limit to study the large deviation rate functions $r(m^2; H)$ and $r(m^2; H_e, H_d)$ controlling the growth of $\langle \mathcal{N}_{\text{tot}}(H) \rangle$ and $\langle \mathcal{N}_{\text{tot}}(H_e, H_d) \rangle$, respectively.
- (b) The Laplace transform can be written exactly for any L , and (in principle) inverted. Such formula exist in general only for the mean number of equilibria at fixed elastic energy, $\int dH_d \langle \mathcal{N}_{\text{tot}}(H_e, H_d) \rangle$, which is studied below.

11.2. Large deviations and rate functions in the large L limit

We will denote $H_e = h_e L$, $H_d = h_d L$ and $H = hL$, where h_e , h_d and h are respectively the elastic, disorder and total energy densities. We expect in the large L limit that

$$\langle \mathcal{N}_{\text{tot}}(H_e, H_d) \rangle \sim e^{r(m^2; h_e, h_d)L} \quad (207)$$

$$\langle \mathcal{N}_{\text{tot}}(H) \rangle \sim e^{r(m^2; h)L} \quad (208)$$

Hence, from the definition of the Laplace transforms (191)

$$\tilde{N}(s_e, s_d) \sim \int dh_e dh_d e^{(r(m^2; h_e, h_d) - s_e h_e - s_d h_d)L} \quad (209)$$

$$\tilde{N}(s, s) \sim \int dh e^{(r(m^2; h) - sh)L} \quad (210)$$

On the other hand from (i) and (ii) above we can write, in the limit of large L

$$\tilde{N}(s_e, s_d) \sim e^{\Gamma(s_e, s_d)L} \quad (211)$$

with

$$\Gamma(s_e, s_d) = r(m^2 + |R''(0)|s_d) + \frac{\sqrt{m^2 + |R''(0)|s_d}}{\sqrt{\kappa}} + \frac{1}{2}R(0)s_d^2 - \frac{m + \sqrt{m^2 + |R''(0)|s_e}}{2\sqrt{\kappa}} \quad (212)$$

One can use a saddle point to estimate the leading large L behaviour of (209) and (210), and we find that the rate functions $r(m^2; h_e, h_d)$ and $r(m^2; h)$ are related to $\Gamma(s_e, s_d)$ and $\Gamma(s, s)$ by Legendre transforms. More precisely one has

$$\Gamma(s_e, s_d) = \max_{h_e, h_d} \{r(m^2; h_e, h_d) - s_e h_e - s_d h_d\} \quad (213)$$

$$\Gamma(s, s) = \max_h \{r(m^2; h) - sh\} \quad (214)$$

Inverting we have

$$r(m^2; h_e, h_d) = \min_{s_e, s_d} \{\Gamma(s_e, s_d) + s_e h_e + s_d h_d\} \quad (215)$$

$$r(m^2; h) = \min_s \{\Gamma(s, s) + sh\} \quad (216)$$

Below we will also study the rates associated to fixing the elastic energy alone, and the disorder energy alone, namely

$$r_e(m^2; h_e) = \min_{s_e} \{ \Gamma(s_e, 0) + s_e h_e \} \quad (217)$$

$$r_d(m^2; h_d) = \min_{s_d} \{ \Gamma(0, s_d) + s_d h_d \} \quad (218)$$

Note the two important general observations, which will be confirmed below by explicit calculations:

- The maximum over h_e of $r_e(m^2; h_e)$ occurs at the field h_e^* which corresponds to $s_e = 0$ and its value is $\Gamma(0, 0) = r(m^2)$. It is easy to check that this property holds from the derivative conditions. The field h_e^* then corresponds to the typical (i.e. the most probable) value of h_e . Same property holds, respectively, for the rate $r_d(m^2; h_d)$ (with typical value h_d^* occurring at $s_d = 0$).
- The form obtained in (212) satisfies that

$$\Gamma(s_e, 0) + \Gamma(0, s_d) = r(m^2) + \Gamma(s_e, s_d) \quad (219)$$

which reflects the independence of the elastic and potential energy noted above. Hence we have

$$r(m^2; h_e, h_d) - r(m^2) = [r_e(m^2; h_e) - r(m^2)] + [r_d(m^2; h_d) - r(m^2)] . \quad (220)$$

In addition one can also show that

$$r(m^2; h) = \max_{h_d} [r_e(m^2; h - h_d) + r_d(m^2; h_d)] - r(m^2) \quad (221)$$

$$= \max_{h_e} [r_e(m^2; h_e) + r_d(m^2; h - h_e)] - r(m^2) \quad (222)$$

and finally, $\max_h r(m^2; h) = r(m^2)$ which is attained at a field h^* , equal to the typical total energy density.

To proceed further, it is convenient to introduce dimensionless variables.⁸ Because we will be interested in the $m \rightarrow 0$ limit, we choose to rescale all observables with respect to the length scale L_c . We define the rescaled energy density and its conjugate variable

$$\tilde{h} := \frac{(R''''(0)\kappa)^{1/3}}{|R''(0)|} h \quad \text{and} \quad \sigma := \frac{|R''(0)|\kappa^{1/3}}{R''''(0)^{2/3}} s . \quad (223)$$

The rates now take the form

$$r(m^2; h_e, h_d) = \frac{1}{L_c} \min_{\sigma_e, \sigma_d} \left\{ \tilde{\Gamma}(\sigma_e, \sigma_d) + \sigma_e \tilde{h}_e + \sigma_d \tilde{h}_d \right\} \quad (224)$$

$$r(m^2; h) = \frac{1}{L_c} \min_{\sigma} \left\{ \tilde{\Gamma}(\sigma, \sigma) + \sigma \tilde{h} \right\} , \quad (225)$$

8. Three main dimensions are involved here : the energy $[\mathcal{H}] = E$, the length $[\tau] = L$ and the field $[u]$. We deduce the dimensions of the main quantities : the correlator $[R(u)] = E^2/L$, the mass $[m] = E^{1/2}L^{-1/2}[u]^{-1}$ and the elastic constant $[\kappa] = EL[u]^{-2}$.

where

$$\tilde{\Gamma}(\sigma_e, \sigma_d) = \tilde{\Lambda}(\mu + \sigma_d) + \frac{\eta}{2} \sigma_d^2 - \frac{1}{2} (\sqrt{\mu + \sigma_e} + \sqrt{\mu}) . \quad (226)$$

$\tilde{\Lambda}(\mu) = L_c \Lambda(1)$ is the (rescaled) generalized Lyapunov exponent (cf. Section 7), defined for $\mu \in \mathbb{R}$ (for reasons which will become clear later, we have preferred to express the rate Γ as a function of the GLE $\Lambda(1) = r(m^2) + 1/L_m$; a rescaled rate \tilde{r} is also defined below). The expression (226) makes clear that the two conjugated parameters belong to different domains : $\sigma_e \in [-\mu, +\infty[$ and $\sigma_d \in \mathbb{R}$, which reflects the fact that $H_e \geq 0$ while $H_d \in \mathbb{R}$. We have also introduced the two dimensionless parameters

$$\mu = (L_c/L_m)^2 \propto m^2 , \quad (227)$$

$$\eta = \frac{R(0)R''''(0)}{R''(0)^2} \geq 1 . \quad (228)$$

The bound on the parameter η will play an important role below and follows from the Gaussian nature⁹ of the disordered potential $V(u, \tau)$ in Eq. (1). This bound is saturated, $\eta = 1$, for harmonic correlations $R(u) = \sigma^2 \cos(u/v_p)$, which corresponds to the charge density wave model studied numerically in Section 5.

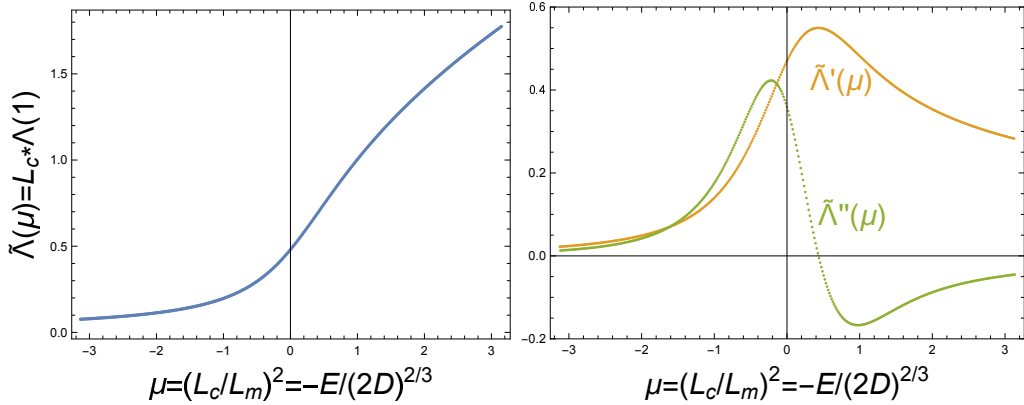


Figure 12: Rescaled GLE computed numerically according to the method described in Subsection 8.1.

We recall that $\tilde{\Lambda}(\mu)$ is a monotonously increasing function of μ , see Fig. 3 and Fig. 12, with the three limiting behaviours obtained in the previous sections

$$\tilde{\Lambda}(\mu) \simeq \begin{cases} -\frac{3}{16\mu} & \text{for } \mu \rightarrow -\infty \\ C + a_1 \mu + \frac{1}{2} a_2 \mu^2 + \mathcal{O}(\mu^3) & \text{for } \mu \rightarrow 0 \\ \sqrt{\mu} + \frac{1}{8\pi\mu} \exp\{-(8/3)\mu^{3/2}\} & \text{for } \mu \rightarrow +\infty \end{cases} \quad (229)$$

9. Since $R(u)$ is the correlator of a Gaussian field, its Fourier transform is positive, $\hat{R}(q) \geq 0$. This property allows to apply the well-known Cauchy-Schwarz inequality $[\int dq f^*(q)g(q)]^2 \leq \int dq |f(q)|^2 \int dq |g(q)|^2$ for square integrable functions to the functions $f(q) = \hat{R}(q)^{1/2}$ and $g(q) = q^2 \hat{R}(q)^{1/2}$, leading to $[\int dq q^2 \hat{R}(q)]^2 \leq \int dq \hat{R}(q) \int dq q^4 \hat{R}(q)$, i.e. $R''(0)^2 \leq R(0) R''''(0)$. QED.

where the behaviour for $\mu \rightarrow -\infty$ is deduced from (78). The function $\tilde{\Lambda}(\mu)$ is smooth and analytic everywhere, in particular near $\mu = 0$, a point of special interest in the present study (see below). The dimensionless coefficient $a_1 \simeq 0.47$ is positive, see Eq. (119). It is also convenient to introduce the rescaled rate $\tilde{r}(\mu) = L_c r(m^2) = \tilde{\Lambda}(\mu) - \sqrt{\mu}$ defined for $\mu \in \mathbb{R}^+$, with the limiting behaviours

$$\tilde{r}(\mu) \simeq \begin{cases} C - \sqrt{\mu} + a_1 \mu + \mathcal{O}(\mu^2) & \text{for } \mu \rightarrow 0^+ \\ \frac{1}{8\pi\mu} \exp\{-(8/3)\mu^{3/2}\} & \text{for } \mu \rightarrow \infty \end{cases} \quad (230)$$

corresponding to (206).

We now study respectively the rates at fixed elastic and disorder energy, and finally at fixed total energy.

11.2.1. Mean number of equilibria constrained by the elastic energy

As a warm up simple exercise, we consider first the number of equilibria constrained by the elastic energy

$$\int dH_d \langle \mathcal{N}_{\text{tot}}(H_e, H_d) \rangle \underset{L \rightarrow \infty}{\sim} \exp\{r_e(m^2; h_e) L\}. \quad (231)$$

Here we only compute the large deviation function $r_e(m^2; h_e)$ (a more precise calculation of the distribution of elastic energy will be presented in Subsection 11.3).

We consider

$$r_e(m^2; h_e) = \frac{1}{L_c} \min_{\sigma_e} \left\{ \tilde{\Gamma}(\sigma_e, 0) + \sigma_e \tilde{h}_e \right\} \quad \text{for } \sigma_e \geq -\mu. \quad (232)$$

It is straightforward to minimize $\tilde{\Gamma}(\sigma_e, 0) + \sigma_e \tilde{h}_e = \tilde{r}(\mu) + (1/2)(\sqrt{\mu} - \sqrt{\sigma_e + \mu}) + \sigma_e \tilde{h}_e$ over σ_e : the function is minimum for $\sigma_e = -\mu + 1/(4\tilde{h}_e)^2$. We deduce

$$L_c r_e(m^2; h_e) = \tilde{r}(\mu) - \frac{\mu}{\tilde{h}_e} \left(\tilde{h}_e - \frac{1}{4\sqrt{\mu}} \right)^2, \quad (233)$$

i.e.

$$r_e(m^2; h_e) - r(m^2) = -\frac{L_c}{L_m^2 \tilde{h}_e} \left(\tilde{h}_e - \frac{L_m}{4L_c} \right)^2 \simeq - \begin{cases} \frac{|R''(0)|}{16\kappa h_e} & \text{as } h_e \rightarrow 0^+ \\ \frac{m^2 h_e}{|R''(0)|} & \text{as } h_e \rightarrow \infty \end{cases}. \quad (234)$$

Writing

$$\int dH_d \frac{\langle \mathcal{N}_{\text{tot}}(H_e, H_d) \rangle}{\langle \mathcal{N}_{\text{tot}} \rangle} \underset{L \rightarrow \infty}{\sim} e^{[r_e(m^2; h_e) - r(m^2)] L} \quad (235)$$

makes clear that (234) is the large deviation function for the elastic energy, controlling the large L behaviour of the distribution of the elastic energy with respect with the annealed measure (63). We see that the rate is maximum at $\tilde{h}_e = \tilde{h}_e^* := 1/(4\sqrt{\mu}) = L_m/(4L_c) \propto 1/m$ (corresponding to $\sigma_e = 0$), which coincides with the most probable

(typical) value of the elastic energy density for the line at equilibrium. Coming back to the original variable, the typical elastic energy density is

$$h_e^* = \frac{|R''(0)|}{4m\sqrt{\kappa}} \simeq \langle h_e \rangle_a, \quad (236)$$

which also corresponds with its annealed average value as indicated by $\langle \dots \rangle_a$. From (234), we deduce the variance of the annealed distribution of the elastic energy density as

$$\text{Var}_a(h_e) \simeq \frac{|R''(0)|^2}{8m^2\kappa} \frac{L_m}{L}. \quad (237)$$

We note a peculiarity in the zero mass limit $m \rightarrow 0$. In that limit, from (236) we see that the typical elastic energy density tends to infinity as $h_e^* \propto m^{-1}$, as well as the fluctuations $\sqrt{\text{Var}_a(h_e)} \propto m^{-3/2}$. This is a genuine feature, understood as follows. We saw in Section 6 that the annealed distribution of displacements obeys the Larkin scaling (see Appendix C), which, in the massless case, goes schematically as $u \sim L^{3/2}$. The simple dimensional estimate $H_e \sim u^2/L$ then leads to an elastic energy growing as $H_e \sim L^2$ instead of L for finite m , meaning that the energy density grows with the length as $h_e \sim L$. This is consistent with an infinite typical energy density in the thermodynamic limit $L \rightarrow \infty$. This behaviour of the elastic energy thus arises because typical stationary configurations wander a lot (with Larkin scaling in L), much further than the ground state (which is known to wander only as $u \sim L^{2/3}$ and to lead to a finite elastic energy density). Below we provide an exact calculation of the distribution of H_e for $m = 0$, which confirms these qualitative arguments (cf. Subsection 11.3.2).

11.2.2. Mean number of equilibria constrained by the disorder energy

In a second stage, we consider the number of equilibria constrained by the disorder energy H_d :

$$\int dH_e \langle \mathcal{N}_{\text{tot}}(H_e, H_d) \rangle \underset{L \rightarrow \infty}{\sim} \exp\{r_d(m^2; h_d) L\}, \quad (238)$$

where the rate is given by

$$r_d(m^2; h_d) = \frac{1}{L_c} \min_{\sigma_d} \left\{ \tilde{\Gamma}(0, \sigma_d) + \sigma_d \tilde{h}_d \right\}, \quad (239)$$

where

$$\tilde{\Gamma}(0, \sigma) = \tilde{\Lambda}(\mu + \sigma) + \frac{\eta}{2} \sigma^2 - \sqrt{\mu} \quad \text{for } \sigma \in \mathbb{R}. \quad (240)$$

Although it is not possible to obtain a simple analytical form, as for the elastic energy, one can establish various general features and limiting behaviours.

The minimizer of Eq. (239) is given by $\sigma_d = \sigma_*$ solution of

$$-\tilde{h}_d = \tilde{\Lambda}'(\mu + \sigma_*) + \eta \sigma_*. \quad (241)$$

We deduce the large deviation function

$$L_c r_d(m^2; h_d) = \tilde{\Lambda}(\mu + \sigma_*) - \sigma_* \tilde{\Lambda}'(\mu + \sigma_*) - \frac{\eta}{2} \sigma_*^2 - \sqrt{\mu}. \quad (242)$$

As discussed above for the elastic energy, from general considerations the maximum of $r_d(m^2; h_d)$ over h_d should equal $r(m^2)$ and occur at the typical field h_d^* corresponding to the argmin value $\sigma_* = 0$. We thus immediately obtain the typical, most probable value of the (dimensionless) disorder energy density as

$$\tilde{h}_d^* = -\tilde{\Lambda}'(\mu) . \quad (243)$$

Because $\tilde{\Lambda}'(\mu) > 0 \forall \mu$ (cf. Fig. 12) we see that the typical disorder energy is *negative*

$$h_d^* = -\frac{|R''(0)|}{(R'''(0)\kappa)^{1/3}} \tilde{\Lambda}'(\mu) < 0 . \quad (244)$$

We recall that $\mu = (L_c/L_m)^2 \propto m^2$. In the limit of zero mass, $m \rightarrow 0$ (absence of external confinement), we can use the value obtained from the numerics $\tilde{\Lambda}'(0) = a_1 \simeq 0.47$ (cf. Fig. 12) to get a good estimate for the typical disorder energy. In the other limit of strong confinement ($L_m \ll L_c$), using (229), we deduce that the typical disorder energy takes the form

$$h_d^* \simeq -\frac{|R''(0)|}{2m\sqrt{\kappa}} \quad \text{for } m \rightarrow \infty , \quad (245)$$

i.e. is twice the elastic energy (236), with the opposite sign. Note that our numerics indicate that $\tilde{\Lambda}'(\mu)$ reaches its maximum at $\mu \approx 0.4$ (when the curvature $\tilde{\Lambda}''(\mu)$ changes in sign). Intuition about ground states would suggest that the lower the mass, the larger the available space for the elastic line to explore better locations in the random potential, hence the lower the typical disorder energy. However here we are dealing with all stationary points, which seems, from our numerics, to behave differently (with the minimum h_d^* occurring at a non zero value of μ).

The study of the typical fluctuations is rather simple : the expansion of (241) at first order in σ_* gives $\sigma_* \simeq -(\tilde{h}_d - \tilde{h}_d^*)/(\tilde{\Lambda}''(\mu) + \eta)$ and, similarly, the expansion of the rate (242) takes the form $L_c r_d(m^2; h_d) = \tilde{r}(\mu) - (1/2)(\tilde{\Lambda}''(\mu) + \eta) \sigma_*^2 + \mathcal{O}(\sigma_*^3)$. We deduce the quadratic behaviour

$$r_d(m^2; h_d) \simeq r(m^2) - \frac{1}{2L_c (\tilde{\Lambda}''(\mu) + \eta)} (\tilde{h}_d - \tilde{h}_d^*)^2 \quad \text{for } \tilde{h}_d \sim \tilde{h}_d^* . \quad (246)$$

Our numerics also indicates that $\tilde{\Lambda}''(\mu)$ is always above ~ -0.17 (Fig. 12). Thus the combination $\eta + \tilde{\Lambda}''(\mu) > 0$ always remain positive, as needed. This combination enters the variance of the disorder energy, from the annealed distribution, as one finds, from (249),

$$\text{Var}_a(\tilde{h}_d) = (\eta + \tilde{\Lambda}''(\mu)) \frac{L_c}{L} \quad \Leftrightarrow \quad \text{Var}_a(h_d) = \left(R(0) + \frac{R''(0)^2}{R'''(0)} \tilde{\Lambda}''(\mu) \right) \frac{1}{L} \quad (247)$$

Because $\eta \geq 1$ and $|\tilde{\Lambda}''(\mu)|$ is bounded by a number of order one, the first expression makes clear that the first term $\eta L_c/L$ gives a good estimate of the variance. Moreover, in the strong confinement limit ($L_m \ll L_c$), the variance is independent of the mass, $\text{Var}_a(h_d) \simeq R(0)/L$, contrary to the typical value which vanishes as $h_d^* \sim 1/m$.

Let us now analyse the large deviations, i.e. the *atypical* fluctuations. The limiting behaviours (229) show that $\tilde{\Lambda}'(\mu + \sigma_*)$ is bounded and decays at $\sigma_* \rightarrow \pm\infty$. This is

supported by numerics (Fig. 12) As a result we get $\sigma_* \simeq -\tilde{h}_d/\eta$ in the tails for $\tilde{h}_d \rightarrow \pm\infty$. We have perform a more detailed analysis of the limiting behaviours of σ_* at large h_d . Putting all together, we obtain the respective behaviours in the three regions :

$$\sigma_* \simeq \begin{cases} -\frac{1}{\eta}\tilde{h}_d - \frac{1}{2\sqrt{\eta|\tilde{h}_d|}} + \mathcal{O}(|\tilde{h}_d|^{-3/2}) & \text{for } \tilde{h}_d \rightarrow -\infty \\ -\frac{1}{\eta + \tilde{\Lambda}''(\mu)}(\tilde{h}_d + \tilde{\Lambda}'(\mu)) & \text{for } \tilde{h}_d + \tilde{\Lambda}'(\mu) \rightarrow 0 \\ -\frac{1}{\eta}\tilde{h}_d + \mathcal{O}(\tilde{h}_d^{-2}) & \text{for } \tilde{h}_d \rightarrow +\infty \end{cases} \quad (248)$$

Correspondingly, we deduce the following behaviours for the large deviation rate function¹⁰

$$L_c [r_d(m^2; h_d) - r(m^2)] \simeq \begin{cases} -\frac{1}{2\eta} \tilde{h}_d^2 + \sqrt{|\tilde{h}_d|/\eta} - \tilde{\Lambda}(\mu) + \mathcal{O}(|\tilde{h}_d|^{-1/2}) & \text{for } \tilde{h}_d \rightarrow -\infty \\ -\frac{1}{2[\eta + \tilde{\Lambda}''(\mu)]} (\tilde{h}_d - \tilde{h}_d^*)^2 & \text{for } \tilde{h}_d \sim \tilde{h}_d^* \\ -\frac{1}{2\eta} \tilde{h}_d^2 - \tilde{\Lambda}(\mu) + \mathcal{O}(\tilde{h}_d^{-1}) & \text{for } \tilde{h}_d \rightarrow +\infty \end{cases} \quad (249)$$

We compare in Fig. 13 these limiting behaviours with the result of a numerical resolution of Eqs. (241,242) : the agreement is excellent.

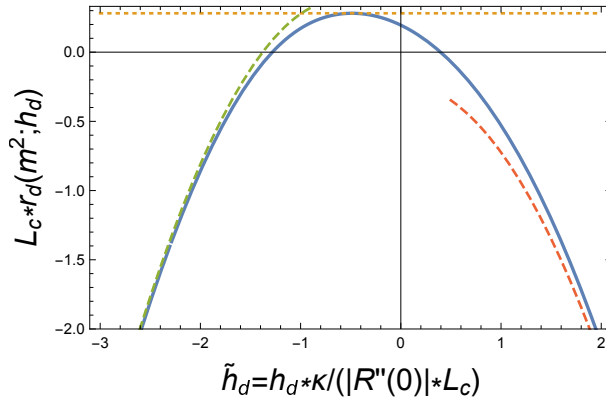


Figure 13: Rate $r_d(m^2; h_d)$ for $\mu = (L_c/L_m)^2 = 0.05$ and $\eta = 1$. The dashed lines correspond to the limiting behaviours (249) ; the dotted horizontal line is $r(m^2)$. The rate was computed by making use of the data for the GLE obtained above and represented in Fig. 12.

An interesting feature is that the decay of the rate at large positive energy is not controlled by the mass, as it was the case for the elastic energy, cf. Eq. (234): instead it has a parabolic shape controlled by $R(0)$:

$$r_d(m^2; h_d) \simeq -\frac{h_d^2}{2R(0)} \quad \text{for } h_d \rightarrow \pm\infty. \quad (250)$$

10. The rate can be deduced from Eq. (242). More directly, one can use the general property $\sigma_*(\tilde{h}_d) = \frac{d}{d\tilde{h}_d} L_c r_d(m^2; h_d)$, i.e. $L_c [r_d(m^2; h_d) - r(m^2)] = \int_{\tilde{h}_d^*}^{\tilde{h}_d} dt \sigma_*(t)$. A similar relation was recently used in Refs. [94, 95] in order to study some properties of random matrices.

We have used the numerical data (Sections 8.1 and 8.2) to compute the rate $r_d(m^2; h_d)$ in order to check our analysis : the agreement is good, as one can see in Fig. 13.

Finally, it is interesting for the following to study the lowest point h_d^{\min} where the rate $r_d(m^2; h_d)$ vanishes : in the small mass limit, $\mu \rightarrow 0$, we obtain numerically $\tilde{h}_d^{\min} \simeq -1.503$ for $\eta = 1$, and using (249), $\tilde{h}_d^{\min} \simeq -2^{2/3}\eta^{1/3} \simeq -1.587\eta^{1/3}$ for $\eta \gg 1$, so that setting $\eta = 1$ in the approximate expression obtained for $\eta \gg 1$ is close to the correct result.

11.2.3. Mean number of equilibria constrained by the total energy

We now study the rate (225) at fixed total energy H . We recall that the total energy can have both signs, contrary to the elastic energy H_e , which is positive. Here also we can obtain the asymptotic behaviours easily. We have now to consider

$$\tilde{\Gamma}(\sigma, \sigma) = \tilde{\Lambda}(\mu + \sigma) - \frac{1}{2}(\sqrt{\mu + \sigma} + \sqrt{\mu}) + \frac{\eta}{2}\sigma^2 \quad \text{for } \sigma \geq -\mu. \quad (251)$$

The sum $\tilde{\Gamma}(\sigma, \sigma) + \sigma\tilde{h}$ is minimum for $\sigma = \sigma_*$ solution of

$$-\tilde{h} = \tilde{\Lambda}'(\mu + \sigma_*) + \eta\sigma_* - \frac{1}{4\sqrt{\mu + \sigma_*}}. \quad (252)$$

As a result

$$r(m^2; h) = \frac{1}{L_c} \left\{ \tilde{\Lambda}(\mu + \sigma_*) - \sigma_* \tilde{\Lambda}'(\mu + \sigma_*) - \frac{1}{4}\sqrt{\mu + \sigma_*} - \frac{1}{2}\sqrt{\mu} - \frac{\mu}{4\sqrt{\mu + \sigma_*}} - \frac{\eta}{2}\sigma_*^2 \right\}. \quad (253)$$

As discussed above, the maximum of $r(m^2; h)$ over h equals $r(m^2)$ and is attained for the typical field \tilde{h}^* corresponding to $\sigma^* = 0$, hence from (252)

$$\tilde{h}^* = -\tilde{\Lambda}'(\mu) + \frac{1}{4\sqrt{\mu}} = \tilde{h}_d^* + \tilde{h}_e^* \quad (254)$$

hence, not surprisingly, the typical total energy is the sum $h^* = h_e^* + h_d^*$ of the typical disorder and elastic energies obtained in the previous sections. In the original units, the typical total energy density reads

$$h^* = \frac{|R''(0)|}{4m\sqrt{\kappa}} \left(1 - 4\sqrt{\mu} \tilde{\Lambda}'(\mu) \right) \quad \text{where } \mu = \left(\frac{L_c}{L_m} \right)^2. \quad (255)$$

From (229) we see that the last factor $(1 - 4\sqrt{\mu} \tilde{\Lambda}'(\mu))$ changes sign as the mass increases and varies from 1 (positive typical energy, elastic energy dominates) for $m \rightarrow 0$, corresponding to weak confinement, to -1 (negative typical energy, disorder energy dominates) for $m \rightarrow +\infty$, corresponding to strong confinement.

The expansion of (252) for $\sigma_* \rightarrow 0$ allows to study the typical fluctuations, in the same way as for the disorder energy. As expected, the variance is given by the sum of variances of elastic and disorder energy computed above :

$$\text{Var}_a(h) = \text{Var}_a(h_e) + \text{Var}_a(h_d) = \frac{R''(0)^2}{R'''(0)L} \left(\eta + \tilde{\Lambda}''(\mu) + \frac{1}{8\mu^{3/2}} \right). \quad (256)$$

We deduce that the fluctuations are dominated by the elastic energy in the weak confinement regime ($L_m \gg L_c$), $\text{Var}_a(h) \simeq \text{Var}_a(h_e) \propto m^{-3}$, while in the strong confinement case ($L_m \ll L_c$) they are dominated by the disorder energy $\text{Var}_a(h) \simeq \text{Var}_a(h_d) \simeq R(0)/L$.

We now derive limiting behaviours for the rate. Asymptotic analysis of (252) using (229) leads to (the analysis is quite similar to the two previous sections)

$$\sigma_* \simeq \begin{cases} -\frac{1}{\eta}\tilde{h} - \frac{1}{4\sqrt{\eta|\tilde{h}|}} + \mathcal{O}(|\tilde{h}|^{-3/2}) & \text{for } \tilde{h} \rightarrow -\infty \\ -\frac{1}{\eta + \tilde{\Lambda}''(\mu) + 1/(8\mu^{3/2})}(\tilde{h} - \tilde{h}^*) & \text{for } \tilde{h} \sim \tilde{h}^* \\ -\mu + \frac{1}{16(\tilde{h} + \tilde{\Lambda}'(0) - \eta\mu)^2} + \mathcal{O}(\tilde{h}^{-5}) & \text{for } \tilde{h} \rightarrow +\infty \end{cases} \quad (257)$$

Correspondingly, using (253) we deduce the following behaviours for the large deviation rate function

$$\begin{aligned} & L_c [r(m^2; h) - r(m^2)] \\ & \simeq \begin{cases} -\frac{1}{2\eta}\tilde{h}^2 + \frac{1}{2}\sqrt{|\tilde{h}|/\eta} + \frac{1}{2}\sqrt{\mu} - \tilde{\Lambda}(\mu) + \mathcal{O}(|\tilde{h}|^{-1/2}) & \text{for } \tilde{h} \rightarrow -\infty \\ -\frac{1}{2[\eta + \tilde{\Lambda}''(\mu) + 1/(8\mu^{3/2})]}(\tilde{h} - \tilde{h}^*)^2 & \text{for } \tilde{h} \sim \tilde{h}^* \\ -\mu\tilde{h} + \frac{1}{2}\sqrt{\mu} - \tilde{\Lambda}(\mu) + \frac{1}{2}\eta\mu^2 + \tilde{\Lambda}(0) + \mathcal{O}(\tilde{h}^{-1}) & \text{for } \tilde{h} \rightarrow +\infty \end{cases} \end{aligned} \quad (258)$$

Using the data of the numerical calculation (Sections 8.1 and 8.2), we have solved numerically (252) and computed the rate (253) : the result is plotted in Fig. 14. We see that the agreement with the limiting behaviours discussed in the text is excellent.

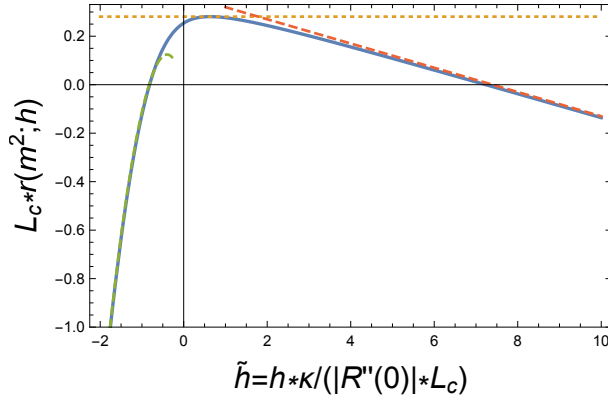


Figure 14: Rate $r(m^2; h)$ for $\mu = (L_c/L_m)^2 = 0.05$ and $\eta = 1$. The dashed lines correspond to the limiting behaviours (258) ; the dotted horizontal line is $r(m^2)$. The rate was computed by making use of the data for the GLE obtained above and represented in Fig. 12.

Let us discuss some main features of this result. In the limit of large total negative energy density we thus obtain the dominant term [corresponding to $-(\eta/2)\sigma_*^2$ in

Eq. (253)]

$$r(m^2; h) \simeq -\frac{h^2}{2R(0)} \quad \text{for } h \rightarrow -\infty. \quad (259)$$

which is identical to the leading behaviour for large negative disorder energy from (250). Since the elastic energy is positive, it is reasonable to expect that the two tails coincide to leading order. Notice by comparing (258) and (249) that they differ however by the prefactor of the next (subleading) order.

Consider now the limit of large positive total energy density. From (258) we obtain

$$r(m^2; h) \simeq -\frac{\mu}{L_c} \tilde{h} = -\frac{m^2}{|R''(0)|} h \quad \text{for } h \rightarrow +\infty. \quad (260)$$

This is the same behaviour as (234), obtained for the elastic energy. Again it is quite reasonable that these two tails coincide, since the disorder energy rate function was found to decay much faster at large positive disorder energy density than the elastic energy one. Hence the elastic energy dominates in that regime. Note however that the next (subleading) order term, which is $\mathcal{O}(1)$, is different for the total and the elastic energy rate functions.

As was already discussed in the context of the elastic energy, the decay of the large deviation function with h is controlled by the mass : when the mass vanishes, $r(0; h)$ is a monotonous function which saturates

$$r(0; h) \simeq \frac{C}{L_c} - \frac{|R''(0)|}{16\kappa h} \quad \text{for } h \rightarrow +\infty. \quad (261)$$

Because $\langle \mathcal{N}_{\text{tot}}(H) \rangle / \langle \mathcal{N}_{\text{tot}} \rangle$ must be a decreasing function of H for $H \rightarrow \pm\infty$, the saturation of the large deviation function (261) for $h \rightarrow +\infty$ needs some explanation, provided at the end of the Subsection 11.3. It has the same physical origin as discussed above for the elastic energy (large wandering of the elastic line at equilibria in the massless case leading to $H \sim L^2$).

As can be seen on Fig. 14, the rate $r(m^2; h)$ is positive for $h \in [h_{\min}, h_{\max}]$. The value h_{\min} provides a *lower bound* on the energy density of the ground state h_{GS} . Indeed one has the convexity exact bound

$$\ln \langle \mathcal{N}_{\text{tot}}(H) \rangle \geq \langle \ln \mathcal{N}_{\text{tot}}(H) \rangle \quad (262)$$

Since when decreasing $H = hL$ the l.h.s vanishes for $h = h_{\min}$, it implies that the r.h.s has already vanished at that point. Since the r.h.s. vanishes when h reaches the typical ground state energy density h_{GS} we deduce that $h_{\min} \leq h_{\text{GS}}$. We now assume small mass $m \rightarrow 0$. For $\eta = 1$, we get numerically $\tilde{h}_{\min} \simeq -0.97$ for $\mu \rightarrow 0$ (Fig. 14). If we assume $\eta \gg 1$, we can use the asymptotic (258) (for $\tilde{h} \rightarrow -\infty$) and deduce $\tilde{h}_{\min} \simeq -\eta^{1/3}$. Reintroducing the dimensional factors, we conclude that the lower bound on the ground state energy density is

$$h_{\min} \simeq \begin{cases} -0.97 \frac{|R''(0)|}{(R'''(0)\kappa)^{1/3}} & \text{and } \eta = 1 \\ -\left(\frac{R(0)|R''(0)|}{\kappa}\right)^{1/3} & \text{and } \eta \gg 1 \end{cases} \quad \text{for } L_c \ll L_m. \quad (263)$$

Similarly, h_{\max} provides an *upper bound* on the highest equilibrium energy density, $h_{\max} \geq h_{\text{HS}}$. For small mass, we can use the asymptotic (258) (for $\tilde{h} \rightarrow +\infty$) to get $\tilde{h}_{\max} \simeq C/\mu \gg 1$, corresponding to

$$h_{\max} \simeq +C \frac{|R''(0)| R'''(0)^{1/3}}{m^2 \kappa^{2/3}} \quad \text{for } L_c \ll L_m. \quad (264)$$

It is interesting to compare the bound \tilde{h}_{\min} ($\simeq -0.97$ for $\eta = 1$ and $\simeq -\eta^{1/3}$, for $\mu = 0$) for the total ground state energy density with the similar bound obtained above for the disorder energy density, $\tilde{h}_d^{\min} \simeq -1.503$ for $\eta = 1$ and $\tilde{h}_d^{\min} \simeq -1.587 \eta^{1/3}$ for $\eta \gg 1$. We have $\tilde{h}_{\min} > \tilde{h}_d^{\min}$ as it should. However the comparison of the two bounds suggest that the elastic energy and the disorder energy are comparable for the *atypical* configurations of the line corresponding to the ground state. This is very different for the *typical* configurations, which are characterized by typical disorder energy density $\tilde{h}_d^* = -\tilde{\Lambda}'(0) \simeq -0.47$ while we show below that the typical elastic energy density is very large, growing with the length $\tilde{h}_e^* \sim L/L_c$, cf. Eq. (275).

11.3. Mean number of equilibria at fixed value of the elastic energy for any L

Let us study the mean number of equilibria at fixed value of the elastic energy H_e . As discussed in Appendix C, the annealed distribution of elastic energy H_e for our model, exactly coincides with the one of the Larkin model. The present calculation, however, which treats carefully the boundary conditions, has not, to our knowledge, been reported previously, even in the context of the Larkin model.

Setting $s_d = 0$ in (201), we obtain

$$\int dH_e dH_d \langle \mathcal{N}_{\text{tot}}(H_e, H_d) \rangle e^{-s_e H_e} = \langle \mathcal{N}_{\text{tot}} \rangle \sqrt{\frac{\det(m^2/\kappa - \partial_\tau^2)}{\det((m^2 + s_e |R''(0)|)/\kappa - \partial_\tau^2)}} \quad (265)$$

Note that since the elastic energy is positive, these are bona-fide Laplace transforms. We can now use the expressions of these determinants, Eq. (46).

11.3.1. Finite mass m

Let us focus on periodic boundary conditions, which leads to the simplest formula, and indicate the results for others. Then we have, with $L_m = \sqrt{\kappa}/m$

$$\int dH_e dH_d \langle \mathcal{N}_{\text{tot}}(H_e, H_d) \rangle e^{-s_e H_e} = \langle \mathcal{N}_{\text{tot}} \rangle \frac{\sinh L/2L_m}{\sinh(\sqrt{1 + \frac{s_e |R''(0)|}{m^2}} L/2L_m)} \quad (266)$$

The natural unit of H_e is $H_{em} = |R''(0)|/m^2$. The quantity of most interest is the annealed (i.e. over samples) probability distribution, $\mathcal{P}_{L,m}(H_e)$, that an equilibrium chosen at random has elastic energy H_e , takes the form (for all classes of boundary conditions)

$$\mathcal{P}_{L,m}(H_e) = \int dH_d \frac{\langle \mathcal{N}_{\text{tot}}(H_e, H_d) \rangle}{\langle \mathcal{N}_{\text{tot}} \rangle} = \frac{1}{H_{em}} f_{L/L_m}(H_e/H_{em}) \quad (267)$$

For the periodic case, we have to compute the inverse Laplace transform

$$f_\ell^{\text{Per}}(\theta) = \mathcal{L}_{s \rightarrow \theta}^{-1} \left[\frac{\sinh(\ell/2)}{\sinh(\sqrt{1+s}\ell/2)} \right]. \quad (268)$$

Note that $f_\ell(\theta)$ integrates to unity since it is a probability distribution for the scaled elastic energy variable θ .

Let us also indicate the result for Dir/Dir

$$f_\ell^{\text{D/D}}(\theta) = \mathcal{L}_{s \rightarrow \theta}^{-1} \left[\sqrt{\frac{\sqrt{1+s} \sinh \ell}{\sinh(\sqrt{1+s}\ell)}} \right] \quad (269)$$

The above formulae can be inverted in principle to obtain $\mathcal{P}_{L,m}(H_e)$ for any L . For periodic boundary condition, using

$$\frac{1}{\sinh(z)} = \sum_{n=-\infty}^{+\infty} \frac{(-1)^n}{z + in\pi}$$

we obtain

$$\begin{aligned} f_\ell^{\text{Per}}(\theta) &= \sinh(\ell/2) \int_0^{+\infty} dt \sum_{n=-\infty}^{+\infty} (-1)^n e^{-in\pi t} \mathcal{L}_{s \rightarrow \theta}^{-1} \left[e^{-\frac{1}{2}\ell t \sqrt{1+s}} \right] \\ &= \sinh(\ell/2) \frac{\ell}{4\sqrt{\pi}\theta^{3/2}} e^{-\theta} \int_0^{+\infty} dt \sum_{n=-\infty}^{+\infty} (-1)^n e^{-in\pi t} t e^{-\ell^2 t^2 / (16\theta)} \\ &= \sinh(\ell/2) \sum_{n=-\infty}^{+\infty} (-1)^n \frac{2e^{-\theta} \left(\ell - 4\pi n \sqrt{\theta} F\left(\frac{2n\pi\sqrt{\theta}}{\ell}\right) \right)}{\sqrt{\pi}\ell^2 \sqrt{\theta}} \end{aligned} \quad (270)$$

where $F(x) = e^{-x^2} \int_0^x dy e^{-y^2}$ the Dawson integral (FDawson in **Mathematica**). Let us further discuss two limits:

In the limit of small $\ell = L/L_m \rightarrow 0$ one sees that the result for the Dirichlet (D/D) boundary conditions converges to $\lim_{\ell \rightarrow 0} f_\ell^{\text{D/D}}(\theta) = \delta(\theta)$ while for the periodic (Per) converges to a non trivial fixed distribution, $\lim_{\ell \rightarrow 0} f_\ell^{\text{Per}}(\theta) = e^{-\theta}/\sqrt{\pi\theta}$. Presumably this is related to the fact that in the later case the center of mass degree of freedom is still free even in that limit, and effectively reduces to a zero dimensional model.

In the limit of large $\ell = L/L_m \gg 1$ one finds

$$f_\ell^{\text{Per}}(\theta) \underset{\ell \gg 1}{\simeq} \mathcal{L}_{s \rightarrow \theta}^{-1} \left[e^{(1-\sqrt{1+s})\ell/2} \right] = \frac{1}{4\sqrt{\pi}\theta^{3/2}} e^{-\frac{(\theta-\ell/4)^2}{\theta}} \quad (271)$$

From this we conclude that for $L/L_m \gg 1$ the leading (i.e. *typical*) fluctuations of the elastic energy are Gaussian

$$H_e \simeq H_{em} \left(\frac{L}{4L_m} + \sqrt{\frac{L}{8L_m}} \chi \right) \quad , \quad H_{em} = \frac{|R''(0)|}{m^2} \quad (272)$$

where χ is a Gaussian random variable of unit variance. The form (271) is furthermore consistent with the *large deviation* rate function (in the notations of the previous section) associated to $H_e = h_e L$, that is

$$r_e(m^2; h_e) = r(m^2) - \frac{H_{em}}{h_e} \left(\frac{h_e}{H_{em}} - \frac{1}{4L_m} \right)^2, \quad (273)$$

which indeed coincides with the Legendre transform w.r.t s_e of $\Gamma(s_e, s_d = 0)$ in Eq. (212), cf. Eq. (234).

11.3.2. Case $m = 0$

In this final paragraph, we consider the distribution of the elastic energy in the zero mass limit. One of our aim is here to clarify the origin of the saturation of the rate $r(m^2; h)$, Eq. (261), or equivalently of the rate $r_e(m^2; h_e)$, as the tail of the distribution of the total energy is controlled by the distribution of the elastic energy. We consider the case of Neumann/Dirichlet boundary conditions, which describes the case where the line is attached by one end, the other end being free. We choose these boundary conditions for the simplicity of the determinant, Eq. (46). From (265), we see that the distribution then takes the form

$$\mathcal{P}_{L,0}(H_e) = \frac{\kappa}{|R''(0)|L^2} \varphi \left(\frac{\kappa H_e}{|R''(0)|L^2} \right) \quad \text{where} \quad \varphi(\theta) = \mathcal{L}_{s \rightarrow \theta}^{-1} \left[\frac{1}{\sqrt{\cosh \sqrt{s}}} \right]. \quad (274)$$

This expression shows that the typical elastic energy *density* grows with the length

$$h_e^* \sim \frac{|R''(0)|L}{\kappa}, \quad \text{i.e.} \quad \tilde{h}_e^* \sim \frac{L}{L_c} \quad (275)$$

in terms of the dimensionless variable introduced above.

In Appendix G, we show that the limiting behaviours of the inverse Laplace transform (274) are

$$\varphi(\theta) \sim \begin{cases} \frac{1}{\theta} \exp \{-1/(16\theta)\} & \text{for } \theta \rightarrow 0 \\ \frac{1}{\sqrt{\theta}} \exp \{-(\pi/2)^2 \theta\} & \text{for } \theta \rightarrow \infty \end{cases}. \quad (276)$$

If the distribution is rewritten under the form $\mathcal{P}_{L,0}(H_e) \sim \exp\{L[r_e(m^2; h_e) - r(m^2)]\}$ for $L \rightarrow \infty$, we have

$$r_e(m^2; h_e) - r(m^2) \simeq \begin{cases} -\frac{|R''(0)|}{16\kappa h_e} & \text{for } h_e \ll |R''(0)|L/\kappa \\ -\frac{\pi^2 \kappa h_e}{4|R''(0)|L^2} & \text{for } h_e \gg |R''(0)|L/\kappa \end{cases} \quad (277)$$

The first behaviour is in exact correspondence with Eq. (261) or Eq. (234) for $m = 0$. The second behaviour ensures the decay of $\mathcal{P}_{L,0}(H_e)$ for large H_e , as it should. This makes clear that the saturation of the rate Eq. (261) only reflects a subtlety concerning the order of the two limits $L \rightarrow \infty$ and $h_e \rightarrow \infty$ when $m = 0$.

12. Conclusion

By extending the Kac-Rice approach to manifolds of finite internal dimension, we have shown that the mean number of equilibria of an elastic line in a random potential in presence of a parabolic confinement, grows exponentially with its length, and developed a theory to calculate the rate of growth r . The mean number equilibria is shown to be related to the expectation value of the modulus of the determinant of the Laplace operator in presence of diagonal disorder, the same operator which features in the Anderson localization problem. The relation is valid for elastic interface of arbitrary internal dimension d . In $d = 1$ (elastic line) using the Gelfand-Yaglom theorem, the rate of growth can be related with the large deviation function of the Lyapunov exponent fluctuations associated to a 1D random Schrödinger problem, but in the negative energy range. This large deviation function (generalized Lyapunov exponent GLE) is given by the lowest eigenvalue of an associated Fokker-Planck operator which is analysed in detail by several complementary techniques.

From these methods, we found that the rate r is described by a universal function of the disorder strength for which we obtained analytical and numerical results. The disorder strength is naturally parameterized using the Larkin length L_c and the dimensionless control parameter is the ratio of L_c to the length L_m imposed by the parabolic confining potential. We extract analytically the asymptotic behaviours of this scaling function for small and large value of the argument. For strong confinement, the rate r is small and given by a non-perturbative (instanton, Lifshitz tail-like) contribution to GLE. For weak confinement, the rate r is found to be proportional to the inverse Larkin length of the pinning theory. We have also discussed the question of counting of stable equilibria. Finally, we have shown how to extend the method to calculate the asymptotic number of equilibria at fixed energy : we have obtained large deviation rate functions controlling the number of equilibria constrained by either the total, the elastic or the disorder energy. These large deviation functions control the distribution of the (total, elastic or disorder) energy density of the line at equilibrium. Some connections with the Larkin model have been discussed.

One of the most interesting application is to study the evolution of the mean number of equilibria as an external force f is turned on. We find that a “topology trivialization” phenomenon occurs, and the rate associated to the mean number of equilibria decreases to zero at some threshold force $f = f_c^{\text{tot}}$ which can be calculated from the above methods. This is related to the so-called depinning transition, which occurs at $f = f_c$, at which all stable equilibria disappear. As a result we showed that f_c^{tot} provides an exact upper bound to f_c , differing only by a factor of order unity. This prediction is confirmed numerically.

From the point of view of Anderson localization, we have also discovered several interesting properties of the generalized Lyapunov exponent (GLE) $\Lambda(q)$. We have shown a crucial difference between the GLE for $q = 1$, which is a non-analytic function of the disorder strength D (for $E \rightarrow -\infty$) while $\Lambda(q)$ is analytic when q is an even integer. It would be interesting to see if the difference persists for larger odd integer arguments. We were able to obtain few exact results for even integer q . The limit of large positive argument $q \rightarrow +\infty$ was analysed, which is related to the large deviations of the wave function (solution of the Cauchy initial value problem) for large values. The analysis of the limit $q \rightarrow -\infty$ of the GLE has remained an open question, which can be related to

the large deviations of the wave function for small values.

The connection discussed here with the generalized Lyapunov exponents of a localization problem opens a bridge between pinning theory and localization theory that should inspire further works.

Acknowledgements

CT acknowledges stimulating discussions and suggestions from Philippe Bougerol, Alain Comtet, Aurélien Grabsch, Jean-Marc Luck, Nicolas Pavloff, Yves Tourigny and Denis Ullmo. We thank David Saykin for sharing his results and writing Appendix E. We thank the PCMI Summer School 2017, where some of this work was performed. The research at King's College London was supported by EPSRC grant EP/N009436/1 The many faces of random characteristic polynomials. This research was also supported by ANR grant ANR-17-CE30-0027-01 RaMaTraF. We are grateful to an anonymous referee for numerous useful remarks.

Appendix A. Boundary conditions and determinants

In this section, we discuss several formulae for the determinant $\det(H - E)$ of the Schrödinger operator to justify and make more precise the formula of the main text and of Appendix B below.

Consider the discrete Hamiltonian which appears in the text, $H_{i,j} = -\Delta_{i,j} + U_i\delta_{i,j}$ and the associated Schrödinger equation

$$\sum_j H_{i,j}\psi_j = -\psi_{i+1} + (2 + U_i)\psi_i - \psi_{i-1} = E\psi_i \quad (\text{A.1})$$

for $i \in \{1, \dots, K\}$; boundary conditions set the values for ψ_0 and ψ_{K+1} .

Appendix A.1. Boundary conditions

There are three natural boundary conditions for the elastic line problem studied in this paper. We detail them here in the discrete and continuum settings.

Appendix A.1.1. Dirichlet boundary conditions

The pinned boundary conditions correspond to setting $\psi_0 = \psi_{K+1} = 0$ in (A.1) ($u_0 = u_{K+1} = 0$ with the notations of the body of the paper). The associated $K \times K$ Laplacian matrix $\Delta = \Delta_{\text{Dir}}$ then reads :

$$\Delta_{\text{Dir}} = \begin{pmatrix} -2 & 1 & 0 & \cdots & 0 \\ 1 & -2 & 1 & 0 & \cdots \\ 0 & 1 & \ddots & \ddots & \\ \vdots & \ddots & \ddots & -2 & 1 \\ 0 & \cdots & 0 & 1 & -2 \end{pmatrix} \quad (\text{A.2})$$

In the continuum limit it corresponds to the usual Laplacian with Dirichlet boundary conditions $\psi(0) = \psi(L) = 0$.

Appendix A.1.2. Neumann boundary conditions

The free boundary conditions : set $\psi_0 = \psi_1$ and $\psi_K = \psi_{K+1}$ in (A.1), i.e. the associated Laplacian $\Delta = \Delta_{\text{Neu}}$ is

$$\Delta_{\text{Neu}} = \begin{pmatrix} -1 & 1 & 0 & \cdots & 0 \\ 1 & -2 & 1 & 0 & \cdots \\ 0 & 1 & \ddots & \ddots & \\ \vdots & \ddots & \ddots & -2 & 1 \\ 0 & \cdots & 0 & 1 & -1 \end{pmatrix} \quad (\text{A.3})$$

In the continuum limit it corresponds to usual Laplacian with Neumann boundary conditions $\psi'(0) = \psi'(L) = 0$.

Appendix A.1.3. Periodic boundary conditions

The periodic boundary conditions, $\psi_0 = \psi_K$, $\psi_{K+1} = \psi_1$, with the associated Laplacian $\Delta = \Delta_{\text{Per}}$ given by

$$\Delta_{\text{Per}} = \begin{pmatrix} -2 & 1 & 0 & \cdots & 1 \\ 1 & -2 & 1 & 0 & \cdots \\ 0 & 1 & \ddots & \ddots & \\ \vdots & \ddots & \ddots & -2 & 1 \\ 1 & \cdots & 0 & 1 & -2 \end{pmatrix} \quad (\text{A.4})$$

In the continuum limit this corresponds to usual Laplacian for $\psi(0) = \psi(L)$ and $\psi'(0) = \psi'(L)$.

Appendix A.2. Determinants

We now discuss separately the formulae for the determinant $\det(H - E)$ for the three types of boundary conditions.

Appendix A.2.1. Pinned boundary conditions (Dirichlet)

We denote by $y_i(E)$ the solution of the initial value problem with

$$y_0 = 0 \quad \text{and} \quad y_1 = 1. \quad (\text{A.5})$$

The K eigenvalues $\{E_\alpha\}_{\alpha=1, \dots, K}$ of the $K \times K$ Hamiltonian H are the solutions of the quantization condition

$$y_{K+1}(E) = 0. \quad (\text{A.6})$$

We see by recursion that $y_2(E) = 2 + U_1 - E$, $y_3(E) = (2 + U_2 - E)(2 + U_1 - E) - 1$, etc. By induction, it is straightforward to prove that $y_{j+1}(E)$ is a polynomial of degree j in E with higher degree term $(-E)^j$. Using these remarks we can write

$$\det(H - E) = \prod_{\alpha=1}^K (E_\alpha - E) = y_{K+1}(E) \quad (\text{A.7})$$

This can now be used for the discrete polymer model, formula (21) in the text, with the correspondence $E = -m^2/\kappa$. As a simple illustration consider the free case with $U_n = -2$. We deduce $y_n = \sin qn/\sin q$ where $E = -2\cos q$. As a consequence the Dirichlet determinant is $\det(H - E) = \sin q(K+1)/\sin q$, corresponding to the spectrum $q_n = n\pi/(K+1)$ with $n = 1, \dots, K$.

Denoting $y(\tau)$ the solution of $(H - E)y(\tau) = 0$ with initial conditions

$$y(0) = 0 \quad \text{and} \quad y'(0) = 1, \quad (\text{A.8})$$

we see that Eq. (A.7) is obviously the discrete version of the Gelfand-Yaglom formula

$$\det(H - E) = 2y(L). \quad (\text{A.9})$$

up to a E independent multiplicative factor which depends on the ultraviolet regularization (the factor chosen here and formulae given below correspond to zeta regularization [62, 96]). Let us illustrate the formula in the free case where $H = -\partial_\tau^2$: setting $\gamma = -E$ for convenience for the following, we find $y(\tau) = \sinh(\sqrt{\gamma}\tau)/\sqrt{\gamma}$ thus $\det(\gamma - \partial_\tau^2) = 2 \sinh(\sqrt{\gamma}L)/\sqrt{\gamma}$. Rewriting the hyperbolic function as an infinite product

$$\det(\gamma - \partial_\tau^2) = 2L \prod_{n=1}^{\infty} \left(1 + \frac{\gamma}{q_n^2}\right), \quad \text{where } q_n = \frac{n\pi}{L} \text{ for } n \in \mathbb{N}^*. \quad (\text{A.10})$$

We recognize the eigenvalues of the Laplacian. In this case we recall the eigenfunctions, $-\partial_\tau^2 \psi_n(\tau) = q_n^2 \psi_n(\tau)$,

$$\psi_n(\tau) = \sqrt{\frac{2}{L}} \sin(q_n \tau) \text{ with } n \in \mathbb{N}^*. \quad (\text{A.11})$$

Appendix A.2.2. Free boundary conditions (Neumann)

$\psi_0 = \psi_1$ and $\psi_K = \psi_{K+1}$. We now denote by $x_i(E)$ the solution of the initial value problem with

$$x_0 = x_1 = 1 \quad (\text{A.12})$$

Now the quantization condition is

$$x_{K+1}(E) = x_K(E) \quad (\text{A.13})$$

Similar argument as above gives

$$\det(H - E) = x_{K+1}(E) - x_K(E). \quad (\text{A.14})$$

In the continuum limit, we consider the solution $x(\tau)$ of the differential equation $(H - E)x(\tau) = 0$, where $H = -\frac{d^2}{d\tau^2} + U(\tau)$, with initial conditions

$$x(0) = 1 \quad \text{and} \quad x'(0) = 0 \quad (\text{A.15})$$

The determinant is then given by

$$\det(H - E) = 2x'(L) \quad (\text{A.16})$$

As in the text, a regularization independent formula is obtained by forming ratio of two such determinants. We illustrate the formula in the free case : setting again $E = -\gamma$ we find $x(\tau) = \cosh(\sqrt{\gamma}\tau)/\sqrt{\gamma}$, thus $\det(\gamma - \partial_\tau^2) = 2\sqrt{\gamma} \sinh(\sqrt{\gamma}L)$, which can also be expressed in terms of the spectrum of eigenvalues $\{q_n^2\}_{n \in \mathbb{N}}$ of the Laplacian:

$$\begin{cases} \psi_0(\tau) = \frac{1}{\sqrt{L}} \\ \psi_n(\tau) = \sqrt{\frac{2}{L}} \cos(q_n \tau) \end{cases}, \quad \text{where } q_n = \frac{n\pi}{L} \text{ with } n \in \mathbb{N} \quad (\text{A.17})$$

Appendix A.2.3. Periodic boundary conditions

For the sake of completeness, let us add a phase and now write the periodic boundary conditions as

$$\psi_K = \psi_0 e^{i\theta} \quad \text{and} \quad \psi_{K+1} = \psi_1 e^{i\theta}, \quad (\text{A.18})$$

(this corresponds to a ring pierced by a magnetic flux). The spectral analysis can be formulated conveniently by introducing two specific solutions $y_i(E)$ and $\tilde{y}_i(E)$ for two different initial value problems corresponding to

$$\begin{cases} y_0 = 0 \\ y_1 = 1 \end{cases} \quad \text{and} \quad \begin{cases} \tilde{y}_{K+1} = 0 \\ \tilde{y}_K = 1 \end{cases} \quad (\text{A.19})$$

We have pointed out above that $y_n(E)$ is a polynomial of degree $n-1$ in E ; similarly $\tilde{y}_n(E)$ a polynomial of degree $K-n-1$. The Wronskian $W_j = y_j \tilde{y}_{j+1} - y_{j+1} \tilde{y}_j$ of the two solutions is constant (starting from (A.1), one finds $W_{j+1} = W_j$), and is simply denoted $W = -\tilde{y}_0 = -y_{K+1}$ (which is the Dirichlet determinant).

The solution of the spectral problem can then be decomposed as $\psi_j = a y_j + b \tilde{y}_j$, where a and b are two constants. Imposing the boundary conditions (A.18) leads to the quantization equation

$$\det \begin{pmatrix} y_K & 1 - \tilde{y}_0 e^{i\theta} \\ e^{i\theta} - y_{K+1} & \tilde{y}_1 e^{i\theta} \end{pmatrix} = 0. \quad (\text{A.20})$$

Expanding this equation gives

$$\det(H - E) = \frac{1}{\tilde{y}_0} + \tilde{y}_0 - \frac{\tilde{y}_1 y_K}{\tilde{y}_0} - 2 \cos \theta. \quad (\text{A.21})$$

As an example of application, we consider the free case ($U_n = -2$) where $y_n = \sin qn / \sin q = \tilde{y}_{K+1-n}$ for energy $E = -2 \cos q$. Some algebra gives $\det(H - E) = 2(\cos qK - \cos \theta) = 2(T_K(-E/2) - \cos \theta)$, where $T_K(x)$ is a Chebyshev polynomial.

We can proceed along the same lines in the continuum : we consider the two solutions $y(\tau)$ and $\tilde{y}(\tau)$ of the differential equation with initial conditions

$$\begin{cases} y(0) = 0 \\ y'(0) = 1 \end{cases} \quad \text{and} \quad \begin{cases} \tilde{y}(L) = 0 \\ \tilde{y}'(L) = -1 \end{cases} \quad (\text{A.22})$$

The determinant is then given by

$$\det(H - E) = y'(L) - \tilde{y}'(0) - 2 \cos \theta \quad (\text{A.23})$$

In the free case we have simply $\tilde{y}(\tau) = y(L - \tau)$ and we find $\det(\gamma - \partial_\tau^2) = 2[\cosh(\sqrt{\gamma}L) - \cos\theta]$, which can again be expanded over the spectrum of eigenvalues

$$\det(\gamma - \partial_\tau^2) = 4 \sin^2(\theta/2) \prod_{n \in \mathbb{Z}} \left(1 + \frac{\gamma}{(q_n - \theta/L)^2} \right) \quad (\text{A.24})$$

We recall also the related eigenfunctions for completeness

$$\psi_n(\tau) = \frac{1}{\sqrt{L}} e^{iq_n \tau}, \quad \text{where } q_n = \frac{2n\pi}{L} \text{ with } n \in \mathbb{Z}. \quad (\text{A.25})$$

For references on functional determinants, cf. Refs. [97, 62, 96] and the review [98].

Appendix B. Pinning of the line for fixed boundary conditions

We provide some additional information for the analysis of § 4.2.3 : we show how the discussion can be extended to the case of a line with fixed endpoints. We can also perform the calculation for an elastic line pinned at its two ends (Dirichlet boundary conditions).¹¹ The Fourier coefficients are

$$\tilde{f}_n = \frac{2f\sqrt{2L}}{n\pi}, \quad n = 2p + 1 \quad (\text{B.1})$$

$$= 0, \quad n = 2p + 2 \quad (\text{B.2})$$

for $p \in \mathbb{N}$. Performing the sum over the modes, $q_n = n\pi/L$ with $n \in \mathbb{N}^*$, one finds that (minus) the argument of the exponential in (45) becomes

$$\frac{Lf^2}{2|R''(0)|} \sum_{n \text{ odd}} \frac{8}{(n\pi)^2} \frac{1}{1 + (L_w/L)^4 [(n\pi)^2 + (L/L_m)^2]^2}. \quad (\text{B.3})$$

In the limit $L_m/L \rightarrow \infty$ (vanishing mass) and $L/L_w \rightarrow \infty$, we find

$$\frac{Lf^2}{2|R''(0)|} \sum_{n \text{ odd}} \frac{8}{(n\pi)^2} = \frac{Lf^2}{2|R''(0)|} \quad (\text{B.4})$$

leading to a value for the second term in (51) *identical* to the case of periodic and Neumann boundary conditions (despite the summation over an infinite set of modes). In addition, we also expect that $\Lambda(1)$, the first term in (51) is independent of the boundary conditions. For instance, in the framework of the Ricatti equation (80) defined in the text, the initial condition is $z(0) = -\infty$ for Dirichlet, and $z(0) = 0$ for Neumann boundary conditions. However, it is known that the rate of growth, i.e. the GLE, does not depend on the initial condition. Hence $\Lambda(1)$, and the rate $r_{\text{tot}}(f)$ in (51) is the same for all three types of boundary conditions, leading to the same value of f_c^{tot} .

11. although it is not the standard one for the depinning problem, where the elastic line is usually free to move, it is a usual setting in the related sandpile problem [99, 100, 101].

Appendix C. The Larkin model

The Larkin model is a simplified model for pinning. Let us recall it here for an elastic line in the continuum (discrete versions, and extensions to higher d are immediate, for reviews see Refs. [1, 2]). In the Larkin model the non-linear random potential term in Eq. (1) is replaced simply by a linear random force term

$$\mathcal{H}_{\text{Lar}}[u(\tau)] = \int_0^L d\tau \left[\frac{\kappa}{2} \left(\frac{\partial u(\tau)}{\partial \tau} \right)^2 + \frac{m^2}{2} u^2(\tau) - \phi(\tau) u(\tau) \right] \quad (\text{C.1})$$

which is centered Gaussian with correlator $\langle \phi(\tau) \phi(\tau') \rangle = -R''(0) \delta(\tau - \tau')$. It amounts to expand $V(u, \tau) = V(0, \tau) + V'(0, \tau) u + \dots$ and discard higher order terms. Being quadratic, there is a unique energy minimum (i.e. a single equilibrium)

$$u_0(\tau) = \int_0^L d\tau' \langle \tau | (m^2 - \kappa \partial_\tau^2)^{-1} | \tau' \rangle \phi(\tau') \quad (\text{C.2})$$

which is distributed as a Gaussian field with correlator

$$\langle u_0(\tau) u_0(\tau') \rangle = |R''(0)| \langle \tau | (m^2 - \kappa \partial_\tau^2)^{-2} | \tau' \rangle = |R''(0)| \int \frac{dq}{2\pi} \frac{\cos q(\tau - \tau')}{(m^2 + \kappa q^2)^2}, \quad (\text{C.3})$$

$$\langle (u_0(\tau) - u_0(\tau'))^2 \rangle = |R''(0)| \int \frac{dq}{\pi} \frac{1 - \cos q(\tau - \tau')}{(m^2 + \kappa q^2)^2} \quad (\text{C.4})$$

where in the second equation we assumed L large enough to ignore boundary conditions: this integral behaves as $L_m^{2\zeta_L}$ where $\zeta_L = 3/2$ is the Larkin roughness exponent.

It is shown that at zero temperature the Larkin model, a zero dimensional version of the elastic line model (1), has the same correlation functions for the field $u(\tau)$, to all orders in perturbation theory in the disorder, as the original model (1) (the so-called dimensional reduction phenomenon). However it lacks the (non-perturbative) feature of multiple equilibria. Indeed, one notes that it depends on a single parameter, $R''(0)$, and lacks the physics of pinning arising from a non vanishing $R'''(0)$. However, it does provide a good approximate description of the correlation functions of the true model (in its ground state) at scales smaller than L_c , or for $m \gg m_c$ (such that $L_{m_c} = L_c$), although even in this regime it lacks the non-perturbative corrections originating from rare events, such as the one obtained in this paper.

The elastic energy at the minimum is easily obtained as

$$H_e^{\text{Lar}} = \frac{1}{2} \int_0^L d\tau \int_0^L d\tau' \phi(\tau) \langle \tau | (m^2 - \kappa \partial_\tau^2)^{-1} | \tau' \rangle \phi(\tau') \quad (\text{C.5})$$

and its Laplace transform is simply obtained by integration over the Gaussian field $\phi(\tau)$ as

$$\langle e^{-s_e H_e^{\text{Lar}}} \rangle = \sqrt{\frac{\det(m^2/\kappa - \partial_\tau^2)}{\det((m^2 + s_e |R''(0)|)/\kappa - \partial_\tau^2)}} \quad (\text{C.6})$$

which is exactly the same factor which occurs in (265). Thus the prediction of the Larkin model (which has a single equilibrium) coincides *exactly* with the *annealed* probability

distribution of the elastic energy of the true model over all equilibria. As an example, by averaging (C.5) over $\phi(\tau)$ one recovers its average (or most probable) value as

$$\lim_{L \rightarrow \infty} \frac{1}{L} \langle H_e^{\text{Lar}} \rangle \simeq \frac{|R''(0)|}{2} \int \frac{dq}{2\pi} \frac{1}{m^2 + \kappa q^2} = \frac{|R''(0)|}{4m\sqrt{\kappa}} \quad (\text{C.7})$$

which is exactly Eq. (236).

In the Larkin model as written in (C.5) the disorder energy is simply $H_d = -2H_e$ and total energy $H = -H_e$, so H_d and H_e are not independent as in the true model (in Section 11.2, the relation $H_d = -2H_e$ was shown to hold only for the typical values in the strong confinement regime, $L_m \ll L_c$). Trying to improve on the model (as adding the $V(0, \tau)$ term from the expansion of the potential) does not lead to a consistent description of H_d . That no such simple approximation exist for H_d and H is corroborated by the results of Section 11.2.2 where the typical disorder energy density is obtained in terms of the (quite non-trivial) GLE of a 1D Anderson localization problem.

Appendix D. Spectrum of the Fokker-Planck generator \mathcal{G}^\dagger in the presence of a non equilibrium stationary state – Spectrum of \mathcal{O}_q

Appendix D.1. Generator of the FPE

We make several remarks on the spectrum of the forward generator

$$\mathcal{G}^\dagger = D \frac{d^2}{dz^2} + \frac{d}{dz} \mathcal{U}'(z) = D \frac{d}{dz} e^{-\mathcal{U}(z)/D} \frac{d}{dz} e^{\mathcal{U}(z)/D} \quad (\text{D.1})$$

when the potential is such that the diffusion is characterized by a non-equilibrium stationary state (NESS) on the full real axis. This situation requires that $\mathcal{U}(z) \rightarrow \pm\infty$ for $z \rightarrow \pm\infty$, and the drift $|\mathcal{U}'(z)|$ grows sufficiently fast at infinity so that the particle is driven in a finite time from $+\infty$ to $-\infty$:

$$\int_{-\infty}^{\infty} dz |\mathcal{U}'(z)|^{-1} < \infty \quad \text{and} \quad \int_{-\infty}^{\infty} dz |\mathcal{U}'(z)|^{-1} < \infty. \quad (\text{D.2})$$

This is the case for the potential $\mathcal{U}(z) = Ez + z^3/3$ considered in the paper.

In order to get some insight, we perform the following non-unitary transformation relating the generator to the Hermitian operator

$$\mathcal{H}_0 = -e^{\mathcal{U}(z)/(2D)} \mathcal{G}^\dagger e^{-\mathcal{U}(z)/(2D)} = -D e^{\mathcal{U}(z)/(2D)} \frac{d}{dz} e^{-\mathcal{U}(z)/D} \frac{d}{dz} e^{\mathcal{U}(z)/(2D)} \quad (\text{D.3})$$

$$= -D \frac{d^2}{dz^2} + \frac{[\mathcal{U}'(z)]^2}{4D} - \frac{\mathcal{U}''(z)}{2}. \quad (\text{D.4})$$

The transformation is well-known in the context of the Fokker-Planck equation (FPE), see for instance Ref. [102] (see also the recent article [66] and references therein). The first equation emphasizes a particular symmetry of the operator, known as “supersymmetry” [103], which rewrites

$$\mathcal{H}_0 = \mathcal{Q}^\dagger \mathcal{Q} \quad \text{where} \quad \mathcal{Q} = -\sqrt{D} e^{-\mathcal{U}(z)/(2D)} \frac{d}{dz} e^{\mathcal{U}(z)/(2D)}. \quad (\text{D.5})$$

This makes clear that \mathcal{H}_0 has a positive spectrum, $\text{Spec}(\mathcal{H}_0) \subset \mathbb{R}^+$, as well as $\text{Spec}(\mathcal{G}^\dagger)$.

The conditions (D.2) imply that the drift grows at infinity so that the potential in the Hamiltonian (D.4) is a confining potential (for the case studied in the paper, the potential behaves as $z^4/(4D)$ at infinity). As a consequence the spectrum of the Hamiltonian and of the generator is *discrete* : we have denoted $\mathcal{E}_n(0)$, $\Phi_n^R(z;0)$ and $\Phi_n^L(z;0)$ the eigenvalues and eigenvectors of the generator, defined by (105,106) for $q=0$. We can also associate to the eigenvalue $\mathcal{E}_n(0)$ the eigenfunction $\Psi_n(z)$ of \mathcal{H}_0 . Making use of $\mathcal{H}_0\Psi_n = \mathcal{E}_n\Psi_n$, $\mathcal{G}^\dagger\Phi_n^R = -\mathcal{E}_n\Phi_n^R$ and $\mathcal{G}\Phi_n^L = -\mathcal{E}_n\Phi_n^L$, if $\mathcal{E}_n(0) > 0$ we get

$$\Psi_n(z) = \Phi_n^R(z;0)e^{\mathcal{U}(z)/(2D)} = \Phi_n^L(z;0)e^{-\mathcal{U}(z)/(2D)} \quad (\text{D.6})$$

which shows that the strictly positive parts of the spectra of the two operators \mathcal{G}^\dagger and \mathcal{H}_0 coincide.

The conditions (D.2) also ensure the existence of null right and left eigenvectors

$$\Phi_0^R(z;0) = \frac{N(E)}{D} e^{-\mathcal{U}(z)/D} \int_{-\infty}^z dz' e^{\mathcal{U}(z')/D} \quad \text{and} \quad \Phi_0^L(z;0) = 1, \quad (\text{D.7})$$

where $N(E)$ is given by the normalization. The right eigenvector is the stationary state for constant current : using the relation between the probability density and the current

$$J_\tau(z) = -D e^{-\mathcal{U}(z)/D} \frac{\partial}{\partial z} \left[e^{\mathcal{U}(z)/D} P_\tau(z) \right], \quad (\text{D.8})$$

we deduce that $P(z) = \Phi_0^R(z;0)$ is the stationary solution of the FPE for a uniform current $J = -N(E)$, where $N(E)$ is the integrated DoS of the random Schrödinger operator (25) introduced in Subsection 7.2.2 (see also Refs. [73, 65, 71, 70, 66]). The inspection of its asymptotic behaviour

$$\Phi_0^R(z;0) \simeq N(E)/|\mathcal{U}'(z)| \simeq N(E) z^{-2} \quad \text{for} \quad z \rightarrow \pm\infty, \quad (\text{D.9})$$

illustrates that the drift $\mathcal{U}'(z) \simeq -z^2$ dominates the diffusion at large z . This also makes clear that the function $\Psi_0(z) = \Phi_0^R(z;0)e^{\mathcal{U}(z)/(2D)}$, solution of $\mathcal{H}_0\Psi_0 = 0$, is *not normalizable*, thus $\mathcal{E}_0(0) = 0$ is not in the spectrum of \mathcal{H}_0 and one says that the “supersymmetry is broken” [103] :¹²

$$\text{Spec}(-\mathcal{G}^\dagger) = \text{Spec}(\mathcal{H}_0) \cup \{\mathcal{E}_0(0) = 0\} \quad (\text{broken SUSY}). \quad (\text{D.10})$$

A consequence of importance for the article is that both

$$\Phi_0^R(z;0) > 0 \quad \text{and} \quad \Phi_1^R(z;0) > 0 \quad (\text{D.11})$$

i.e. have no node, where the second condition follows from the fact that $\Phi_1^R(z;0)$ is related to the ground state Ψ_1 of \mathcal{H}_0 . Since Ψ_n for $n \geq 1$ is the $(n-1)$ -th excited state of the Hamiltonian, it has $n-1$ nodes, like $\Phi_n^R(z;0)$.

12. When the potential $\mathcal{U}(z)$ confines the particle such that an equilibrium state (with zero current) exists, the two null eigenvectors are $\Phi_0^R(z;0) = c \exp\{-\mathcal{U}(z)/D\}$ and $\Phi_0^L(z;0) = 1$ so that the wave function $\Psi_0(z) = c \exp\{-\mathcal{U}(z)/(2D)\}$ is normalizable and the zero mode also belongs to the spectrum of the Hamiltonian. This is the case of “good susy” where the spectra exactly coincide, $\text{Spec}(-\mathcal{G}^\dagger) = \text{Spec}(\mathcal{H}_0)$. Note that the condition (D.6) ensures the detailed balance property in this case.

We now briefly discuss the asymptotic behaviour of the eigenvectors. We assume that $\mathcal{U}(z) \rightarrow \pm\infty$ for $z \rightarrow \pm\infty$ like in the paper. The asymptotic behaviour of the eigenfunctions of \mathcal{H}_0 is given by the WKB form $\Psi_n(z) \simeq [p(z)]^{-1/2} \exp \pm \int dz p(z)$ where $p(z) = \sqrt{[\mathcal{U}'(z)/2D]^2 - \mathcal{U}''(z)/2D - \mathcal{E}_n/D}$. With the condition that $\mathcal{U}'(z)$ grows at infinity, we can expand its integral as $\int dz p(z) \simeq \pm \mathcal{U}(z)/(2D) \mp \frac{1}{2} \ln |\mathcal{U}'(z)|$ for $z \rightarrow \pm\infty$. As a consequence, the two asymptotic behaviours for the wave function are

$$\Psi_n(z) \sim \begin{cases} e^{-\mathcal{U}(z)/(2D)} & \text{for } z \rightarrow +\infty \\ \frac{1}{|\mathcal{U}'(z)|} e^{\mathcal{U}(z)/(2D)} & \text{for } z \rightarrow -\infty \end{cases} \quad (\text{D.12})$$

which is obviously normalizable. Correspondingly, the right and left eigenvectors of the generator behave asymptotically as

$$\Phi_n^R(z; 0) \sim \begin{cases} e^{-\mathcal{U}(z)/D} \\ \frac{1}{|\mathcal{U}'(z)|} \end{cases} \quad \text{and} \quad \Phi_n^L(z; 0) \sim \begin{cases} 1 \\ \frac{1}{|\mathcal{U}'(z)|} e^{\mathcal{U}(z)/D} \end{cases} \quad \text{for } z \rightarrow \pm\infty \quad (\text{D.13})$$

Appendix D.2. The spectrum of \mathcal{O}_q

We now make some remark on the spectrum of the operator $\mathcal{O}_q = \mathcal{G}^\dagger + qz$ of importance for the paper. The similar non-unitary transformation is possible

$$\mathcal{H}_q = -e^{\mathcal{U}(z)/(2D)} \mathcal{O}_q e^{-\mathcal{U}(z)/(2D)} = \mathcal{H}_0 - qz, \quad (\text{D.14})$$

which leads to a Hermitian operator. \mathcal{H}_q also describes a quantum particle trapped in a confining potential, hence has a discrete spectrum. However the presence of the additional potential term $-qz$ breaks the supersymmetry. It is not possible to construct explicitly the state $\Phi_0^R(z; q)$ like for $q = 0$, which makes the discussion more complicated. From a continuity argument, we expect also the property

$$\text{Spec}(-\mathcal{O}_q) = \text{Spec}(\mathcal{H}_q) \cup \{\mathcal{E}_0(q)\}, \quad (\text{D.15})$$

what we have verified by diagonalisation of the discretised operators for several values of q .

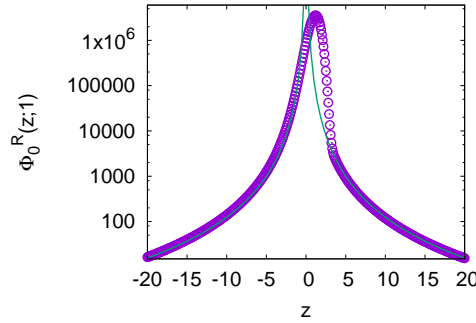


Figure D.15: Function $\Phi_0^R(z; q)$ (not normalized) for $k = 1$ and $q = 1$. The line is $\propto |z|^{-3}$.

Some asymptotic analysis is also possible. Starting from the differential equation $\mathcal{O}_q \Phi_n^R(z; q) = -\mathcal{E}_n(q) \Phi_n^R(z; q)$, we obtain that the two independent asymptotic behaviours are

$$|z|^{-2-q} \quad \text{and} \quad |z|^q e^{-\mathcal{U}(z)/D}, \quad (\text{D.16})$$

which corresponds to (D.13) for $q = 0$. All “excited state” $n \geq 1$ are in correspondence with eigenfunctions of (D.14) and thus present the exponential behaviour $z^q e^{-\mathcal{U}(z)/D}$ for $z \rightarrow +\infty$. Like for $q = 0$, the first right eigenvector is the only one with algebraic behaviour on both sides $\Phi_0^R(z; q) \sim |z|^{-2-q}$ for $z \rightarrow \pm\infty$ (see Fig. D.15).

Appendix E. WKB calculation for the ground state of the Fokker-Planck operator (written by David Saykin)

We consider the spectral problem defined by Eq. (105) for $q = 1$. A closely related problem was considered recently in Ref. [104]. In order to make the equation of the Schrödinger type, one performs the transformation : $\Phi(z) = \psi(z) \exp[\frac{1}{2}(|E|z - \frac{z^3}{3})]$

$$-\psi'' + \left[\frac{1}{4}(z^2 - |E|)^2 - 2z - \mathcal{E} \right] \psi = 0. \quad (\text{E.1})$$

As we have seen in Section 8, one seeks for a solution $\Phi_0^R(z; q = 1)$ presenting a power law decay at infinity, implying an exponential blow up of $\psi(z)$ as $z \rightarrow +\infty$, however this does not preclude us from solving the problem using conventional WKB analysis.

Let us rescale the coordinate as $z \mapsto |E|^{-1/4}y$ and introduce $g \equiv (4|E|^{3/2})^{-1}$ and $2\nu \equiv 1 + \mathcal{E}/\sqrt{|E|}$. One recovers the shifted double-well potential in a more standard form :

$$-\psi'' + \left[g \left(y^2 - \frac{1}{4g} \right)^2 - 4\sqrt{g}y + 1 - 2\nu \right] \psi = 0, \quad (\text{E.2})$$

The desired eigenfunction satisfies the boundary conditions

$$\psi \sim A_- \frac{\exp \int_0^y |k(x)| dx}{\sqrt{|k(y)|/g}}, \quad \text{as } y \rightarrow -\infty, \quad (\text{E.3})$$

$$\psi \sim A_+ \frac{\exp \int_0^y |k(x)| dx}{\sqrt{|k(y)|/g}} + A'_+ \frac{\exp - \int_0^y |k(x)| dx}{\sqrt{|k(y)|/g}}, \quad \text{as } y \rightarrow +\infty, \quad (\text{E.4})$$

where

$$|k(y)|^2 = g \left(y^2 - \frac{1}{4g} \right)^2 - 4\sqrt{g}y + 1 - 2\nu. \quad (\text{E.5})$$

The energy parameter ν is expected to behave asymptotically as $\nu \sim -2\#g \exp(-\frac{1}{3g})$ for $g \rightarrow +0$.

Hermite equation. Let us introduce the notations $y_{\pm} = y \mp \frac{1}{2\sqrt{g}}$, $\nu_+ = \nu$ and $\nu_- = \nu - 2$. Near the minima of the potential $|y_{\pm}| \ll \frac{1}{\sqrt{g}}$, Eq. (E.2) reduces to the Hermite equation

$$[-\partial^2 + y_{\pm}^2 - (2\nu_{\pm} + 1)] \chi(y_{\pm}) \approx 0, \quad |y_{\pm}| \ll \frac{1}{\sqrt{g}}. \quad (\text{E.6})$$

The solution of this differential equation is known as the Hermite function used in Section 9, or, equivalently, the parabolic cylinder functions $\psi_\nu^{\text{osc}}(y) = \sqrt{2}^\nu D_\nu(\sqrt{2}y)$ (see also Section 9). We deduce the asymptotic

$$\psi_\nu^{\text{osc}}(y) \sim \begin{cases} (2y)^\nu e^{-\frac{y^2}{2}}, & y \rightarrow +\infty \\ \cos \pi \nu (-2y)^\nu e^{-\frac{y^2}{2}} + \frac{\sqrt{\pi}}{\Gamma(-\nu)} (-y)^{-\nu-1} e^{\frac{y^2}{2}}, & y \rightarrow -\infty \end{cases} \quad (\text{E.7})$$

The second linearly independent solution may be chosen as $\bar{\psi}_\nu^{\text{osc}}(y) = -\cos \pi \nu \psi_\nu^{\text{osc}}(y) + \psi_\nu^{\text{osc}}(-y)$, with asymptotic behaviour

$$\bar{\psi}_\nu^{\text{osc}}(y) \sim \begin{cases} \frac{\sqrt{\pi}}{\Gamma(-\nu)} y^{-\nu-1} e^{\frac{y^2}{2}}, & y \rightarrow +\infty \\ \sin^2 \pi \nu (-2y)^\nu e^{-\frac{y^2}{2}} - \frac{\cos \pi \nu \sqrt{\pi}}{\Gamma(-\nu)} (-y)^{-\nu-1} e^{\frac{y^2}{2}}, & y \rightarrow -\infty \end{cases} \quad (\text{E.8})$$

Note that, when $\nu \in \mathbb{N}_0$, the solution becomes $\psi_n^{\text{osc}}(y) = (2y)^n e^{-\frac{y^2}{2}}$, $\Gamma(-n) \bar{\psi}_n^{\text{osc}}(y) = \sqrt{\pi} y^{-n-1} e^{\frac{y^2}{2}}$.

Matching. In order to match the global WKB solutions with Hermite-like solutions approximating the solution in the neighbourhood of the points $\frac{\pm 1}{2\sqrt{g}}$, one expands the semiclassical exponent $S(y) = \int_0^y k(x) dx - \frac{1}{2} \ln(k(y)/g)$ in the vicinity of these points :

$$\text{I} : S(y_- < 0) \sim \frac{1}{12g} - \frac{y_-^2}{2} - \ln(-4\sqrt{g}y_+) + \left(\nu - \frac{1}{2}\right) \ln(\sqrt{g}y_+) + \mathcal{O}(g) + \mathcal{O}(y_-^3) \quad (\text{E.9})$$

$$\text{II} : S(y_- > 0) \sim -\frac{1}{12g} + \frac{y_-^2}{2} + \ln(4\sqrt{g}y_+) - \left(\nu - \frac{1}{2}\right) \ln(\sqrt{g}y_+) + \mathcal{O}(g) + \mathcal{O}(y_-^3) \quad (\text{E.10})$$

$$\text{III} : S(y_+ < 0) \sim \frac{1}{12g} - \frac{y_+^2}{2} + \ln(-4\sqrt{g}y_+) + \left(\nu - \frac{1}{2}\right) \ln(\sqrt{g}y_+) + \mathcal{O}(g) + \mathcal{O}(y_+^3) \quad (\text{E.11})$$

$$\text{IV} : S(y_+ > 0) \sim -\frac{1}{12g} + \frac{y_+^2}{2} - \ln(4\sqrt{g}y_+) - \left(\nu - \frac{1}{2}\right) \ln(\sqrt{g}y_+) + \mathcal{O}(g) + \mathcal{O}(y_+^3) \quad (\text{E.12})$$

Starting from $y = -\infty$, one connects A_- to A_+ , A'_+ passing the turning points (of second order) with the help of Eqs. (E.7), (E.8). Here one omits lower indices $y_\pm \mapsto y$ to make

equations more readable :

$$\text{I : } \psi(y_- < 0) \sim A_- e^{\frac{1}{12g}} (4\sqrt{g}^{\frac{3}{2}-\nu})^{-1} (-y)^{\nu-2} e^{-y^2/2} \quad (\text{E.13})$$

$$\begin{aligned} \text{II : } \psi(y_- > 0) &\sim \cos \pi \nu_- A_- e^{\frac{1}{12g}} (4\sqrt{g}^{\frac{3}{2}-\nu})^{-1} y^{\nu-} e^{-\frac{y^2}{2}} \\ &+ \frac{2^{-\nu-} \sqrt{\pi}}{\Gamma(-\nu_-)} A_- e^{\frac{1}{12g}} (4\sqrt{g}^{\frac{3}{2}-\nu})^{-1} y^{-\nu-1} e^{\frac{y^2}{2}} \end{aligned} \quad (\text{E.14})$$

$$\sim C_- e^{\frac{1}{12g}} (4\sqrt{g}^{\frac{3}{2}-\nu})^{-1} y^{\nu-2} e^{-y^2/2} + C_+ e^{-\frac{1}{12g}} 4\sqrt{g}^{\frac{3}{2}-\nu} y^{-\nu+1} e^{y^2/2} \quad (\text{E.15})$$

$$\text{III : } \psi(y_+ < 0) \sim C_+ e^{\frac{1}{12g}} 4\sqrt{g}^{\nu+\frac{1}{2}} (-y)^{\nu} e^{-y^2/2} + C_- e^{-\frac{1}{12g}} (4\sqrt{g}^{\nu+\frac{1}{2}})^{-1} (-y)^{-\nu-1} e^{y^2/2} \quad (\text{E.16})$$

$$\text{IV : } \psi(y_+ > 0)$$

$$\begin{aligned} &\sim \left[\cos \pi \nu C_+ e^{\frac{1}{12g}} 4\sqrt{g}^{\nu+\frac{1}{2}} + \frac{\Gamma(-\nu)}{\sqrt{\pi}} 2^{\nu} \sin^2 \pi \nu C_- e^{-\frac{1}{12g}} (4\sqrt{g}^{\nu+\frac{1}{2}})^{-1} \right] y^{\nu} e^{-y^2/2} \\ &+ \left[\frac{2^{-\nu} \sqrt{\pi}}{\Gamma(-\nu)} C_+ e^{\frac{1}{12g}} 4\sqrt{g}^{\nu+\frac{1}{2}} - \cos \pi \nu C_- e^{-\frac{1}{12g}} (4\sqrt{g}^{\nu+\frac{1}{2}})^{-1} \right] y^{-\nu-1} e^{y^2/2} \end{aligned} \quad (\text{E.17})$$

$$\sim A_+ e^{-\frac{1}{12g}} (4\sqrt{g}^{\nu+\frac{1}{2}})^{-1} y^{-\nu-1} e^{y^2/2} + A'_+ e^{\frac{1}{12g}} 4\sqrt{g}^{\nu+\frac{1}{2}} y^{\nu} e^{-y^2/2}. \quad (\text{E.18})$$

C_{\pm} are the coefficients of the semiclassical expansion under the potential barrier.

$$\psi \left(|y| \lesssim \frac{1}{2\sqrt{g}} \right) \sim C_+ \frac{\exp \int_0^y |k(x)| dx}{\sqrt{|k(y)|/g}} + C_- \frac{\exp - \int_0^y |k(x)| dx}{\sqrt{|k(y)|/g}}. \quad (\text{E.19})$$

$$C_+ = \frac{e^{\frac{1}{6g}}}{4\sqrt{g}^{3-2\nu}} \frac{2^{-\nu} \sqrt{\pi}}{\Gamma(2-\nu)} A_-, \quad C_- = \cos \pi \nu A_-. \quad (\text{E.20})$$

Finally, the coefficients A_+ , A_- are given by

$$A_+/A_- = \frac{e^{\frac{1}{3g}}}{\Gamma(-\nu)\Gamma(2-\nu)} \frac{4\pi}{g} \left(\frac{g}{2} \right)^{2\nu} - \cos^2 \pi \nu, \quad (\text{E.21})$$

$$A'_+/A_- = \frac{\cos \pi \nu e^{\frac{1}{6g}}}{\Gamma(2-\nu)} \frac{\sqrt{g}^{2\nu-3}}{2^{\nu+2}} - \cos \pi \nu \sin^2 \pi \nu \frac{e^{-\frac{1}{6g}} \Gamma(-\nu) 2^{\nu-4}}{\sqrt{\pi} \sqrt{g}^{2\nu-1}}. \quad (\text{E.22})$$

One could expect that the correct boundary condition at $+\infty$ is $A'_+ = 0$, however this is not the case. Instead, let us exploit $A_+ = A_-$, cf. Eq. (117) of the paper. This leads to

$$\nu \simeq -\frac{g}{2\pi} \exp \left(-\frac{1}{3g} \right), \quad g \ll 1. \quad (\text{E.23})$$

Substitution of this result leads to $A'_+/A_- \sim \frac{1}{4g} \sqrt{\pi/g} e^{\frac{1}{6g}} \gg 1$. This means that the solution of the initial problem at $+\infty$ has corrections of order $\psi(z) \sim A_+ |z|^{-3} + \dots + \# \exp(|E|z - z^3/3)$, $z \rightarrow +\infty$, as well as monomial corrections.

Using $g = s/4 = 1/(4|E|^{3/2})$, we can relate (E.23) with the quantity of interest in the paper :

$$\Lambda(1) = -\mathcal{E}_0(1) = \sqrt{|E|}(1-2\nu) \simeq \sqrt{|E|} + \frac{1}{4\pi|E|} e^{-4|E|^{3/2}/3}. \quad (\text{E.24})$$

This coincides with the energy dependence of the pre-exponential function obtained by a neat numerical analysis (Section 8), and demonstrates the statement below Eq. (121) about the dimensionless factor $1/(4\pi) \simeq 0.079577$.

Appendix F. Action S_q of the WKB treatment in the $s \rightarrow 0$ limit

In this appendix, we analyse the action (161) of the WKB treatment presented in Section 9 and prove that its $s \rightarrow 0$ behaviour is given by Eqs. (162,163). For this purpose, we introduce the function

$$F_q(s) := 2s S_q = \int_{-1}^{1-\sqrt{s}} d\zeta \sqrt{(1-\zeta^2)^2 - 4s(q+1)\zeta + 4sq(1-\sqrt{s}) - s^2}. \quad (\text{F.1})$$

As it is quite obvious that $F_q(0) = 4/3$, this allows one to extract easily the leading term of the action $S_q \simeq 2/(3s)$ by considering

$$F'_q(s) = 2 \int_{-1}^{1-\sqrt{s}} d\zeta \frac{q - (q+1)\zeta - (3/2)q\sqrt{s} - s/2}{\sqrt{(1-\zeta^2)^2 - 4s(q+1)\zeta + 4sq(1-\sqrt{s}) - s^2}}. \quad (\text{F.2})$$

The integral is logarithmically divergent in the $s \rightarrow 0$ limit. This makes clear that we can safely neglect the two terms $-(3/2)q\sqrt{s} - s/2$ in the numerator, which contribute as $\mathcal{O}(\sqrt{s} \ln s)$ to $F'_q(s)$.

In the limit $s \rightarrow 0$, the integral is dominated by the two boundaries. Because the logarithmic divergences are cut off in two different manners, it is convenient to split the integral into two parts, which we analyse separately :

$$F'_q(s) = G_-(s) + G_+(s) + \mathcal{O}(\sqrt{s} \ln s) \quad (\text{F.3})$$

where

$$G_-(s) := 2 \int_{-1}^0 d\zeta \frac{q - (q+1)\zeta}{\sqrt{f(\zeta)}} \quad \text{and} \quad G_+(s) := 2 \int_0^{1-\sqrt{s}} d\zeta \frac{q - (q+1)\zeta}{\sqrt{f(\zeta)}} \quad (\text{F.4})$$

and

$$f(\zeta) = (1 - \zeta^2)^2 - 4s(q+1)\zeta + 4sq(1 - \sqrt{s}) - s^2. \quad (\text{F.5})$$

Term G_-

Inspection of the Taylor expansion of the function f near $\zeta = -1$

$$f(\zeta) \underset{\zeta \sim -1}{\simeq} 4s(2q+1) - s(4q\sqrt{s} + s) - 4s(q+1)(\zeta+1) + 4(\zeta+1)^2 \quad (\text{F.6})$$

makes clear that the constant term cut off the logarithmic divergence of the integral at a scale $\delta\zeta = \mathcal{O}(\sqrt{s})$, so that the linear term can be neglected :

$$G_-(s) \underset{s \rightarrow 0}{\simeq} 2 \int_{-1}^0 d\zeta \frac{q - (q+1)\zeta}{\sqrt{s(2q+1) + (\zeta+1)^2}} \quad (\text{F.7})$$

$$\simeq (2q+1) \int_{\sqrt{s(2q+1)}}^0 \frac{dy}{y} \simeq - \left(q + \frac{1}{2} \right) \ln s \quad (\text{F.8})$$

In order to obtain the subleading constant term, we consider the integral

$$\begin{aligned} A_-(s) &:= \int_{-1}^0 d\zeta \frac{q - (q+1)\zeta}{\sqrt{s(2q+1) + (\zeta+1)^2}} \\ &= (2q+1) \ln \left(\frac{1}{\sqrt{s(2q+1)}} + \sqrt{\frac{1}{s(2q+1)} + 1} \right) - (q+1) \left[\sqrt{s(2q+1) + 1} - \sqrt{s(2q+1)} \right] \end{aligned} \quad (\text{F.9})$$

It is straightforward to show that

$$\lim_{s \rightarrow 0} [G_-(s) - A_-(s)] = q + 1 - \ln 2 \quad (\text{F.10})$$

from which we conclude that

$$G_-(s) \underset{s \rightarrow 0}{\simeq} - \left(q + \frac{1}{2} \right) \ln [s(2q + 1)] + 2q \ln 2 + \mathcal{O}(\sqrt{s}) \quad (\text{F.11})$$

Term G_+

We proceed in a similar manner for the second term. The starting point is the Taylor expansion

$$f(\zeta) \underset{\zeta \sim 1 - \sqrt{s}}{\simeq} - [8\sqrt{s} + \mathcal{O}(s)] (\zeta - 1 + \sqrt{s}) + 4(\zeta - 1 + \sqrt{s})^2 \quad (\text{F.12})$$

which shows that we have now to consider the integral

$$\begin{aligned} A_+(s) &:= \int_0^{1-\sqrt{s}} d\zeta \frac{q - (q+1)\zeta}{\sqrt{2\sqrt{s}(1-\sqrt{s}-\zeta) + (\zeta-1+\sqrt{s})^2}} \\ &= -\ln \left(\frac{1}{\sqrt{s}} + \sqrt{\frac{1}{s} + 1} \right) + (q+1)\sqrt{1-s} \end{aligned} \quad (\text{F.13})$$

Using that

$$\lim_{s \rightarrow 0} [G_+(s) - A_+(s)] = -(q+1) + (2q+1) \ln 2 \quad (\text{F.14})$$

we conclude that

$$G_+(s) \underset{s \rightarrow 0}{\simeq} \frac{1}{2} \ln s + 2q \ln 2 + \mathcal{O}(s) \quad (\text{F.15})$$

Conclusion

Gathering the two expressions (F.11,F.15), we finally obtain

$$F'(s) \underset{s \rightarrow 0}{=} -q \ln s + 4q \ln 2 - \left(q + \frac{1}{2} \right) \ln(2q+1) + \mathcal{O}(\sqrt{s} \ln s) \quad (\text{F.16})$$

An integration, with $F(0) = 4/3$, leads to (162,163).

Appendix G. An inverse Laplace transform

We study in this appendix the function defined by its Laplace transform

$$\varphi(\theta) = \mathcal{L}_{s \rightarrow \theta}^{-1} \left[\frac{1}{\sqrt{\cosh \sqrt{s}}} \right] \quad \text{for } \theta \geq 0. \quad (\text{G.1})$$

A direct calculation of the inverse Laplace is quite tricky due to the complicate analytic structure of the function $\sqrt{\cosh \sqrt{s}}$, which presents numbers of branch cuts in the complex plane of the variable $s = x + iy$: a succession of segments on the real axis,

$[-\pi^2(2n+3/2)^2, -\pi^2(2n+1/2)^2]$ for $n \in \mathbb{N}$, and parabolas intersecting those segments, $-x + [y/(2m\pi)]^2 = (m\pi)^2$ for non zero odd integers m .

Instead, we consider

$$(\varphi * \varphi)(\theta) = \mathcal{L}_{s \rightarrow \theta}^{-1} \left[\frac{1}{\cosh \sqrt{s}} \right] \quad (\text{G.2})$$

which can be easily computed thanks to residue's theorem

$$(\varphi * \varphi)(\theta) = \pi \sum_{n=0}^{\infty} (-1)^n (2n+1) \exp \left\{ -\frac{\pi^2}{4} (2n+1)^2 \theta \right\}. \quad (\text{G.3})$$

This first representation is useful to analyse the $\theta \rightarrow \infty$ limit. Using a Poisson formula given in an appendix of Ref. [105], we obtain the other useful representation

$$(\varphi * \varphi)(\theta) = \frac{1}{\sqrt{\pi} \theta^{3/2}} \sum_{n=0}^{\infty} (-1)^n (2n+1) \exp \left\{ -\frac{(n+1/2)^2}{\theta} \right\}, \quad (\text{G.4})$$

appropriate to describe the $\theta \rightarrow 0$ limit.

We now relate the two limiting behaviours

$$(\varphi * \varphi)(\theta) \simeq \begin{cases} \frac{1}{\sqrt{\pi} \theta^{3/2}} \exp \{-1/(4\theta)\} & \text{for } \theta \rightarrow 0 \\ \pi \exp \{-\pi^2 \theta / 4\} & \text{for } \theta \rightarrow \infty \end{cases} \quad (\text{G.5})$$

to the corresponding one for $\varphi(\theta)$. We use the two following remarks :

- We introduce $w(x) = c x^{-\alpha} e^{-x-1/(16x)}$ for $x > 0$. Some algebra gives

$$(w * w)(x) = c^2 (x/2)^{-2\alpha+1} e^{-x} \int_1^{\infty} du \frac{u^{\alpha-3/2}}{\sqrt{u-1}} e^{-u/(4x)}$$

with $(w * w)(x) \sim x^{-2\alpha+1/2} e^{-1/(4x)}$ for $x \rightarrow 0$.

- Now considering the function $p(x) = [b^{\alpha+1}/\Gamma(\alpha+1)] x^{\alpha} e^{-bx}$ for $x > 0$, it is easy to get

$$(p * p)(x) = \frac{b^{2\alpha+2}}{\Gamma(2\alpha+2)} x^{2\alpha+1} e^{-bx}$$

Using the first remark for $\alpha = 1$ and the second remark for $\alpha = -1/2$, we can relate the limiting behaviours (G.5) to

$$\varphi(\theta) \sim \begin{cases} \frac{1}{\theta} e^{-1/(16\theta)} & \text{for } \theta \rightarrow 0 \\ \frac{1}{\sqrt{\theta}} e^{-\pi^2 \theta / 4} & \text{for } \theta \rightarrow \infty \end{cases}. \quad (\text{G.6})$$

References

- [1] G. Blatter, M. V. Feigel'man, V. B. Geshkenbein, A. I. Larkin, and V. M. Vinokur, Vortices in high-temperature superconductors, *Rev. Mod. Phys.* **66**, 1125–1388 (1994).
- [2] P. Le Doussal, Novel phases of vortices in superconductors, *Int. J. Mod. Phys. B* **24**, 3855–3914 (2010), in *BCS: 50 years*, L. N. Cooper and D. Feldman (eds.), World Scientific, 2011.

- [3] T. Halpin-Healy and Y.-C. Zhang, Kinetic roughening phenomena, stochastic growth, directed polymers and all that. Aspects of multidisciplinary statistical mechanics, Phys. Rep. **254**(46), 215–414 (1995).
- [4] P. Calabrese, P. L. Doussal, and A. Rosso, Free-energy distribution of the directed polymer at high temperature, Europhys. Lett. **90**, 20002 (2010).
- [5] V. Dotsenko, Bethe ansatz derivation of the Tracy-Widom distribution for one-dimensional directed polymers, Europhys. Lett. **90**, 20003 (2010).
- [6] V. Dotsenko, Replica Bethe ansatz derivation of the Tracy-Widom distribution of the free energy fluctuations in one-dimensional directed polymers, J. Stat. Mech. , P07010 (2010).
- [7] T. Sasamoto and H. Spohn, One-dimensional Kardar-Parisi-Zhang equation: an exact solution and its universality, Phys. Rev. Lett. **104**, 230602 (2010).
- [8] G. Amir, I. Corwin, and J. Quastel, Probability distribution of the free energy of the continuum directed random polymer in $1 + 1$ dimensions, Commun. Pure Appl. Math. **64**, 466–537 (2011).
- [9] K. Johansson, Shape Fluctuations and Random Matrices, Commun. Math. Phys. **209**(2), 437–476 (2000).
- [10] J.-M. Azaïs and M. Wschebor, *Level Sets and Extrema of Random Processes and Fields*, John Wiley & Sons, 2009.
- [11] Y. V. Fyodorov, High-Dimensional Random Fields and Random Matrix Theory, Markov Processes Related Fields **21**, 483–518 (2015).
- [12] A. Auffinger, G. Ben Arous, and J. Cerny, Random matrices and complexity of spin glasses, Commun. Pure. Appl. Math. **66**, 165 (2013).
- [13] A. Auffinger and G. Ben Arous, Complexity of random smooth functions on the high-dimensional sphere, Ann. Probab. **41**(6), 4214–4247 (2013).
- [14] L. I. Nicolaescu, Complexity of random smooth functions on compact manifolds, Indiana Univ. Math. J. **63**, 1037 (2014).
- [15] E. Subag and O. Zeitouni, The extremal process of critical points of the pure p-spin spherical spin glass model, Probab. Theory Related Fields **168**(3), 773–820 (2017).
- [16] V. Cammarota and I. Wigman, Fluctuations of the total number of critical points of random spherical harmonics, Stochastic Processes and their Applications **127**(12), 3825–3869 (2017).
- [17] Y. V. Fyodorov and B. A. Khoruzhenko, Nonlinear analogue of the May-Wigner instability transition, Proc. Natl. Acad. Sci. (USA) **113**, 6827 (2016).
- [18] M. S. Longuet-Higgins, Reflection and refraction at a random moving surface. II. Number of specular points in a Gaussian surface, J. Opt. Soc. Am. **50**, 845 (1960).
- [19] B. I. Halperin and M. Lax, Impurity-Band Tails in the High-Density Limit. I. Minimum Counting Methods, Phys. Rev. **148**, 722–740 (1966).
- [20] A. Weinrib and B. I. Halperin, Distribution of maxima, minima, and saddle points of the intensity of laser speckle patterns, Phys. Rev. B **26**, 1362–1368 (1982).
- [21] I. Freund, Saddles, singularities, and extrema in random phase fields, Phys. Rev. E **52**, 2348–2360 (1995).
- [22] Y. V. Fyodorov, Complexity of Random Energy Landscapes, Glass Transition, and Absolute Value of the Spectral Determinant of Random Matrices, Phys. Rev. Lett. **92**, 240601 (2004).
- [23] A. J. Bray and D. S. Dean, Statistics of Critical Points of Gaussian Fields on Large-Dimensional Spaces, Phys. Rev. Lett. **98**, 150201 (2007).
- [24] Y. V. Fyodorov and I. Williams, Replica Symmetry Breaking Condition Exposed by Random Matrix Calculation of Landscape Complexity, J. Stat. Phys. **129**(5), 1081–1116 (2007).
- [25] Y. V. Fyodorov and C. Nadal, Critical Behavior of the Number of Minima of a Random Landscape at the Glass Transition Point and the Tracy-Widom Distribution, Phys. Rev. Lett. **109**, 167203 (2012).
- [26] G. Parisi, Computing the number of metastable states in infinite-range models, in *Les Houches summer school, Session LXXXIII*, edited by A. Bovier and *et al*, volume 83, pages 295–329, Amsterdam, 2005, Elsevier.
- [27] A. Annibale, A. Cavagna, I. Giardinà, and G. Parisi, Supersymmetric complexity in the Sherrington-Kirkpatrick model, Phys. Rev. E **68**, 061103 (2003).
- [28] Y. V. Fyodorov and P. Le Doussal, Topology Trivialization and Large Deviations for the Minimum in the Simplest Random Optimization, J. Stat. Phys. **154**(1), 466–490 (2014).
- [29] G. Wainrib and J. Touboul, Topological and Dynamical Complexity of Random Neural Networks, Phys. Rev. Lett. **110**, 118101 (2013).
- [30] Y. V. Fyodorov, Topology trivialization transition in random non-gradient autonomous ODEs on a sphere, J. Stat. Mechanics: Theor. Exp. **2016**, 124003 (2016).

- [31] M. R. Douglas, B. Shiffman, and S. Zelditch, Critical Points and supersymmetric vacua, I, Commun. Math. Phys. **252**, 325 (2004).
- [32] M. R. Douglas, B. Shiffman, and S. Zelditch, Critical Points and supersymmetric vacua, III: String/M models, Commun. Math. Phys. **265**, 617 (2006).
- [33] R. Easter, A. H. Guth, and A. Masoumi, Counting Vacua in Random Landscapes, preprint hep-th arXiv:1612.05224 (2016).
- [34] Y. V. Fyodorov, Counting stationary points of random landscapes as a random matrix problem, Acta Phys. Pol. B **36**(9), 2699–2707 (2005).
- [35] P. Le Doussal, M. Müller, and K. J. Wiese, Cusps and shocks in the renormalized potential of glassy random manifolds: How functional renormalization group and replica symmetry breaking fit together, Phys. Rev. B **77**, 064203 (2008).
- [36] L. Balents, J.-P. Bouchaud, and M. Mezard, The large scale energy landscape of randomly pinned objects, J. Phys. I (France) **6**, 1007 (1996).
- [37] M. Mézard and G. Parisi, Replica field theory for random manifolds, J. Phys. I (France) **1**, 809 (1991).
- [38] D. S. Fisher, Interface Fluctuations in Disordered Systems: $5 - \epsilon$ Expansion and Failure of Dimensional Reduction, Phys. Rev. Lett. **56**, 1964–1967 (1986).
- [39] P. Le Doussal, Exact results and open questions in first principle functional RG, Ann. Phys. **325**, 49 (2009).
- [40] P. Le Doussal and K. J. Wiese, Size distributions of shocks and static avalanches from the functional renormalization group, Phys. Rev. E **79**, 051106 (2009).
- [41] D. S. Fisher, Sliding charge-density waves as a dynamic critical phenomenon, Phys. Rev. B **31**, 1396–1427 (1985).
- [42] A. Rosso and W. Krauth, Roughness at the depinning threshold for a long-range elastic string, Phys. Rev. E **65**, 025101 (2002).
- [43] A. B. Kolton, S. Bustingorry, E. E. Ferrero, and A. Rosso, Uniqueness of the thermodynamic limit for driven disordered elastic interfaces, J. Stat. Mech.: Theor. Exp. **2013**, P12004 (2013).
- [44] V. Démery, V. Lecomte, and A. Rosso, The effect of disorder geometry on the critical force in disordered elastic systems, J. Stat. Mech.: Theor. Exp. **2014**, P03009 (2014).
- [45] V. Démery, A. Rosso, and L. Ponson, From microstructural features to effective toughness in disordered brittle solids, Europhys. Lett. **105**(3), 34003 (2014).
- [46] P. Le Doussal and K. J. Wiese, Driven particle in a random landscape: Disorder correlator, avalanche distribution, and extreme value statistics of records, Phys. Rev. E **79**, 051105 (2009).
- [47] A. A. Fedorenko, P. Le Doussal, and K. J. Wiese, Universal distribution of threshold forces at the depinning transition, Phys. Rev. E **74**, 041110 (2006).
- [48] A. Rosso, P. Le Doussal, and K. J. Wiese, Avalanche-size distribution at the depinning transition: A numerical test of the theory, Phys. Rev. B **80**, 144204 (2009).
- [49] P. Le Doussal, K. J. Wiese, and P. Chauve, Two-loop functional renormalization group theory of the depinning transition, Phys. Rev. B **66**, 174201 (2002).
- [50] G. Huber, M. Pradas, A. Pumir, and M. Wilkinson, Persistent stability of a chaotic system, Physica A **492**, 517–523 (2018).
- [51] K. B. Efetov and A. I. Larkin, Charge-density wave in a random potential, Sov. Phys. JETP **45**(6), 1236–1241 (1977).
- [52] G. Parisi and N. Sourlas, Random Magnetic Fields, Supersymmetry, and Negative Dimensions, Phys. Rev. Lett. **43**, 744–745 (1979).
- [53] T. Giamarchi and P. Le Doussal, Elastic theory of pinned flux lattices, Phys. Rev. Lett. **72**, 1530–1533 (1994).
- [54] D. S. Fisher, Random fields, random anisotropies, nonlinear σ models, and dimensional reduction, Phys. Rev. B **31**, 7233–7251 (1985).
- [55] D. E. Feldman, Quasi-long-range order in the random anisotropy Heisenberg model: Functional renormalization group in $4 - \epsilon$ dimensions, Phys. Rev. B **61**, 382–390 (2000).
- [56] D. E. Feldman, Quasi-long range order in glass states of impure liquid crystals, magnets, and superconductors, Int. J. Mod. Phys. B **15**(22), 2945–2976 (2001).
- [57] K. J. Wiese and P. L. Doussal, Functional Renormalization for Disordered Systems, Basic Recipes and Gourmet Dishes, Markov Processes Relat. Fields **13**, 777–818 (2007), preprint arXiv:cond-mat/0611346.
- [58] A. A. Middleton, Asymptotic uniqueness of the sliding state for charge-density waves, Phys. Rev. Lett. **68**(5), 670 (1992).
- [59] C. Baesens and R. S. MacKay, Gradient dynamics of tilted Frenkel-Kontorova models, Nonlinearity

- 11, 949 (1998).
- [60] M. W. Hirsch, Systems of Differential Equations that are Competitive or Cooperative II: Convergence Almost Everywhere, *SIAM J. Math. Anal.* **16**(3), 423 (1985).
 - [61] I. S. Gradshteyn and I. M. Ryzhik, *Table of integrals, series and products*, Academic Press, fifth edition, 1994.
 - [62] C. Texier, ζ -regularised spectral determinants for metric graphs, *J. Phys. A: Math. Theor.* **43**, 425203 (2010).
 - [63] D. C. Herbert and R. Jones, Localized states in disordered systems, *J. Phys. C: Solid St. Phys.* **4**(10), 1145 (1971).
 - [64] D. J. Thouless, A relation between the density of states and range of localization for one-dimensional random systems, *J. Phys. C: Solid St. Phys.* **5**, 77 (1972).
 - [65] J.-M. Luck, *Systèmes désordonnés unidimensionnels*, CEA, collection Aléa Saclay, Saclay, 1992.
 - [66] A. Grabsch, C. Texier, and Y. Tourigny, One-dimensional disordered quantum mechanics and Sinai diffusion with random absorbers, *J. Stat. Phys.* **155**(2), 237–276 (2014).
 - [67] I. M. Gel'fand and A. M. Yaglom, Integration in functional spaces and its applications in quantum physics, *J. Math. Phys.* **1**(1), 48–69 (1960).
 - [68] S. Levit and U. Smilansky, A theorem on infinite products of eigenvalues of Sturm-Liouville type operators, *Proc. Am. Math. Soc.* **65**, 299 (1977).
 - [69] I. V. Kolokolov, Statistical geometry of chaotic two-dimensional transport, *JETP Lett.* **92**, 107 (2010).
 - [70] A. Comtet, J.-M. Luck, C. Texier, and Y. Tourigny, The Lyapunov exponent of products of random 2×2 matrices close to the identity, *J. Stat. Phys.* **150**(1), 13–65 (2013).
 - [71] A. Comtet, C. Texier, and Y. Tourigny, Lyapunov exponents, one-dimensional Anderson localisation and products of random matrices, *J. Phys. A: Math. Theor.* **46**, 254003 (2013), Special issue “Lyapunov analysis: from dynamical systems theory to applications”.
 - [72] B. I. Halperin, Green's Functions for a Particle in a One-Dimensional Random Potential, *Phys. Rev.* **139**(1A), A104–A117 (1965).
 - [73] I. M. Lifshits, S. A. Gredeskul, and L. A. Pastur, *Introduction to the theory of disordered systems*, John Wiley & Sons, 1988.
 - [74] G. Paladin and A. Vulpiani, Anomalous scaling in multifractal objects, *Phys. Rep.* **156**(4), 147–225 (1987).
 - [75] G. Paladin and A. Vulpiani, Anomalous scaling and generalized Lyapunov exponents of the one-dimensional Anderson model, *Phys. Rev. B* **35**, 2015–2020 (1987).
 - [76] A. Crisanti, G. Paladin, and A. Vulpiani, *Products of random matrices in statistical physics*, Springer-Verlag, 1993, Springer Series in Solid-State Sciences vol. **104**.
 - [77] T. N. Antsygina, L. A. Pastur, and V. A. Slyusarev, Localization of states and kinetic properties of one-dimensional disordered systems, *Sov. J. Low Temp. Phys.* **7**(1), 1–21 (1981).
 - [78] H. Schomerus and M. Titov, Statistics of finite-time Lyapunov exponents in a random time-dependent potential, *Phys. Rev. E* **66**, 066207 (2002).
 - [79] A. Cohen, Y. Roth, and B. Shapiro, Universal distributions and scaling in disordered systems, *Phys. Rev. B* **38**(17), 12125–12132 (1988).
 - [80] K. Ramola and C. Texier, Fluctuations of random matrix products and 1D Dirac equation with random mass, *J. Stat. Phys.* **157**(3), 497–514 (2014).
 - [81] J.-P. Bouchaud, A. Georges, D. Hansel, P. Le Doussal, and J.-M. Maillard, Rigorous bounds and the replica method for products of random matrices, *J. Phys. A: Math. Gen.* **19**, L1145–L1152 (1986).
 - [82] J.-P. Bouchaud, A. Georges, and P. Le Doussal, Fluctuations of the Lyapunov exponent and intermittency in dynamical and disordered systems: the example of 1D localization, in *Proceedings of the Meeting on Dynamical Systems*, Rome, Italy, 1986, Preprint LPTENS 86/34.
 - [83] J. B. Pendry, Symmetry and transport of waves in one-dimensional disordered systems, *Adv. Phys.* **43**(4), 461–542 (1994).
 - [84] C. Texier, Individual energy level distributions for one-dimensional diagonal and off-diagonal disorder, *J. Phys. A: Math. Gen.* **33**, 6095–6128 (2000).
 - [85] C. Hagendorf and C. Texier, Breaking supersymmetry in a one-dimensional random Hamiltonian, *J. Phys. A: Math. Theor.* **41**, 405302 (2008).
 - [86] L. D. Landau and E. Lifchitz, *Mécanique quantique*, Mir, 1966, tome 3.
 - [87] A. Garg, Tunnel splittings for one dimensional potential wells revisited, *Am. J. Phys.* **68**, 430 (2000).
 - [88] D.-Y. Song, Tunneling and energy splitting in an asymmetric double-well potential, *Ann. Phys.*

- 323**(12), 2991–2999 (2008).
- [89] C. Texier, *Mécanique quantique*, Dunod, Paris, second edition, 2015.
 - [90] A. Nikiforov and V. Ouvarov, *Fonctions spéciales de la physique mathématique*, Mir, Moscou, 1983.
 - [91] C. W. Gardiner, *Handbook of stochastic methods for physics, chemistry and the natural sciences*, Springer, 1989.
 - [92] R. Zillmer and A. Pikovsky, Multiscaling of noise-induced parametric instability, *Phys. Rev. E* **67**, 061117 (2003).
 - [93] K. Mallick and P. Marcq, Anomalous diffusion in nonlinear oscillators with multiplicative noise, *Phys. Rev. E* **66**, 041113 (2002).
 - [94] A. Grabsch and C. Texier, Capacitance and charge relaxation resistance of chaotic cavities – Joint distribution of two linear statistics in the Laguerre ensemble of random matrices, *Europhys. Lett.* **109**, 50004 (2015).
 - [95] A. Grabsch and C. Texier, Distribution of spectral linear statistics on random matrices beyond the large deviation function – Wigner time delay in multichannel disordered wires, *J. Phys. A: Math. Theor.* **49**, 465002 (2016).
 - [96] J. M. Harrison, K. Kirsten, and C. Texier, Spectral determinants and Zeta functions of Schrödinger operators on metric graphs, *J. Phys. A: Math. Theor.* **45**, 125206 (2012).
 - [97] J. Desbois, Spectral determinant of Schrödinger operators on graphs, *J. Phys. A: Math. Gen.* **33**, L63 (2000).
 - [98] A. Comtet, J. Desbois, and C. Texier, Functionals of the Brownian motion, localization and metric graphs, *J. Phys. A: Math. Gen.* **38**, R341–R383 (2005).
 - [99] D. Dhar, The Abelian sandpile and related models, *Physica A* **263**(1-4), 4–25 (1999), Proceedings of the 20th IUPAP International Conference on Statistical Physics.
 - [100] G. Pruessner, *Self-organised criticality: theory, models and characterisation*, Cambridge University Press, 2012.
 - [101] P. Le Doussal and K. J. Wiese, Exact Mapping of the Stochastic Field Theory for Manna Sandpiles to Interfaces in Random Media, *Phys. Rev. Lett.* **114**, 110601 (2015).
 - [102] H. Risken, *The Fokker-Planck Equation: Methods of Solution and Applications*, Springer, Berlin, 1989.
 - [103] G. Junker, *Supersymmetric methods in quantum and statistical physics*, Springer, 1996.
 - [104] D. R. Saykin, K. S. Tikhonov, and Y. I. Rodionov, Landau levels with magnetic tunneling in a Weyl semimetal and magnetoconductance of a ballistic p – n junction, *Phys. Rev. B* **97**, 041202 (2018).
 - [105] C. Texier and C. Hagendorf, Effect of boundaries on the spectrum of a one-dimensional random mass Dirac Hamiltonian, *J. Phys. A: Math. Theor.* **43**, 025002 (2010).